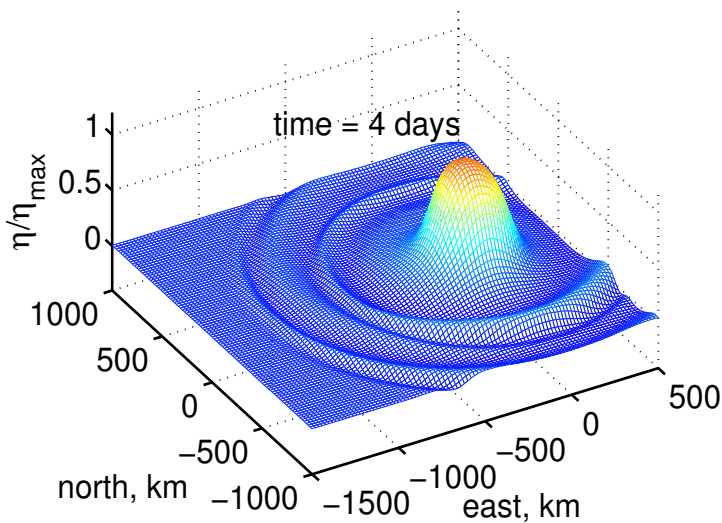


a Coriolis tutorial

Part I: Rotating reference frames and the Coriolis force

Part II: Geostrophic adjustment and potential vorticity



James F. Price
Woods Hole Oceanographic Institution
Woods Hole, Massachusetts, 02543
www.whoi.edu/science/PO/people/jprice

Version 4.3.3

September 24, 2010

This essay is an introduction to rotating reference frames and to the effects of Earth's rotation on the large scale flows of the atmosphere and ocean. It is intended for students who are beginning a quantitative study of Earth science and geophysical fluid dynamics and who have some background in classical mechanics and applied mathematics.

Part I uses a very simple single parcel model to derive and illustrate the equation of motion appropriate to a steadily rotating reference frame. Two inertial forces account for accelerations due to the rotating reference frame, a centrifugal force and a Coriolis force. In the case of an Earth-attached reference frame, the centrifugal force is indistinguishable from gravitational mass attraction and is subsumed into

the gravity field. The Coriolis force has a very simple mathematical form, $-2\mathbf{\Omega} \times \mathbf{V}'M$, where $\mathbf{\Omega}$ is Earth's rotation vector, \mathbf{V}' is the velocity observed from the rotating frame and M is the parcel mass. The Coriolis force is perpendicular to the velocity and so tends to change velocity direction, but not velocity amplitude, i.e., the Coriolis force does no work.

If the Coriolis force is the only force acting on a moving parcel, then the velocity vector of the parcel will be continually deflected anti-cyclonically. These free motions, often termed inertial oscillations, are a first approximation of the upper ocean currents that are generated by a transient wind event. If the Coriolis force is balanced by a steady force, say a pressure gradient, then the resulting wind or current will be in a direction that is perpendicular to the pressure gradient force. An approximate geostrophic momentum balance of this kind is the defining characteristic of the large scale, low frequency circulation of the atmosphere and oceans outside of the tropics.

Part II uses a single-layer fluid model to solve several problems in geostrophic adjustment; a one- or two-dimensional mass anomaly is released from rest and allowed to evolve under gravity and rotation. The fast time scale response includes gravity waves with phase speed C that tend to spread the mass anomaly. If the anomaly has a horizontal scale that exceeds several times the radius of deformation, $R_d = C/f$, where $f = 2\Omega \sin(\textit{latitude})$ is the Coriolis parameter, then the Coriolis force will arrest the spreading and yield a quasi-steady, geostrophic balance.

An exact geostrophic balance would be exactly steady, while it is evident that the atmosphere and the ocean evolve continually. Departures from exact geostrophy can arise in many ways including as a consequence of frictional drag with a boundary, and from the latitudinal variation of f . The latter beta-effect imposes a marked anisotropy onto the atmosphere and the ocean — eddies and long waves propagate phase westward and the major ocean gyres are strongly compressed onto the western sides of ocean basins. These and other low frequency phenomenon are often best interpreted as a consequence of potential vorticity conservation, the geophysical fluid equivalent of angular momentum conservation. Earth's rotation contributes planetary vorticity $= f$, that is generally considerably larger than the relative vorticity of winds and currents. Small changes in the latitude or thickness of a fluid column may convert planetary vorticity to relative vorticity, $\nabla \times \mathbf{V}'$, succinctly accounting for some of the most important large scale, low frequency phenomena, e.g., westward propagation.

Contents

1	Large-scale flows of the atmosphere and ocean.	4
1.1	Classical mechanics observed from a rotating Earth	9
1.2	The goal and the plan of this essay	11
1.3	About this essay	13
2	Part I: Rotating reference frames and the Coriolis force.	14
2.1	Kinematics of a linearly accelerating reference frame	14
2.2	Kinematics of a rotating reference frame	17
2.2.1	Transforming the position, velocity and acceleration vectors	17
2.2.2	Stationary \Rightarrow Inertial; Rotating \Rightarrow Earth-Attached	23
2.2.3	Remarks on the transformed equation of motion	25
3	Inertial and noninertial descriptions of elementary motions.	27
3.1	Switching sides	28
3.2	To get a feel for the Coriolis force	30
3.2.1	Zero relative velocity	30
3.2.2	With relative velocity	31
3.3	An elementary projectile problem	33
3.3.1	From the inertial frame	34
3.3.2	From the rotating frame	35
3.4	Appendix to Section 3: Circular motion and polar coordinates.	37
4	A reference frame attached to the rotating Earth.	38
4.1	Cancellation of the centrifugal force	38
4.1.1	Earth's (slightly chubby) figure	39
4.1.2	Vertical and level in an accelerating reference frame	40
4.1.3	The equation of motion for an Earth-attached frame	41
4.2	Coriolis force on motions in a thin, spherical shell	42
4.3	Why do we insist on the rotating frame equations?	44
4.3.1	Inertial oscillations from an inertial frame	44
4.3.2	Inertial oscillations from the rotating frame	48
5	A dense parcel on a slope.	50
5.1	Inertial and geostrophic motion	52

1	<i>LARGE-SCALE FLOWS OF THE ATMOSPHERE AND OCEAN.</i>	4
5.2	Energy budget	55
6	Part II: Geostrophic adjustment and potential vorticity.	56
6.1	The shallow water model	57
6.2	Solving and diagnosing the shallow water system	59
6.2.1	Energy balance	60
6.2.2	Potential vorticity balance	60
6.3	Linearized shallow water equations	64
7	Models of the Coriolis parameter.	64
7.1	Case 1, $f = 0$, nonrotating	65
7.2	Case 2, $f = \text{constant}$, an f -plane,	69
7.3	Case 3, $f = f_0 + \beta y$, a β -plane,	75
7.3.1	Beta-plane phenomena	76
7.3.2	Rossby waves; low frequency waves on a beta plane	79
7.3.3	Modes of potential vorticity conservation	84
7.3.4	Some of the varieties of Rossby waves	86
8	Summary of the essay.	88
9	Supplementary material.	90
9.1	Matlab and Fortran source code	90
9.2	Additional animations	91

1 Large-scale flows of the atmosphere and ocean.

The large-scale, low frequency flows of Earth’s atmosphere and ocean take the form of circulations around centers of high or low pressure. Global-scale circulations include the broad belt of westerly wind that encircles the mid-latitudes in both hemispheres (Fig. 1) and gyres that fill ocean basins (Fig. 2). Smaller scale circulations often dominate the weather. Hurricanes and mid-latitude storms, for example, have a more or less circular flow around a low pressure center, and many regions of the ocean are filled with slowly revolving eddies having a diameter of several hundred kilometers (Figs. 2 and 3). The pressure anomaly that is associated with each of these circulations can be understood as the direct consequence of mass excess (high pressure) or deficit (low pressure) in the overlying fluid.

What is at first surprising is that large scale mass anomalies of the kind seen in Figs. 1 and 2 persist for many days or weeks in the absence of an external energy source. The flow of mass that would be

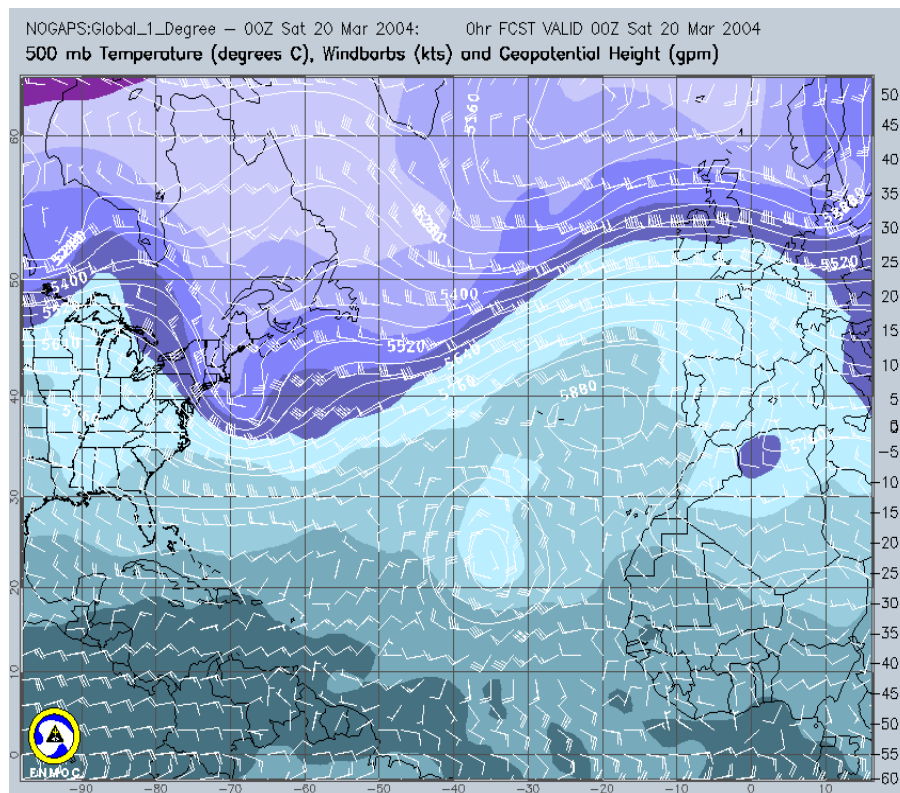


Figure 1: A weather map showing conditions at 500 mb over the North Atlantic on 20 March, 2004, produced by the Fleet Numerical Meteorology and Oceanography Center (500 mb is a middle level of the atmosphere). Variables are temperature (colors, scale at right is $^{\circ}\text{C}$), the height of the 500 mb pressure surface (white contours, values are meters above sea level) and the wind vector (as 'barbs' at the rear of the vector, one thin barb = 10 knots $\approx 5 \text{ m s}^{-1}$, one heavy barb = 50 knots). Several important phenomenon that will be discussed throughout the text are evident on this map. (1) The winds at mid-latitudes were mainly westerly, i.e., winds that blow from the west toward the east. The broad band of westerly winds often includes one or several maxima, or jet stream(s), here between about 40° to 50° N. (2) Within the westerly wind band, the 500 mb surface sloped upward toward lower latitude. There was thus a small, but significant component of gravity that was parallel to this surface, $-g\nabla\eta$, and directed from south to north. The largest slope was roughly 500 m per 1000 km within the jet stream where wind speed was also largest, roughly $U \approx 40 \text{ m s}^{-1}$. (3) Wind vectors appear to be nearly parallel to the contours of constant height everywhere poleward of about 10° latitude. The wind and pressure fields were thus in an approximately steady, geostrophic balance, $0 \approx -g\partial\eta/\partial y - fU$, where f is the Coriolis parameter and fU is the Coriolis force (per unit mass), the topic of Part I of this essay. (4) Any particular realization of the jet stream is likely to exhibit wave-like undulations. The longest such undulations often appear to be almost stationary with respect to Earth, and so must be propagating westward with respect to the spatially-averaged westerly wind. On this day the jet stream made a trough (southerly dip) near the east coast of the US, and a ridge near northwestern Europe. This is a fairly common jet stream configuration that transports relatively warm, moist air toward Northern Europe (Seager, R., D. S. Battisti, J. Yin, N. Gordon, N. Naik, A. C. Clement and M. Cane, 'Is the Gulf Stream responsible for Europe's mild winters?', Q. J. R. Meteorol. Soc., **128**, pp. 1-24, 2002.)

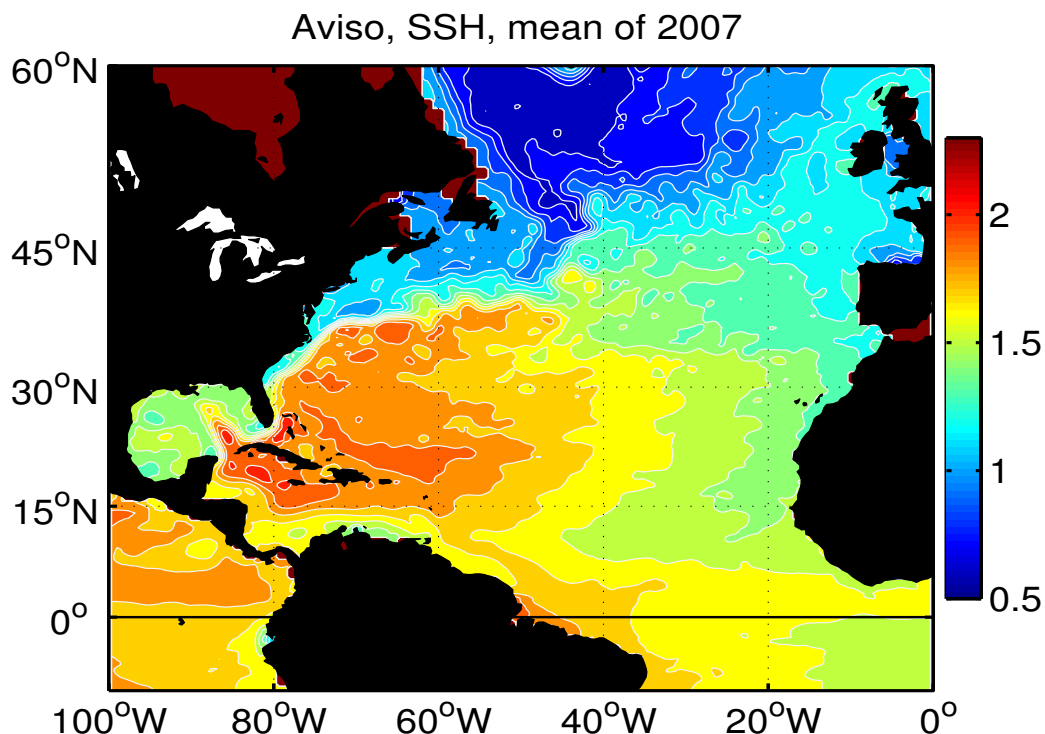


Figure 2: The 2007 annual mean of sea surface height (SSH). These remarkable data are thanks to the Aviso project (with support from Cnes, <http://www.aviso.oceanobs.com/duacs/>). The color scale at right is in meters. The region depicted here is comparable to that of Fig.1, and the field has a very similar meaning; SSH is effectively a constant pressure, frictionless surface that is displaced slightly but significantly from level. The change in SSH is only about 2 m from a low in the western subpolar gyre (55° N and 50° W) to a high in the western subtropical gyre and Caribbean Sea (25° N and 70° W). Note that by far the largest gradient of SSH is found just inside the western boundary of the subtropical gyre and is much less over the central and eastern regions. This marked east-west asymmetry is typical of ocean gyres. What keeps SSH displaced away from level? We do not have direct measurement of ocean currents on anything close to the same resolution, but nevertheless we can be confident that the horizontal gravitational force associated with this tilted SSH is nearly balanced by the Coriolis force acting upon horizontal currents, i.e., we infer a geostrophic momentum balance, just as in the atmospheric westerlies of Fig. 1.

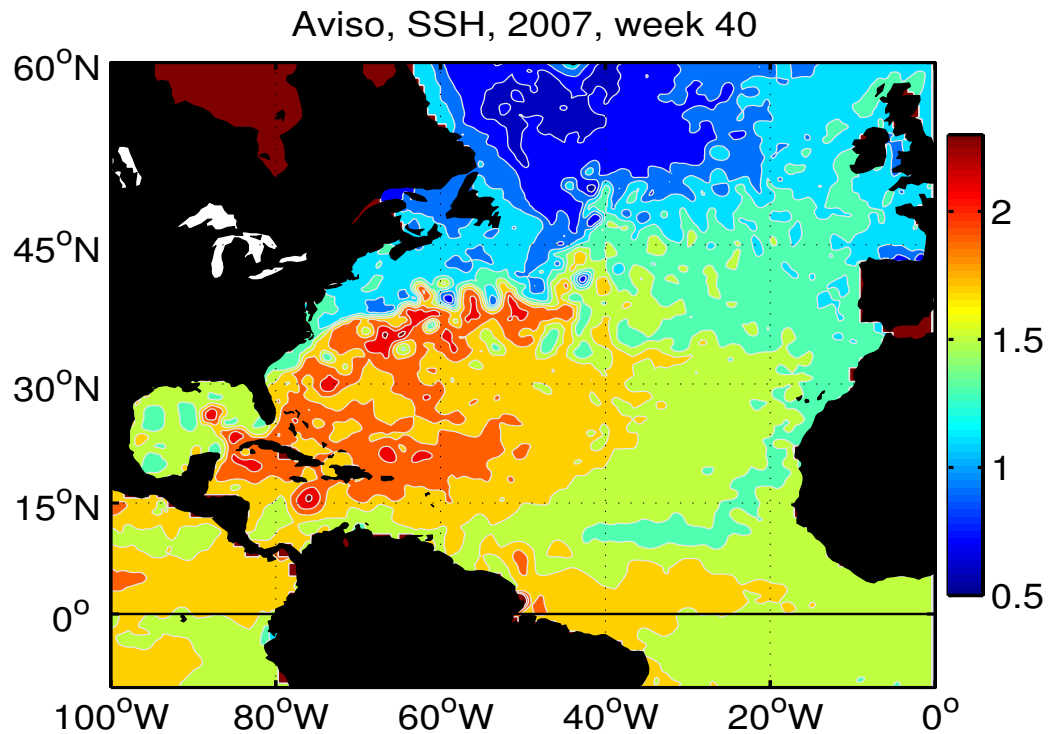


Figure 3: A snapshot of SSH over the North Atlantic ocean from week 40 of 2007 (thanks to the Aviso project). Compared with the previous year-long mean, this field shows considerable variability on scales of several hundred kilometers, often termed the oceanic mesoscale (*meso* is Greek for middle), and a considerably narrower western boundary current. If you are viewing on Acrobat Reader you can animate the field by clicking on the image. You will see that the mesoscale eddies persist as identifiable features for many weeks. Eddies that are near the western boundary are carried northward and eastward by the western boundary current system (from south to north, the Loop Current, Gulf Stream, and North Atlantic Current). Eddies that are within the central subtropical gyre and outside of strong time-mean currents move steadily westward. An important goal of this essay (Section 7.3) is to understand the mechanism of this westward propagation and the closely related east-west asymmetry of ocean gyres.

expected to accelerate down the pressure gradient and disperse the associated mass anomaly does not occur. Instead, large-scale, low frequency winds and currents are observed to flow in a direction that is almost parallel to lines of constant pressure; the sense of the flow is clockwise around high pressure centers (northern hemisphere) and anticlockwise around low pressure centers. The direction of flow is reversed in the southern hemisphere. From this we can infer that the pressure gradient force, which is normal to lines of constant pressure, must be balanced approximately by a second force, the Coriolis force,^{1,2} that must act to deflect (accelerate) horizontal winds and currents to the right of the velocity vector in the northern hemisphere and to the left of the velocity vector in the southern hemisphere.³ A balance between a pressure gradient force and the deflecting Coriolis force is called a geostrophic balance, and a near-geostrophic momentum balance is the defining characteristic of large scale, low frequency atmospheric and oceanic flows outside of equatorial regions.

We attribute quite profound physical consequences to the Coriolis force, and yet we cannot point to a physical interaction as the cause of the Coriolis force in the direct and simple way that we can relate hydrostatic pressure anomalies to the mass field. Rather, the Coriolis force arises from our common practice to observe and analyze the atmosphere and ocean using an Earth-attached and thus rotating, noninertial reference frame. The Coriolis force thus arises from motion itself, and in this regard the Coriolis force is distinct from other important forces in ways and with consequences that are the theme of Part I of this essay. In Part II we will examine some of the consequences of Earth's rotation, and take a different and in some ways more direct view of Earth's rotation, *viz.*, that it imparts a kind of gyroscopic rigidity to winds and currents that can be understood from the conservation of potential vorticity, the fluid equivalent of angular momentum.

¹Footnotes provide references, extensions or qualifications of material discussed in the main text, and homework assignments; they may be skipped on first reading.

²After the French physicist and engineer, Gaspard-Gustave de Coriolis, 1792-1843, whose seminal contributions include the systematic derivation of the rotating frame equation of motion and the development of the gyroscope. An informative history of the Coriolis force is by A. Persson, 'How do we understand the Coriolis force?', *Bull. Am. Met. Soc.*, **79**(7), 1373-1385 (1998).

³You must be wondering 'What's it do right on the equator?' (and see S. Adams, *It's Obvious You Won't Survive by Your Wits Alone*, p. 107, Andrews and McNeil Press, Kansas City, Kansas, 1995). By symmetry we would expect that the horizontal deflection due to the Coriolis force must vanish along the equator. The contrast between mid-latitude and equatorial wind and pressure relationships is thus of great interest here, and we will return to the equator at several points in this essay. A question for you: How would you characterize the equatorial wind and pressure relationship of Fig. 1? One specific chart may not be particularly revealing, so take a look at the 500 hPa charts (heights, winds and temperatures) available online at http://www.nrlmry.navy.mil/metoc/nogaps/NOGAPS_global_net.html (you may have to type this address into your web browser).

1.1 Classical mechanics observed from a rotating Earth

This essay proceeds inductively, developing concepts one by one rather than deriving them from a comprehensive starting point. In that spirit, our first model of a geophysical fluid will be a single, isolated particle. So long as we are concerned just with the Coriolis force (Part I), we can be content with a point-like particle. In Part II we will begin to consider the rotation of the particle, and for that purpose we will need the first spatial derivatives of velocity, e.g., $\partial u/\partial y$ and thus a particle with finite size, in fluid usage, a 'parcel'. But whether point-like or not, a single parcel model is a drastic, and for most purposes untenable idealization. Winds and currents, like all fluid flows, are made up of a continuum of parcels that interact in three-dimensions. Nevertheless, a single parcel is an appropriate first step in a hierarchy of models because the Coriolis force depends only upon the local velocity of a parcel and not upon the spatial derivative of velocity or pressure around the parcel. Thus the phenomena that arise in the single parcel model are found also in much more realistic fluid models and in the real atmosphere and ocean. The converse is certainly not true; many of the most interesting and important phenomena of fluid flows are not within the domain of the single parcel model, e.g., gravity waves, and so we will be careful not to over-interpret or extrapolate our single parcel results. But here's a promise: The intuition that you will gain by studying the Coriolis force in this simplified context will carry over intact to a study of much more realistic fluid models that we will come to in Sections 6 and 7, by then knowing quite a lot about the Coriolis force.

If our parcel is observed from an inertial reference frame⁴, then the classical (Newtonian) equation of motion is just

$$\frac{d(M\mathbf{V})}{dt} = \mathbf{F} + \mathbf{g}_*M,$$

where d/dt is an ordinary time derivative, \mathbf{V} is the velocity in a three-dimensional space, and M is the parcel's mass. The parcel mass (or fluid density) will be presumed constant in all that follows, and the equation of motion rewritten as

$$\frac{d\mathbf{V}}{dt}M = \mathbf{F} + \mathbf{g}_*M. \quad (1)$$

Unless it is noted otherwise, the acceleration that would be directly observable in a given reference frame will be the left-hand side of an equation of motion, and the forces (everything else) will be on the right-hand side. Here, \mathbf{F} is the sum of the forces that we can specify *a priori* given the complete

⁴'Inertia' has Latin roots *in+artis* meaning without art or skill and secondarily, resistant to change. Since Newton's *Principia*, physics usage has emphasized the latter: a parcel having inertia will remain at rest, or if in motion, continue without change unless subjected to an external force. By 'reference frame' we mean a coordinate system that serves to arithmetize the position of parcels, a clock to tell the time, and an observer who makes an objective record of positions and times. A reference frame may or may not be attached to a physical object. In this essay we suppose purely classical physics so that measurements of length and of time are identical in all reference frames. This common sense view of space and time begins to fail when velocities approach the speed of light, which is not an issue here. An inertial reference frame is one in which all parcels have the property of inertia and in which the total momentum is conserved, i.e., all forces occur as action-reaction force pairs. How this plays out in the presence of gravity will be discussed briefly in Section 3.1.

knowledge of the environment, e.g., a pressure gradient, or frictional drag with the ground or adjacent parcels, and \mathbf{g}_* is gravitational mass attraction. These are said to be central forces insofar as they are effectively instantaneous and they act in a radial direction between parcels (and in the case of gravitational mass attraction, between parcels and the Earth). Central forces occur as action-reaction force pairs, the sum of which is zero. Given the single parcel model used up through Section 5, it is appropriate to make two sweeping simplifications of \mathbf{F} : 1) we will specify \mathbf{F} independently of the motion of surrounding parcels, and, 2) we will make no allowance for the continuity of volume of a fluid flow, i.e., that two parcels can not occupy the same point in space.⁵

This inertial reference frame equation of motion has two fundamental properties that we note here because we are about to give them up:

Global conservation. For each of the central forces acting on the parcel there will be a corresponding reaction force acting on the part of the environment that sets up the force. Thus the global time rate of change of momentum (global means parcel plus the environment) due to the sum of all of the central forces $\mathbf{F} + \mathbf{g}_*M$ is zero, i.e., global momentum is conserved. Usually our attention is focused on the local problem, i.e., the parcel only, with global conservation taken for granted and not analyzed explicitly.

Invariance to Galilean transformation. Eqn. (1) should be invariant to a steady (linear) translation of the reference frame, often called a Galilean transformation. A constant velocity added to \mathbf{V} will cause no change in the time derivative, and if added to the environment should as well cause no change in the forces \mathbf{F} or \mathbf{g}_*M . Like the global balance just noted, this property is not invoked frequently, but is a powerful guide to the appropriate forms of the forces \mathbf{F} . For example, a frictional force that satisfies Galilean invariance should depend upon the difference of the velocity with respect to a surface or adjacent parcels, and not the velocity only.

When it comes to the practical analysis of the atmosphere or ocean we always use a reference frame that is attached to the rotating Earth — true (literal) inertial reference frames are simply not accessible. Some of the reasons for this are discussed in a later section, 4.3; for now we are concerned with the consequence that, because of the Earth's rotation, an Earth-attached reference frame is significantly noninertial for the large-scale motions of the atmosphere and ocean. The equation of motion (1) transformed into an Earth-attached reference frame (examined in detail in Sections 2 and 4.1) is

$$\frac{d\mathbf{V}'}{dt}M = -2\boldsymbol{\Omega} \times \mathbf{V}'M + \mathbf{F}' + \mathbf{g}M, \quad (2)$$

where the prime on a vector indicates that it is observed from the rotating frame, $\boldsymbol{\Omega}$ is Earth's rotation

⁵In Section 6 we will consider a fluid model in which the main force on parcels is the gradient of pressure, which is determined largely by the continuity of volume requirement: as fluid parcels converge into a given volume, the pressure will increase, eventually enough to disperse the parcels away from the volume. How rapidly the pressure increases and how rapidly the fluid responds depends upon the stiffness and the mass density of the fluid, i.e., the properties that determine wave propagation speed.

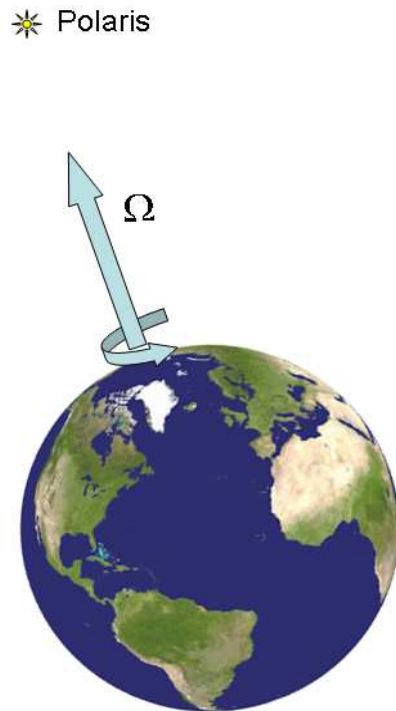


Figure 4: Earth's rotation vector, Ω , maintains a nearly steady direction that points close to the North Star, Polaris. This very simple image is meant to convey a very profound physical fact: Ω defines a specific direction with respect to the universe for Earth-bound observers. That this direction is toward Polaris is accidental. But that there is a specific direction is reflected in the anisotropy of many large-scale circulation phenomena, e.g., the east-west asymmetry of the ocean gyres (Fig. 2) and the westward propagation of Rossby waves and oceanic eddies (Figs. 1 and 3, and discussed further in Section 7.3).

vector, $\mathbf{g}M$ is the time-independent inertial force, gravitational mass attraction plus the centrifugal force associated with Earth's rotation called 'gravity' and discussed further in Section 4.1. Our main interest is the term, $-2\boldsymbol{\Omega} \times \mathbf{V}'M$, commonly called the Coriolis force in geophysics. The Coriolis force has a very simple mathematical form; it is always perpendicular to the parcel velocity and will thus act to deflect the velocity unless it is balanced by another force, e.g., very often a pressure gradient as noted in the opening paragraph and Fig. 1.

1.2 The goal and the plan of this essay

Eqn. (2) applied to geophysical flows is not controversial. If our intentions were strictly practical we could accept the Coriolis force as given, as we do a few fundamental concepts of classical mechanics, e.g., mass and gravitational mass attraction, and move on to applications. However, the Coriolis force is not a fundamental concept of that kind and yet for many students (and more) it has a similar, mysterious quality. The plan and the goal of Part I of this essay is to take a rather slow and careful journey from Eqn. (1) to (2) so that at the end we should understand and so be able to explain:⁶

⁶'Explanation is indeed a virtue; but still, less a virtue than an anthropocentric pleasure.' B. van Frassen, 'The pragmatics of explanation', in *The Philosophy of Science*, Ed. by R. Boyd, P. Gasper and J. D. Trout. (The MIT Press, Cambridge Ma,

Q1) The origin of the term $-2\Omega \times \mathbf{V}'M$, and in what respect it is appropriate to call it the Coriolis 'force'. We have already hinted that the Coriolis term is a kind of inertial force (reviewed in Section 2.1) that arises from the rotation of a reference frame. The origin of the Coriolis force is thus mainly a matter of kinematics, i.e., more mathematical than physical, and we begin in Section 2.2 with the transformation of the inertial frame equation of motion Eqn. (1) into a rotating reference frame and Eqn. (2). The best choice of a word or words to label the Coriolis term is less clear than is Eqn. (2) itself; we will stick with just plain 'Coriolis force' on the basis of what the Coriolis term does, considered in Sections 3 - 6, and summarized on closing in Section 7.

Q2) The global conservation and Galilean transformation properties of Eqn. (2) and absence of the centrifugal force. Two simple applications of the rotating frame equation of motion are considered in Section 3. These illustrate the often marked difference between inertial and rotating frame descriptions of the same motion, and they also show that the rotating frame equation of motion does *not* retain these fundamental properties. Eqn. (2) applies on a rotating Earth or a planet, where the centrifugal force associated with planetary rotation is exactly canceled (Section 4). The rotating frame equation of motion thus treats only the comparatively small relative velocity, i.e., winds and currents. This is a great advantage compared with the inertial frame equation of motion and more than compensates for the (admittedly) peculiar properties of the Coriolis force.

Q3) The new modes of motion in Eqn. (2) compared with Eqn. (1). Eqn. (2) admits two modes of motion dependent upon the Coriolis force; a free oscillation, often called an inertial oscillation, and forced, steady motion, called a geostrophic wind or current when the force \mathbf{F}' is a pressure gradient.⁷

Part II considers some of the consequences of Earth's rotation in the context of a simple, single layer fluid model, and the phenomenon of geostrophic adjustment: a ridge or an eddy of dense fluid is released from rest and allowed to evolve freely. The aims are to understand:

Q4) The circumstances that lead to a near geostrophic balance. As we will see in Section 7, a geostrophic balance is almost inevitable for large scale, low frequency motions of the atmosphere or ocean. The key thing in this is to define what we mean by large scale (depends upon stratification and f) and low frequency (low compared to f).

Q5) How small but systematic departures from geostrophic balance may lead to time-dependent, low frequency motions, and east-west asymmetry. Given an eddy or long wave that is in approximate geostrophic balance, the variation of the Coriolis force with latitude, often called the beta-effect, leads

1999).

⁷By now you may be thinking that all this talk of 'forces, forces, forces' is tedious and archaic. Modern dynamics is more likely to be developed around the concepts of energy, action and minimization principles, which are very useful in some special classes of fluid flow. However, it remains that the majority of fluid mechanics proceeds along the path of Eqn. (1) laid down by Newton. In part this is because mechanical energy is not conserved in most real fluid flows and in part because the interaction between a fluid parcel and its surroundings is often at issue, friction for example, and is usually best-described in terms of forces.

to some of the most interesting and important phenomenon of geophysical flows — westward propagation of long waves in the jet stream (Fig. 1) and of mesoscale eddies in the ocean (Fig. 3).

1.3 About this essay

This essay been written especially for students who are beginning a quantitative study of Earth science and geophysical fluid dynamics and who have some preparation in classical mechanics and applied mathematics. Rotating reference frames and the Coriolis force are a topic in most classical mechanics texts and in most fluid mechanics textbooks that treat geophysical flows.⁸ There is nothing fundamental and new added here, but the hope is that this essay will make a useful supplement to these and other sources⁹ by providing greater mathematical detail and physical background (in Part I) than is possible in most fluid dynamics texts, while emphasizing geophysical phenomena (in Part II) that are missed or outright misconstrued in many physics texts.¹⁰ Geophysical fluid dynamics is all about fluids in motion, and the electronic version of this essay is able to display animations that provide a much more vivid depiction of fluid motion than is possible in a hardcopy.

There is a fairly marked change in level of detail and in scope in going from Part I to Part II. Part I derives the rotating frame equation of motion (Eqn. 2) in sufficient depth and detail to serve as a primary reference on that fairly narrow topic. Part II, Section 6 introduces but does not derive a shallow water fluid model that is then applied to several problems in geostrophic adjustment in Section 7. Part II is best viewed as a supplement to the excellent, comprehensive GFD texts by Gill, Cushman-Roisin, and Pedlosky.⁸ The scope changes from a narrow focus on the Coriolis force in Part I to a description and analysis of the somewhat diverse phenomena that arise in the geostrophic adjustment experiments of Part II. Inertio-gravity waves and Rossby waves play a very large role and so become the apparent center

⁸Classical mechanics texts in order of increasing level: A. P. French, *Newtonian Mechanics* (W. W. Norton Co., 1971); A. L. Fetter and J. D. Walecka, *Theoretical Mechanics of Particles and Continua* (McGraw-Hill, NY, 1990); C. Lanczos, *The Variational Principles of Mechanics* (Dover Pub., NY, 1949). A clear treatment by variational methods is by L. D. Landau and E. M. Lifshitz *Mechanics*, (Pergamon, Oxford, 1960). Textbooks on geophysical fluid dynamics emphasize mainly the consequences of Earth's rotation; excellent introductions at about the level of this essay are by J. R. Holton, *An Introduction to Dynamic Meteorology*, 3rd Ed. (Academic Press, San Diego, 1992), and by B. Cushman-Roisin, *Introduction to Geophysical Fluid Dynamics* (Prentice Hall, Engelwood Cliffs, New Jersey, 1994). Somewhat more advanced and highly recommended for the topic of geostrophic adjustment is A. E. Gill, *Atmosphere-Ocean Dynamics* (Academic Press, NY, 1982) and for waves generally, J. Pedlosky, *Waves in the Ocean and Atmosphere*, (Springer, 2003).

⁹There are several essays or articles that, like this one, aim to clarify the Coriolis force. A fine treatment in great depth is by H. M. Stommel and D. W. Moore, *An Introduction to the Coriolis Force* (Columbia Univ. Press, 1989); the present Section 4.1 owes a great deal to their work. A detailed analysis of particle motion including the still unresolved matter of the apparent southerly deflection of dropped particles is by M. S. Tiersten and H. Soodak, 'Dropped objects and other motions relative to a noninertial earth', *Am. J. Phys.*, **68**(2), 129–142 (2000). A good web page for general science students is <http://www.ems.psu.edu/%7Efraser/Bad/BadFAQ/BadCoriolisFAQ.html>

¹⁰The Coriolis force also has engineering applications; it is exploited to measure the angular velocity required for vehicle control systems, <http://www.siliconsensing.com>, and to measure mass transport in fluid flow, <http://www.micromotion.com>.

of attention. An implicit goal of Part II is to introduce and motivate the practice of experimentation via numerical modeling. Numerical models are an indispensable tool of atmospheric and oceanic science, and yet numerical modeling receives scant attention in some graduate curriculum. Many of the homework assignments are aimed at encouraging exploration and hypothesis testing by way of numerical experimentation. The model source codes listed in Section 9 are intended to facilitate this.

This document may be freely copied and distributed for all educational purposes. It may be cited via the MIT Open Course Ware address: James F Price, 12.808 Supplemental Material, Topics in Fluid Dynamics: Dimensional Analysis, the Coriolis Force, and Lagrangian and Eulerian Representations, <http://ocw.mit.edu/ans7870/resources/price/index.htm> (date accessed) License: Creative commons BY-NC-SA. The most recent version of this text and the source codes are on the author's public-access web page linked in Section 9. Comments and questions may be addressed directly to jprice@whoi.edu.

Acknowledgments. Financial support during preparation of this essay was provided by the Academic Programs Office of the Woods Hole Oceanographic Institution. Additional salary support has been provided by the U.S. Office of Naval Research. Terry McKee of WHOI is thanked for her expert assistance with Aviso data. Tom Farrar of WHOI, Pedro de la Torre of KAUST and Ru Chen of MIT/WHOI are thanked for carefully proof reading a draft of this essay.

2 Part I: Rotating reference frames and the Coriolis force.

The first step toward understanding the origin of the Coriolis force is to describe the origin of inertial forces in the simplest possible context, a pair of reference frames that are represented by displaced coordinate axes, Fig. (5). Frame one is labeled X and Z and frame two is labeled X' and Z' . Only relative motion is significant, but there is no harm in assuming that frame one is stationary and that frame two is displaced by a time-dependent vector, $\mathbf{X}_o(t)$. The measurements of position, velocity, etc. of a given parcel will thus be different in frame two vs. frame one. Just how the measurements differ is a matter of kinematics; there is no physics involved until we define the acceleration of frame two and use the accelerations to write an equation of motion, e.g., Eqn. (2).

2.1 Kinematics of a linearly accelerating reference frame

If the position vector of a given parcel is \mathbf{X} when observed from frame one, then from within frame two the same parcel will be observed at the position

$$\mathbf{X}' = \mathbf{X} - \mathbf{X}_o.$$

The position vector of a parcel thus depends upon the reference frame. Suppose that frame two is translated and possibly accelerated with respect to frame one, while maintaining a constant orientation

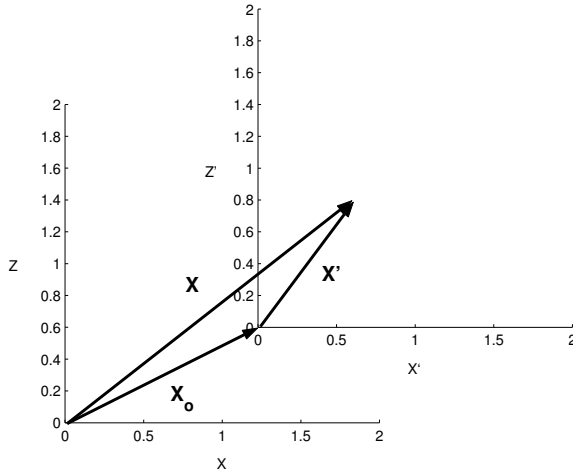


Figure 5: Two reference frames are represented by coordinate axes that are displaced by the vector \mathbf{X}_o that is time-dependent. In this Section 2.1 we consider only a relative translation, so that frame two maintains a fixed orientation with respect to frame one. The rotation of frame two will be considered beginning in Section 2.2.

(rotation will be considered shortly). If the velocity of a parcel observed in frame one is $d\mathbf{X}/dt$, then in frame two the same parcel will be observed to have velocity

$$\frac{d\mathbf{X}'}{dt} = \frac{d\mathbf{X}}{dt} - \frac{d\mathbf{X}_o}{dt}.$$

The accelerations are similarly $d^2\mathbf{X}/dt^2$ and

$$\frac{d^2\mathbf{X}'}{dt^2} = \frac{d^2\mathbf{X}}{dt^2} - \frac{d^2\mathbf{X}_o}{dt^2}. \quad (3)$$

We are going to assume that frame one is an inertial reference frame, i.e., that parcels observed in frame one have the property of inertia so that their momentum changes only in response to a force, \mathbf{F} , i.e., Eqn. (1). From Eqn. (1) and from Eqn. (3) we can easily write down the equation of motion for the parcel as it would be observed from frame two:

$$\frac{d^2\mathbf{X}'}{dt^2}M = -\frac{d^2\mathbf{X}_o}{dt^2}M + \mathbf{F}' + \mathbf{g}_*M. \quad (4)$$

Terms of the sort $-(d^2\mathbf{X}_o/dt^2)M$ appearing in the frame two equation of motion (4) will be called 'inertial forces', and when these terms are nonzero, frame two is said to be 'noninertial'. As an example, suppose that frame two is subject to a constant acceleration, $d^2\mathbf{X}_o/dt^2 = \mathbf{A}$ that is upward and to the right in Fig. (5). From Eqn. (4) it is evident that all parcels observed from within frame two would then appear to be subject to an inertial force, $-\mathbf{A}M$, directed downward and to the left, and which is exactly opposite the acceleration of frame two with respect to frame one. An inertial force results when we multiply this acceleration by the mass of the parcel, and so an inertial force is exactly proportional to the mass of the parcel, regardless of what the mass is. Clearly, it is the acceleration, $-\mathbf{A}$, that is imposed by the accelerating reference frame, and not a force *per se*. In this regard, inertial forces are indistinguishable from gravitational mass attraction. If in addition the inertial force is

dependent only upon position (centrifugal force due to Earth's rotation is an example, Section 4.1), as is gravitational mass attraction, then it might as well be added with \mathbf{g}_* to denote a single, time-independent acceleration field, usually termed gravity and denoted by \mathbf{g} . Indeed, it is only this gravity field, \mathbf{g} , that can be observed directly, for example by pendulum experiments (more in Section 4.1). But unlike gravitational mass attraction, there is no physical interaction between particles involved in an inertial force, and hence there is no action-reaction force pair. Global momentum conservation thus does not obtain in the presence of inertial forces. There is indeed something equivocal about this phenomenon we are calling an inertial force, and it is not unwarranted that some authors have deemed these terms 'virtual' or 'fictitious correction' forces.¹¹

Whether an inertial force is problematic or not depends entirely upon whether $d^2\mathbf{X}_o/dt^2$ is known or not. If it should happen that the acceleration of frame two is not known, then all bets are off. For example, imagine observing the motion of a pendulum within an enclosed trailer that was moving along in irregular, stop-and-go traffic. The pendulum would be observed to lurch forward and backward unexpectedly, and we would soon conclude that dynamics in such an uncontrolled, noninertial reference frame was going to be a very difficult endeavor. We could at least infer that an inertial force was to blame if it was observed that all of the physical objects in the trailer, observers included, experienced exactly the same unaccounted acceleration. Very often we do know the relevant inertial forces well enough to use noninertial reference frames with great precision, e.g., Earth's gravity field is well-known from extensive and ongoing survey and the Coriolis force can be readily calculated.

In the specific example of reference frame translation considered here we could just as well transform the observations made from frame two back into the inertial frame one, use the inertial frame equation of motion to make a calculation, and then transform back to frame two if required. By that tactic we could avoid altogether the seeming delusion of an inertial force. However, when it comes to the observation and analysis of Earth's atmosphere and ocean, there is really no choice but to use an Earth-attached and thus rotating and noninertial reference (discussed in Section 4.3). That being so, we have to contend with the Coriolis force, an inertial force that arises from the rotation of an Earth-attached frame. The kinematics of rotation add a small complication that is taken up in the next section. But if you followed the development of Eqn. (4), then you already understand the essential origin of the Coriolis force.

¹¹The latter is by J. D. Marion, *Classical Mechanics of Particles and Systems* (Academic Press, NY, 1965), who describes the plight of a rotating observer as follows (the double quotes are his): '... the observer must postulate an additional force - the centrifugal force. But the "requirement" is an artificial one; it arises solely from an attempt to extend the form of Newton's equations to a non inertial system and this may be done only by introducing a fictitious "correction force". The same comments apply for the Coriolis force; this "force" arises when attempt is made to describe motion relative to the rotating body.' Rotating observers do indeed have to contend with inertial forces that are not found in otherwise comparable inertial frames, but these inertial forces are not *ad hoc* corrections as Marion's quote (taken out of context) might seem to imply.

2.2 Kinematics of a rotating reference frame

The second step toward understanding the origin of the Coriolis force is to learn the equivalent of Eqn. (4) for the case of a steadily rotating (rather than linearly accelerating) reference frame. From here on it is necessary to develop the component-wise description of vectors alongside the geometric form used to now.

Reference frame one will again be assumed to be stationary and defined by a triad of orthogonal unit vectors, \mathbf{e}_1 , \mathbf{e}_2 and \mathbf{e}_3 (Fig. 6). A parcel P can then be located by a position vector \mathbf{X}

$$\mathbf{X} = \mathbf{e}_1 x_1 + \mathbf{e}_2 x_2 + \mathbf{e}_3 x_3, \quad (5)$$

where the Cartesian (rectangular) components, x_i , are the projection of \mathbf{X} onto each of the unit vectors in turn. It is useful to rewrite Eqn. (5) using matrix notation. The unit vectors are made the elements of a row matrix,

$$\mathbb{E} = [\mathbf{e}_1 \ \mathbf{e}_2 \ \mathbf{e}_3], \quad (6)$$

and the components x_i are taken to be the elements of a column matrix,

$$\mathbb{X} = \begin{bmatrix} x_1 \\ x_2 \\ x_3 \end{bmatrix}. \quad (7)$$

Eqn. (5) may then be written in a way that conforms with the usual matrix multiplication rules as

$$\mathbf{X} = \mathbb{E}\mathbb{X}. \quad (8)$$

The vector \mathbf{X} and its time derivatives are presumed to have an objective existence, i.e., they represent something physical that is unaffected by our arbitrary choice of a reference frame. Nevertheless, the way these vectors appear clearly does depend upon the reference frame (Fig. 6) and for our purpose it is essential to know how the position, velocity and acceleration vectors will appear when they are observed from a steadily rotating reference frame. In a later part of this section we will identify the rotating reference frame as an Earth-attached reference frame and the stationary frame as one aligned on the distant fixed stars. It is assumed that the motion of the rotating frame can be represented by a time-independent rotation vector, Ω . The \mathbf{e}_3 unit vector can be aligned with Ω with no loss of generality, Fig. (6a). We can go a step further and align the origins of the stationary and rotating reference frames because the Coriolis force is independent of position (Section 2.2).

2.2.1 Transforming the position, velocity and acceleration vectors

Position: Back to the question at hand: how does this position vector look when viewed from a second reference frame that is rotated through an angle θ with respect to the first frame? The answer is

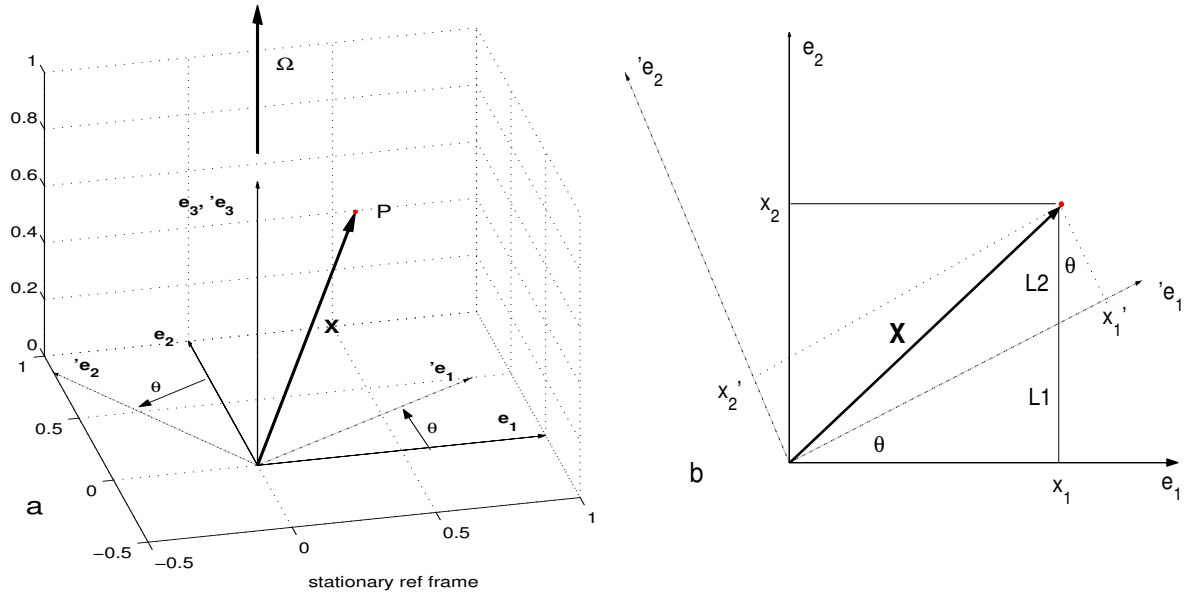


Figure 6: (a) A parcel P is located by the tip of a position vector, \mathbf{X} . The stationary reference frame has solid unit vectors that are presumed to be time-independent, and a second, rotated reference frame has dashed unit vectors that are labeled \mathbf{e}'_i . The reference frames have a common origin, and rotation is about the \mathbf{e}_3 axis. The unit vector \mathbf{e}_3 is thus unchanged by this rotation and so $\mathbf{e}'_3 = \mathbf{e}_3$. This holds also for $\Omega' = \Omega$, and so we will use Ω exclusively. The angle θ is counted positive when the rotation is counterclockwise. (b) The components of \mathbf{X} in the stationary reference frame are x_1, x_2, x_3 , and in the rotated reference frame they are x'_1, x'_2, x'_3 .

that the vector 'looks' like the components appropriate to the rotated reference frame, and so we need to find the projection of \mathbf{X} onto the unit vectors that define the rotated frame. The details are shown in Fig. (6b); notice that $x_2 = L1 + L2$, $L1 = x_1 \tan \theta$, and $x'_2 = L2 \cos \theta$. From this it follows that $x'_2 = (x_2 - x_1 \tan \theta) \cos \theta = -x_1 \sin \theta + x_2 \cos \theta$. By a similar calculation we can find that $x'_1 = x_1 \cos(\theta) + x_2 \sin(\theta)$. The component x'_3 that is aligned with the axis of the rotation vector is unchanged, $x'_3 = x_3$, and so the set of equations for the primed components may be written as a column vector

$$\mathbb{X}' = \begin{bmatrix} x'_1 \\ x'_2 \\ x'_3 \end{bmatrix} = \begin{bmatrix} x_1 \cos \theta + x_2 \sin \theta \\ -x_1 \sin \theta + x_2 \cos \theta \\ x_3 \end{bmatrix}. \quad (9)$$

By inspection this can be factored into the product

$$\mathbb{X}' = \mathbb{R} \mathbb{X}, \quad (10)$$

where \mathbb{X} is the matrix of stationary frame components and \mathbb{R} is the rotation matrix,

$$\mathbb{R}(\theta) = \begin{bmatrix} \cos \theta & \sin \theta & 0 \\ -\sin \theta & \cos \theta & 0 \\ 0 & 0 & 1 \end{bmatrix}. \quad (11)$$

This θ is the angle displaced by the rotated reference frame and is positive counterclockwise. The position vector observed from the rotated frame will be denoted by \mathbf{X}' ; to construct \mathbf{X}' we sum the rotated components, \mathbb{X}' , times a set of unit vectors that are fixed and thus

$$\boxed{\mathbf{X}' = \mathbf{e}_1 x'_1 + \mathbf{e}_2 x'_2 + \mathbf{e}_3 x'_3 = \mathbb{E} \mathbb{X}'} \quad (12)$$

For example, the position vector \mathbf{X} of Fig. (6) is at an angle of about 45° counterclockwise from the \mathbf{e}_1 unit vector and the rotated frame is at $\theta = 30^\circ$ counterclockwise from the stationary frame one. That being so, the position vector viewed from the rotated reference frame, \mathbf{X}' , makes an angle of $45^\circ - 30^\circ = 15^\circ$ with respect to the \mathbf{e}_1 (fixed) unit vector seen within the rotated frame, Fig. (7). As a kind of verbal shorthand we might say that the position vector has been 'transformed' into the rotated frame by Eqs. (9) and (12). But since the vector has an objective existence, what we really mean is that the components of the position vector are transformed by Eqn. (9) and then summed with fixed unit vectors to yield what should be regarded as a new vector, \mathbf{X}' , the position vector that we observe from the rotated (or rotating) reference frame.¹²

Velocity: The velocity of parcel P seen in the stationary frame is just the time rate of change of the position vector seen in that frame,

$$\frac{d\mathbf{X}}{dt} = \frac{d}{dt} \mathbb{E} \mathbb{X} = \mathbb{E} \frac{d\mathbb{X}}{dt},$$

since \mathbb{E} is time-independent. The velocity of parcel P as seen from the rotating reference frame is similarly

$$\frac{d\mathbf{X}'}{dt} = \frac{d}{dt} \mathbb{E} \mathbb{X}' = \mathbb{E} \frac{d\mathbb{X}'}{dt},$$

which indicates that the time derivatives of the rotated components are going to be very important in what follows. For the first derivative we find

$$\frac{d\mathbf{X}'}{dt} = \frac{d(\mathbb{R}\mathbb{X})}{dt} = \frac{d\mathbb{R}}{dt} \mathbb{X} + \mathbb{R} \frac{d\mathbb{X}}{dt}. \quad (13)$$

¹²If the somewhat formal-looking Eqs. (9) through (12) do not have an immediate and concrete meaning for you, then the remainder of this important section will probably be a loss. Some questions/assignments to help you along: 1) Verify Eqs. (9) and (12) by some direct experimentation, i.e., try them and see. 2) Show that the transformation of the vector components given by Eqs. (10) and (11) leaves the magnitude of the vector unchanged, i.e., $|\mathbf{X}'| = |\mathbf{X}|$. 3) Verify that $\mathbb{R}(\theta_1)\mathbb{R}(\theta_2) = \mathbb{R}(\theta_1 + \theta_2)$ and that $\mathbb{R}(\theta)^{-1} = \mathbb{R}(-\theta)$, where \mathbb{R}^{-1} is the inverse (and also the transpose) of the rotation matrix. 4) Show that the unit vectors that define the rotated frame can be related to the unit vectors of the stationary frame by $\mathbb{E} = \mathbb{E}\mathbb{R}^{-1}$ and hence the unit vectors observed from the stationary frame turn the opposite direction of the position vector observed from the rotating frame (and thus the reversed prime). The components of an ordinary vector (a position vector or velocity vector) are thus said to be *contravariant*, meaning that they rotate in a sense that is opposite the rotation of the coordinate system. What, then, can you make of $\mathbb{E}\mathbf{X}' = \mathbb{E}\mathbb{R}^{-1}\mathbb{R}\mathbf{X}$? A concise and clear reference on matrix representations of coordinate transformations is by J. Pettofrezzo *Matrices and Transformations* (Dover Pub., New York, 1966). An excellent all-around reference for undergraduate-level applied mathematics including coordinate transformations is by M. L. Boas, *Mathematical Methods in the Physical Sciences, 2nd edition* (John Wiley and Sons, 1983).

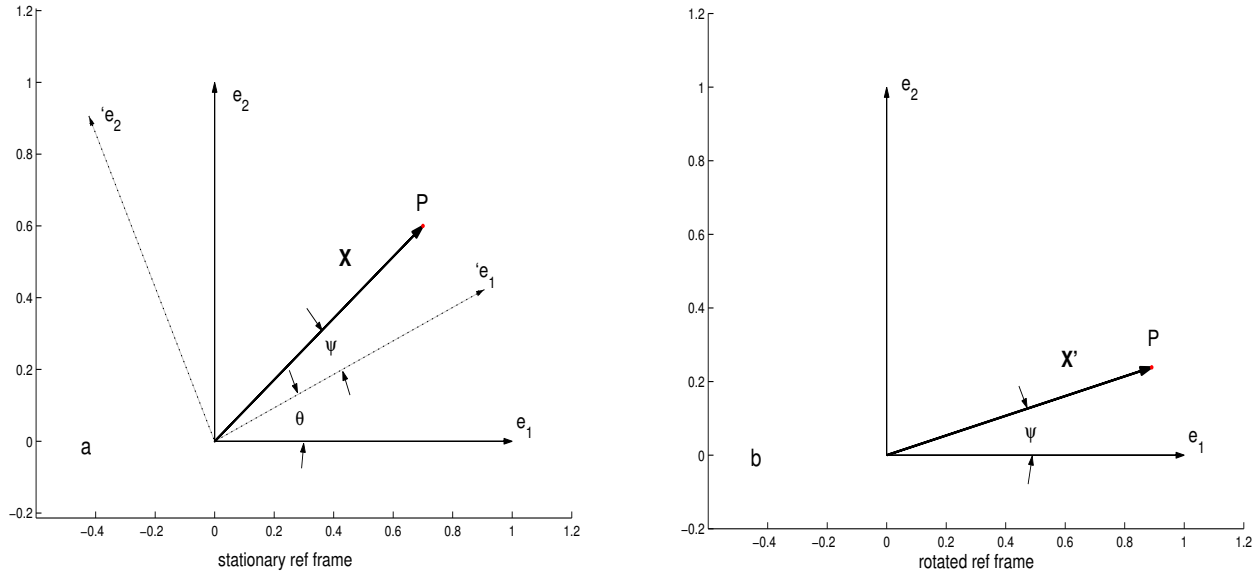


Figure 7: (a) The position vector \mathbf{X} seen from the stationary reference frame. (b) The position vector as seen from the rotated frame, denoted by \mathbf{X}' . Note that in the rotated reference frame the unit vectors are labeled e_i since they are fixed; when these unit vectors are seen from the stationary frame, as on the left, they are labeled \hat{e}_i . If the position vector is stationary in the stationary frame, then $\theta + \psi = \text{constant}$. The angle ψ then changes as $d\psi/dt = -d\theta/dt = -\Omega$, and thus the vector \mathbf{X}' appears to rotate at the same rate but in the opposite sense as does the rotating reference frame.

The second term on the right side of Eqn. (13) represents velocity components from the stationary frame that have been transformed into the rotating frame, as in Eqn. (10). If the rotation angle θ was constant so that \mathbb{R} was independent of time, then the first term on the right side would vanish and the velocity components would transform exactly as do the components of the position vector. In that case there would be no Coriolis force.

When the rotation angle is time-varying, as it will be here, the first term on the right side of Eqn. (13) is non-zero and represents a velocity component that is induced solely by the rotation of the reference frame. With Earth-attached reference frames in mind, we are going to take the angle θ to be

$$\theta = \theta_0 + \Omega t,$$

where Ω is Earth's rotation rate, a constant defined below (and θ_0 is unimportant). Though Ω is constant, the associated reference frame is nevertheless accelerating and is noninertial in the same way that circular motion at a steady speed is accelerating because the direction of the velocity vector is continually changing. Given this $\theta(t)$, the time-derivative of the rotation matrix is

$$\frac{d\mathbb{R}}{dt} = \Omega \begin{bmatrix} -\sin \theta(t) & \cos \theta(t) & 0 \\ -\cos \theta(t) & -\sin \theta(t) & 0 \\ 0 & 0 & 0 \end{bmatrix}, \tag{14}$$

which, notice, this has all the elements of \mathbb{R} , but shuffled around. By inspection, this matrix can be factored into the product of a matrix \mathbb{C} and \mathbb{R} as

$$\frac{d\mathbb{R}}{dt} = \Omega \mathbb{C}\mathbb{R}(\theta(t)), \quad (15)$$

where the matrix \mathbb{C} is

$$\mathbb{C} = \begin{bmatrix} 0 & 1 & 0 \\ -1 & 0 & 0 \\ 0 & 0 & 0 \end{bmatrix} = \begin{bmatrix} 1 & 0 & 0 \\ 0 & 1 & 0 \\ 0 & 0 & 0 \end{bmatrix} \mathbb{R}(\pi/2). \quad (16)$$

Multiplication by \mathbb{C} acts to knock out the component $(\)_3$ that is parallel to Ω and causes a rotation of $\pi/2$ in the plane perpendicular to Ω . Substitution into Eqn. (13) gives the velocity components appropriate to the rotating frame

$$\frac{d(\mathbb{R}\mathbf{X})}{dt} = \Omega \mathbb{C}\mathbb{R}\mathbf{X} + \mathbb{R} \frac{d\mathbf{X}}{dt}, \quad (17)$$

or using the prime notation $(\)'$ to indicate multiplication by \mathbb{R} , then

$$\boxed{\frac{d\mathbf{X}'}{dt} = \Omega \mathbb{C}\mathbf{X}' + \left(\frac{d\mathbf{X}}{dt}\right)'} \quad (18)$$

The second term on the right side of Eqn. (18) is just the rotated velocity components and is present even if Ω vanished (a rotated but not a rotating reference frame). The first term on the right side represents a velocity that is induced by the rotation rate of the rotating frame; this induced velocity is proportional to Ω and makes an angle of $\pi/2$ radians to the right of the position vector in the rotating frame (assuming that $\Omega > 0$).

To calculate the vector form of this term we can assume that the parcel P is stationary in the stationary reference frame so that $d\mathbf{X}/dt = 0$. Viewed from the rotating frame, the parcel will appear to move clockwise at a rate that can be calculated from the geometry (Fig. 8). Let the rotation in a time interval δt be given by $\delta\psi = -\Omega\delta t$; in that time interval the tip of the vector will move a distance $|\delta\mathbf{X}'| = |\mathbf{X}'|\sin(\delta\psi) \approx |\mathbf{X}'|\delta\psi$, assuming the small angle approximation for $\sin(\delta\psi)$. The parcel will move in a direction that is perpendicular (instantaneously) to \mathbf{X}' . The velocity of parcel P as seen from the rotating frame and due solely to the coordinate system rotation is thus $\lim_{\delta t \rightarrow 0} \frac{\delta\mathbf{X}'}{\delta t} = -\Omega \times \mathbf{X}'$, the vector cross-product equivalent of $\Omega\mathbb{C}\mathbf{X}'$ (Fig. 9). The vector equivalent of Eqn. (18) is then

$$\boxed{\frac{d\mathbf{X}'}{dt} = -\Omega \times \mathbf{X}' + \left(\frac{d\mathbf{X}}{dt}\right)'} \quad (19)$$

The relation between time derivatives given by Eqn. (19) is general; it applies to all vectors, e.g., velocity vectors, and moreover, it applies for vectors defined at all points in space. Hence the relationship between the time derivatives may be written as an operator equation,

$$\boxed{\frac{d(\)'}{dt} = -\Omega \times (\)' + \left(\frac{d(\)}{dt}\right)'} \quad (20)$$

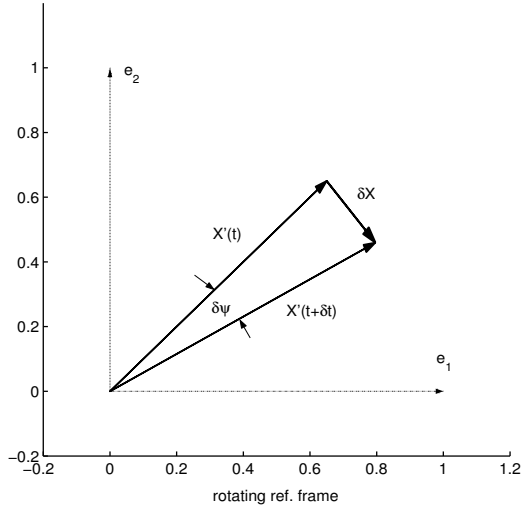


Figure 8: The position vector \mathbf{X}' seen from the rotating reference frame. The unit vectors that define this frame, \hat{e}_i , appear to be stationary when viewed from within this frame, and hence we label them with e_i (not primed). Assume that $\Omega > 0$ so that the rotating frame is turning counterclockwise with respect to the stationary frame, and assume that the parcel P is stationary in the stationary reference frame so that $d\mathbf{X}/dt = 0$. Parcel P as viewed from the rotating frame will then appear to move clockwise at a rate that can be calculated from the geometry.

that is valid for all vectors.¹³ From left to right the terms are: 1) the time rate of change of a vector as seen in the rotating reference frame, 2) the cross-product of the rotation vector with the vector and 3) the time rate change of the vector as seen in the stationary frame and then rotated into the rotating frame. One way to describe Eqn. (20) is that the time rate of change and prime operators do not commute, the difference being the cross-product term which, notice, represents a time rate change in the *direction* of the vector, but not the magnitude. Term 1) is the time rate of change that we observe directly or that we seek to solve when we are working from the rotating frame.

Acceleration: Our goal is to relate the accelerations seen in the two frames and so we differentiate Eqn. (18) once more and after rearrangement of the kind used above find that the components satisfy

$$\boxed{\frac{d^2\mathbf{X}'}{dt^2} = 2\Omega\mathbb{C}\frac{d\mathbf{X}'}{dt} + \Omega^2\mathbb{C}^2\mathbf{X}' + \left(\frac{d^2\mathbf{X}}{dt^2}\right)'} \quad (21)$$

The middle term on the right includes multiplication by the matrix $\mathbb{C}^2 = \mathbb{C}\mathbb{C}$,

$$\mathbb{C}^2 = \begin{bmatrix} 1 & 0 & 0 \\ 0 & 1 & 0 \\ 0 & 0 & 0 \end{bmatrix} \mathbb{R}(\pi/2) \begin{bmatrix} 1 & 0 & 0 \\ 0 & 1 & 0 \\ 0 & 0 & 0 \end{bmatrix} \mathbb{R}(\pi/2) = \begin{bmatrix} 1 & 0 & 0 \\ 0 & 1 & 0 \\ 0 & 0 & 0 \end{bmatrix} \mathbb{R}(\pi) = - \begin{bmatrix} 1 & 0 & 0 \\ 0 & 1 & 0 \\ 0 & 0 & 0 \end{bmatrix},$$

that knocks out the component corresponding to the rotation vector Ω and reverses the other two components; the vector equivalent of $\Omega^2\mathbb{C}^2\mathbf{X}'$ is thus $-\Omega \times \Omega \times \mathbf{X}'$ (Fig. 9). The vector equivalent of

¹³Imagine arrows taped to a turntable with random orientations. Once the turntable is set into (solid body) rotation, all of the arrows will necessarily rotate at the same rotation rate regardless of their position or orientation. The rotation will, of course, cause a translation of the arrows that depends upon their location, but the rotation rate is necessarily uniform, and this holds regardless of the physical quantity that the vector represents. This is of some importance for our application to a rotating Earth, since Earth's motion includes a rotation about the polar axis, as well as an orbital motion around the Sun and yet we represent Earth's rotation by a single vector.

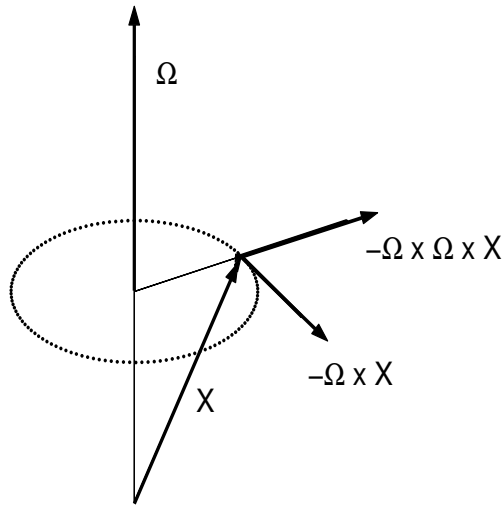


Figure 9: A schematic showing the relationship of a vector \mathbf{X} , and various cross-products with a second vector Ω (note the signs). The vector \mathbf{X} is shown with its tail perched on the axis of the vector Ω as if it were a position vector. This helps us to visualize the direction of the cross-products, but it is important to note that the relationship among the vectors and vector products shown here holds for all vectors, regardless of where they are defined in space or the physical quantity, e.g., position or velocity, that they represent.

Eqn. (21) is then¹⁴

$$\boxed{\frac{d^2 \mathbf{X}'}{dt^2} = -2\Omega \times \frac{d\mathbf{X}'}{dt} - \Omega \times \Omega \times \mathbf{X}' + \left(\frac{d^2 \mathbf{X}}{dt^2}\right)'} \quad (22)$$

Note the similarity with Eqn. (3). From left to right the terms of this equation are 1) the acceleration as seen in the rotating frame, 2) the Coriolis term, 3) the centrifugal¹⁵ term, and 4) the acceleration as seen in the stationary frame and then rotated into the rotating frame. As before, term 1) is the acceleration that we directly observe or analyze when we are working from the rotating reference frame.

2.2.2 Stationary \Rightarrow Inertial; Rotating \Rightarrow Earth-Attached

The third and final step in this derivation of the Coriolis force is to specify what we mean by an inertial reference frame, and so define the rotation rate of frame two. To make frame one inertial we presume that the unit vectors \mathbf{e}_i could in principle be aligned on the distant, 'fixed stars'.¹⁶ The rotating frame

¹⁴The relationship between the stationary and rotating frame velocity vectors given by Eqs. (18) and (19) is clear visually and becomes intuitive given just a little experience. It is not so easy to intuit the corresponding relationship between the accelerations given by Eqs. (22) and (21). Hence, to understand the transformation of acceleration there is no choice but to understand the mathematical steps (to be able to reproduce, be able to explain) going from Eqn. (18) to Eqn. (21) and/or from Eqn. (19) to Eqn. (22).

¹⁵'Centrifugal' and 'centripetal' have Latin roots, *centri+fugere* and *centri+peter*, meaning center-fleeing and center-seeking, respectively. Taken literally they would indicate the sign of a radial force, for example. However, they are very often used to mean the specific term $\omega^2 r$, i.e., centrifugal force when it is on the right side of an equation of motion and centripetal acceleration when it is on the left side.

¹⁶'Fixed' is a matter of degree; certainly the Sun and the planets do not qualify, but even some nearby stars move detectably over the course of a year. The intent is that the most distant stars should serve as sign posts for the spatially-averaged mass

two is presumed to be attached to Earth, and the rotation rate Ω is then given by the rate at which the same fixed stars are observed to rotate overhead, one revolution per *sidereal* day (Latin for from the stars), 23 hrs, 56 min and 4.09 sec, or

$$\Omega = 7.2921 \times 10^{-5} \text{ rad s}^{-1}. \quad (23)$$

Earth's rotation rate is very nearly constant, and the axis of rotation maintains a nearly steady bearing on a point on the celestial sphere that is close to the North Star, Polaris (Fig. 4). The rotation vector thus provides a definite orientation of Earth within the universe, and the rotation rate has an absolute significance. For example, the rotation rate sensors noted in footnote 10 read out Earth's rotation rate with respect to the fixed stars as a kind of gage pressure, called 'Earth rate'.¹⁷

of the universe on the hypothesis that inertia arises whenever there is an acceleration (linear or rotational) with respect to the mass of the universe as a whole. This grand idea was expressed most forcefully by the Austrian philosopher and physicist Ernst Mach, and is often termed Mach's Principle (see, e.g., J. Schwinger, *Einstein's Legacy* Dover Publications, 1986; M. Born, *Einstein's Theory of Relativity*, Dover Publications, 1962). Mach's Principle seems to be in accord with all empirical data, including the magnitude of the Coriolis force. However, Mach's Principle is not, in and of itself, the fundamental mechanism of inertia. A new hypothesis takes the form of so-called vacuum stuff (or Higgs field) that is presumed to pervade all of space and so provide a local mechanism for resistance to accelerated motion (see P. Davies, 'On the meaning of Mach's principle', <http://www.padrak.com/ine/INERTIA.html>). The debate between Newton and Leibniz over the reality of absolute space, which had seemed to go in favor of relative space, Leibniz and Mach's Principle, has been renewed in the search for a physical origin of inertia.

Observations on the fixed stars are a very precise means to define rotation rate, but can not, in general, be used to define the linear translation or acceleration of a reference frame. The only way to know if a reference frame that is aligned on the fixed stars is inertial is to carry out mechanics experiments and test whether Eqn.(1) holds and global momentum is conserved. If yes, the frame is inertial.

¹⁷For our purpose we can presume that Ω is constant. In fact, there are small but observable variations of Earth's rotation rate due mainly to changes in the atmospheric and oceanic circulation and due to mass distribution within the cryosphere, see B. F. Chao and C. M. Cox, 'Detection of a large-scale mass redistribution in the terrestrial system since 1998,' *Science*, **297**, 831–833 (2002), and R. M. Ponte and D. Stammer, 'Role of ocean currents and bottom pressure variability on seasonal polar motion,' *J. Geophys. Res.*, **104**, 23393–23409 (1999). The direction of Ω with respect to the celestial sphere also varies detectably on time scales of tens of centuries on account of precession, so that Polaris has not always been the pole star (Fig. 4), even during historical times. The slow variation of Earth's orbital parameters (slow for our present purpose) are an important element of climate, see e.g., J. A. Rial, 'Pacemaking the ice ages by frequency modulation of Earth's orbital eccentricity,' *Science*, **285**, 564–568 (1999).

As well, Earth's motion within the solar system and galaxy is much more complex than a simple spin around the polar axis. Among other things, the Earth orbits the Sun in a counterclockwise direction with a rotation rate of $1.9910 \times 10^{-7} \text{ s}^{-1}$, which is about 0.3% of the rotation rate Ω . Does this orbital motion enter into the Coriolis force, or otherwise affect the dynamics of the atmosphere and oceans? The short answer is no and yes. We have already accounted for the rotation of the Earth with respect to the fixed stars. Whether this rotation is due to a spin about an axis centered on the Earth or due to a solid body rotation about a displaced center is not relevant for the Coriolis force *per se*, as noted in the discussion of Eqn. (20). However, since Earth's polar axis is tilted significantly from normal to the plane of the Earth's orbit around the Sun (the tilt implied by Fig. (4)), we can ascribe Earth's rotation Ω to spin alone. The orbital motion about the Sun combined with Earth's finite size gives rise to tidal forces, which are small but important spatial variations of the centrifugal/gravitational balance that holds for the Earth-Sun and for the Earth-Moon as a whole (described particularly well by French⁸). A question for you: What is the rotation rate of the Moon? Hint, make a sketch of the Earth-Moon orbital system and consider what we observe of the Moon from Earth. What would the Coriolis and centrifugal forces be on the Moon?

A sidereal day is only a few minutes less than a solar day, and so in a purely numerical sense, $\Omega \approx \Omega_{solar} = 2\pi/24$ hours, which is certainly easier to remember than is Eqn. (23). For the purpose of a rough estimate, the small numerical difference between Ω and Ω_{solar} is not significant. However, the difference between Ω and Ω_{solar} can be told in numerical simulations and in well-resolved field observations, and, if we accept Mach's Principle,¹⁶ the physical difference between Ω and Ω_{solar} is highly significant.

Assume that the inertial frame equation of motion is

$$\frac{d^2\mathbb{X}}{dt^2}M = \mathbb{F} + \mathbb{G}_*M \quad \text{and} \quad \frac{d^2\mathbf{X}}{dt^2}M = \mathbf{F} + \mathbf{g}_*M \quad (24)$$

(\mathbb{G}_* is the component matrix of \mathbf{g}_*). The acceleration and force can always be viewed from another reference frame that is rotated (but not rotating) with respect to the first frame,

$$\left(\frac{d^2\mathbb{X}}{dt^2}\right)'M = \mathbb{F}' + \mathbb{G}'_*M \quad \text{and} \quad \left(\frac{d^2\mathbf{X}}{dt^2}\right)'M = \mathbf{F}' + \mathbf{g}'_*M, \quad (25)$$

as if we had chosen a different set of fixed stars or multiplied both sides of Eqn. (22) by the same rotation matrix. This equation of motion preserves the global conservation and Galilean transformation properties of Eqn. (24). To find the rotating frame equation of motion, we use Eqs. (21) and (22) to eliminate the rotated acceleration from Eqn. (25) and then solve for the acceleration seen in the rotating frame: the components are

$$\boxed{\frac{d^2\mathbb{X}'}{dt^2}M = 2\Omega\mathbb{C}\frac{d\mathbb{X}'}{dt}M - \Omega^2\mathbb{C}^2\mathbb{X}'M + \mathbb{F}' + \mathbb{G}'_*M} \quad (26)$$

and the vector equivalent is

$$\boxed{\frac{d^2\mathbf{X}'}{dt^2}M = -2\boldsymbol{\Omega} \times \frac{d\mathbf{X}'}{dt}M - \boldsymbol{\Omega} \times \boldsymbol{\Omega} \times \mathbf{X}'M + \mathbf{F}' + \mathbf{g}'_*M} \quad (27)$$

Eqn. (27) has the form of Eqn. (4), the difference being that the noninertial reference frame is rotating rather than merely translating. If the origin of this noninertial reference frame was also accelerating, then we would have a third inertial force term, $-(d^2\mathbf{X}_o/dt^2)M$. Notice that we are not yet at Eqn. (2); in Section 4.1 we will indicate why the centrifugal force and gravitational mass attraction terms are combined into \mathbf{g} .

2.2.3 Remarks on the transformed equation of motion

Once we have in hand the transformation rule for accelerations, Eqn.(22), the path to the rotating frame equation of motion is short and direct — if Eqn. (25) holds in a given reference frame, say an inertial

frame, then Eqs. (26) and (27) hold exactly in a frame that rotates at the constant rate and direction Ω with respect to the first frame. The rotating frame equation of motion includes two terms that are dependent upon the rotation vector, the Coriolis term, $-2\Omega \times (d\mathbf{X}'/dt)$, and the centrifugal term, $-\Omega \times \Omega \times \mathbf{X}'$. These terms are sometimes written on the left side of an equation of motion as if they were going to be regarded as part of the acceleration, i.e.,

$$\frac{d^2 \mathbf{X}'}{dt^2} M + 2\Omega \times \frac{d\mathbf{X}'}{dt} M + \Omega \times \Omega \times \mathbf{X}' M = \mathbf{F}' + \mathbf{g}^* M. \quad (28)$$

If we compare the left side of Eqn. (28) with Eqn. (22) it is evident that the rotated acceleration is equal to the rotated force,

$$\left(\frac{d^2 \mathbf{X}}{dt^2} \right)' M = \mathbf{F}' + \mathbf{g}^* M,$$

which is well and true and the same as Eqn. (25).¹⁸ However, it is crucial to understand that the left side of Eqn. (28), $(d^2 \mathbf{X}/dt^2)'$ is *not* the acceleration that we observe or seek to analyze when we use a rotating reference frame; the acceleration we observe in a rotating frame is $d^2 \mathbf{X}'/dt^2$. Once we solve for $d^2 \mathbf{X}'/dt^2$, it follows that the Coriolis and centrifugal terms are, figuratively or literally, sent to the right side of the equation of motion where they are interpreted as if they were forces.

When the Coriolis and centrifugal terms are regarded as forces — as we intend they should be when we use a rotating reference frame — they have some peculiar properties. From Eqn. (28) (and Eqn. (4)) we can see that the centrifugal and Coriolis terms are inertial forces and are exactly proportional to the mass of the parcel observed, M , whatever that mass may be. The acceleration field for these inertial forces arises from the rotational acceleration of the reference frame, combined with relative velocity for the Coriolis force. They differ from central forces \mathbf{F} and $\mathbf{g}^* M$ in the respect that there is no physical interaction that causes the Coriolis or centrifugal force and hence there is no action-reaction force pair. As a consequence the rotating frame equation of motion does not retain the global conservation of momentum that is a fundamental property of the inertial frame equation of motion and central forces (an example of this nonconservation is described in Section 3.4). Similarly, we note here only that invariance to Galilean transformation is lost since the Coriolis force involves the velocity rather than velocity derivatives. Thus \mathbf{V}' is an absolute velocity in the rotating reference frame of the Earth. If we need to call attention to these special properties of the Coriolis force, then the usage Coriolis *inertial* force seems appropriate because it is free from the taint of unreality that goes with 'virtual force', 'fictitious correction force', etc., and because it gives at least a hint at the origin of the Coriolis force. It is important to be aware of these properties of the rotating frame equation of motion, and also to be assured that in most analysis of geophysical flows they are of no great practical

¹⁸Recall that $\Omega = \Omega'$ and so we could put a prime on every vector in this equation. That being so, we would be better off to remove the visually distracting primes and simply note that the resulting equation holds in a steadily rotating reference frame. We will hang onto the primes for now, since we will be considering both inertial and rotating reference frames until Section 5.

consequence. What is important is that the rotating frame equation of motion offers a very significant gain in simplicity compared to the inertial frame equation of motion (discussed in Section 4.3).

The Coriolis and centrifugal forces taken individually have simple interpretations. From Eqn. (27) it is evident that the Coriolis force is normal to the velocity, $d\mathbf{X}'/dt$, and to the rotation vector, $\boldsymbol{\Omega}$. The Coriolis force will thus tend to cause the velocity to change direction but not magnitude, and is appropriately termed a deflecting force as noted in Section 1. The centrifugal force is in a direction perpendicular to and directed away from the axis of rotation. Notice that the Coriolis force is independent of position, while the centrifugal force clearly is not. The centrifugal force is independent of time. How these forces effect dynamics in simplified conditions will be considered further in Sections 3, 4.3 and 5.

3 Inertial and noninertial descriptions of elementary motions.

To appreciate some of the properties of a noninertial reference frame we will now analyze several examples of elementary motions whose inertial frame dynamics will be very familiar. The object will be to compare the same motions when they are observed from a noninertial reference frame, and the goal will be to understand how the accelerations and the inertial forces — gravity, centrifugal and Coriolis — depend upon the reference frame.

There is an important difference between what we will term contact forces, \mathbf{F} , that act over the surface of the parcel, and the acceleration due to gravity, gM , which is an inertial force that acts throughout the body of the parcel (and note that in this section we will not distinguish between g and g^*) (Table 1). To measure the contact forces we could enclose the parcel in a wrap-around strain gage that measures and reads out the vector sum of the tangential and normal stresses acting on the surface of the parcel. To measure gravity we could measure the direction of a plumb line, which defines vertical and the alignment of the \mathbf{e}_z unit vector. The magnitude of the acceleration could then be measured by observing the period of oscillation of a simple pendulum.¹⁹

¹⁹A plumb line is nothing more than a weight, the plumb bob, that hangs from a string, the plumb line (and *plumbum* is Latin for lead, Pb). When the plumb bob is at rest, the plumb line is parallel to the local acceleration field. If the weight is displaced and released, it becomes a simple pendulum, and the period of oscillation, P , can be used to infer the magnitude of the acceleration, $g = L/(P/2\pi)^2$, where L is the length of the plumb line. If the reference frame is attached to the rotating Earth, then the measured inertial acceleration includes a contribution from the centrifugal force, discussed in Section 4.1. The motion of the pendulum will be effected also by the Coriolis force, and in this context a simple pendulum is often termed a Foucault pendulum, discussed further in a later footnote 29. In this section we consider gravity, rather than gravitational mass attraction and centrifugal force due to Earth's rotation considered separately. When centrifugal force arises here, it will be due to the rotation of a rapidly rotating reference frame and noted explicitly.

A characterization of the forces on geophysical flows.

	central?	inertial?	Galilean invariant?	position only?
contact forces	yes	no	yes	no
grav. mass attraction	yes	yes	yes	yes
centrifugal	no	yes	yes	yes
Coriolis	no	yes	no	no

Table 1: Contact forces on fluid parcels are pressure gradients (normal to a surface) and frictional forces (mainly tangential to a surface). The centrifugal force noted here is that associated with Earth's rotation. By 'position only' we mean that the gravitational mass attraction is dependent upon the parcel position on Earth (times mass), but not the parcel velocity, for example. In this table we have ignored electromagnetic forces that are usually small.

3.1 Switching sides

In this section we will evaluate the equations of motion, Eqn. (24) and (27), for truly elementary motions. Nevertheless, the analysis is slightly subtle insofar as the terms that represent accelerations and inertial forces will seem to change identity, as if by fiat, when we change reference frames. To understand that there is more going on than merely relabeling and reinterpreting terms in an arbitrary way, it will be very helpful make a sketch of each case beginning with the acceleration.

Consider a parcel of known, fixed mass M that is at rest and in contact with the ground, say, in a reference frame where the acceleration of gravity is known from independent observations, e.g., pendulum experiments. The strain gauge will read out a contact force F_z , which is upwards, from the perspective of the parcel. The vertical component of the equation of motion for the parcel is then

$$\frac{d^2 z}{dt^2} M = F_z - g.$$

As before, we will write the observable acceleration on the left side of the equation of motion (even when we regard it as known) and list the forces on the right side. In this case the acceleration $d^2 z/dt^2 = 0$, and so

$$0 = F_z - gM, \tag{29}$$

which indicates a static force balance between the upward contact force, F_z , and the downward force due to gravity. Now suppose that we observe the same parcel from a reference frame that is in free-fall and accelerating downwards at the rate $-g$.²⁰ When viewed from this reference frame, the parcel

²⁰Gravitational mass attraction is an inertial force and a central force that has a very long range. Consider two gravitating bodies and a reference frame attached to one of them, say parcel one, which will then be observed to be at rest. If parcel two is then found to accelerate towards parcel one, the total momentum of the system (parcel one plus parcel two) will not be

appears to be accelerating upwards at the rate g that is just the complement of the acceleration of the free-falling frame. In this frame there is no gravitational force (imagine astronauts floating in space and attempting pendulum experiments) and so the only force we recognize as acting on the parcel is the contact force, F_z , which is unchanged from the case before. The equation of motion for the parcel observed from this free-falling reference frame is then

$$\frac{d^2 z'}{dt^2} M = F_z,$$

or if we evaluate the acceleration, $d^2 z' / dt^2 = g$,

$$gM = F_z. \quad (30)$$

Notice that in going from Eqn. (29) to the free-falling frame Eqn. (30) the contact force is unchanged (invariant) while the term involving g has switched sides; gM is an inertial force in the reference frame appropriate to Eqn. (29) and is transformed into an acceleration (times M) in the free-falling reference frame described by Eqn. (30). The equations of motion makes perfectly good sense either way, but what we observe as an acceleration in one frame appears as an inertial force in the other frame. As we will see next, the same kind of switching sides happens with centrifugal and Coriolis inertial forces when we transform to or from a rotating reference frame.

Now consider the horizontal motion of this parcel, so that gravity and the vertical component of the motion will be ignored. We will presume that $\mathbf{F} = 0$, and hence the inertial frame equation of motion expanded in polar coordinates (derived in Section 3.4 and repeated here for convenience),

$$\frac{d^2 \mathbf{X}}{dt^2} M = \left(\frac{d^2 r}{dt^2} - r\omega^2 \right) M \mathbf{e}_r + \left(2\omega \frac{dr}{dt} + r \frac{d\omega}{dt} \right) M \mathbf{e}_\theta = F_r \mathbf{e}_r + F_\theta \mathbf{e}_\theta,$$

vanishes term by term. Suppose that the same parcel is viewed from a steadily rotating reference frame and that it is at a distance r' from the origin of the rotating frame. Viewed from this frame, the parcel will have a velocity $\mathbf{V}' = -\boldsymbol{\Omega} \times \mathbf{X}'$ and will appear to be moving around a circle of radius $r' = \text{constant}$ and in a direction opposite the rotation of the reference frame, $\omega' = -\Omega$, just as in Figure (8). The rotating frame equation of motion in polar coordinates is

$$\begin{aligned} \frac{d^2 \mathbf{X}'}{dt^2} M &= \left(\frac{d^2 r'}{dt^2} - r' \omega'^2 \right) M \mathbf{e}'_r + \left(2\omega' \frac{dr'}{dt} + r' \frac{d\omega'}{dt} \right) M \mathbf{e}'_\theta \\ &= \left(r' \Omega^2 M + 2\Omega \omega' r' M + F'_r \right) \mathbf{e}'_r + \left(-2\Omega \frac{dr'}{dt} M + F'_\theta \right) \mathbf{e}'_\theta. \end{aligned} \quad (31)$$

conserved, i.e., in effect, gravity would not be recognized as a central force. A reference frame attached to one of the parcels is thus noninertial. To define an inertial reference frame in the presence of mutually gravitating bodies we can use the center of mass of the system, and then align on the fixed stars. This amounts to putting the entire system into free-fall with respect to any larger scale (external to this system) gravitational mass attraction (for more on gravity and inertial reference frames see <http://plato.stanford.edu/entries/spacetime-iframes/>).

We presume that we can read the strain gage from this rotating frame just as well, and $F'_r = F'_\theta = 0$. All of the azimuthal component terms vanish individually, but three of the radial component terms are nonzero,

$$-r'\omega'^2 = r'\Omega^2 + 2\Omega\omega'r', \quad (32)$$

and indicate an interesting balance between the centripetal acceleration, $-r'\omega'^2$ (the acceleration we observe and the left hand side), and the sum of the centrifugal and Coriolis inertial forces (the right hand side, divided by M , and note that $\omega' = -\Omega$).²¹ Interesting perhaps, but disturbing as well; a parcel that was at rest in the inertial frame has acquired a rather complex momentum balance when observed from a rotating reference frame. It is sorely tempting to deem the Coriolis and centrifugal terms to be 'virtual', or 'fictitious, correction' forces to acknowledge this discomfort.¹¹ To be consistent, we would have do the same for the centripetal acceleration term. But labeling terms this way serves mainly to obscure the fundamental issue — accelerations and inertial forces are relative to a reference frame. As we found in the example of a free-falling reference frame, this applies just as much for gravitational mass attraction as it does for centrifugal and Coriolis forces.

3.2 To get a feel for the Coriolis force

The centrifugal force is something that we encounter in daily life. For example, a runner having $V = 5 \text{ m s}^{-1}$ and making a moderately sharp turn, radius $R = 15 \text{ m}$, will easily feel the centrifugal force, $(V^2/R)M \approx 0.15gM$, and will compensate instinctively by leaning toward the center of the turn. It is unlikely that a runner would think of this centrifugal force as virtual or fictitious.

The Coriolis force associated with Earth's rotation is very small by comparison, only about $2\Omega VM \approx 10^{-4}gM$ for a runner. To experience the Coriolis force in the same direct way that we can feel the centrifugal force, i.e., to feel it in our bones, will thus require a platform having a rotation rate that exceeds Earth's rotation rate by a factor of about 10^4 . A typical merry-go-round having a rotation rate $\Omega = 2\pi/12 \text{ rad s}^{-1} = 0.5 \text{ rad s}^{-1}$ is ideal. We are now going to calculate the forces that we would feel while sitting or walking about on a merry-go-round, and so will need to estimate a body mass, say $M = 75 \text{ kg}$ (approximately the standard airline passenger before the era of super-sized meals and passengers).

3.2.1 Zero relative velocity

To start, let's presume that we are sitting quietly near the outside radius $r = 6 \text{ m}$ of a merry-go-round that it is rotating at a steady rate, $\Omega = 0.5 \text{ rad s}^{-1}$. How does the momentum balance of our motion

²¹Two problems for you: 1) Given the polar coordinate velocity, Eqn. (42), show that Eqn. (31) can be derived also from the vector form of the equation of motion, Eqn. (27). 2) Sketch the balance of forces in a case where the rotation rate Ω is positive and then again where it is negative. Is this consistent with Eqn. (32)?

depend upon the reference frame?

Viewed from an approximate **inertial frame** outside of the merry-go-round (fixed stars are not required given the rapid rotation rate), the polar coordinate momentum balance Eqn. (31) with $\omega = \Omega$ and $dr/dt = d\omega/dt = F_\theta = 0$ reduces to a two term radial balance,

$$-r\Omega^2 M = F_r, \quad (33)$$

in which a centripetal acceleration ($\times M$) is balanced by an inward-directed radial (contact) force, F_r . We can readily evaluate the former and find $-r\Omega^2 M = F_r = -112$ N, which is equal to the weight on a mass of $F_r/g = 11.5$ kg for a nominal g . This is just what the strain gauge (the one on the seat of your pants) reads out.

Viewed from the **rotating reference frame**, i.e., our seat on the merry-go-round, we are stationary and of course not accelerating. To evaluate the rotating frame momentum equation, Eqn. 31, we thus set $\omega' = 0$, $r' = \text{constant}$, and are left with a two term radial force balance,

$$0 = r'\Omega^2 M + F'_r. \quad (34)$$

The physical conditions are unchanged and thus the strain gage reads out exactly as before, and $F'_r = F_r = -112$ N. What has changed is that the term $r'\Omega^2 M$, an acceleration in the inertial frame, is now on the right side of the momentum equation and is the centrifugal force. Within the rotating frame, the centrifugal force is quite vivid; it appears that we are being pushed outwards, or centrifugally, by an inertial force that is opposed by the centripetal contact force F'_r . This is exactly the relationship between weight and a contact force described in Section 3.1. The centrifugal force produces a radial acceleration on every stationary object that depends only upon the radius, r' . For example, a plumb line makes an angle to the vertical of $\arctan(r'\Omega^2/g)$, where the vertical direction and g are in the absence of rotation. The centrifugal force thus contributes to the direction and magnitude of the time-independent acceleration field observed in the rotating frame, an important point that we will return to in Section 4.1.

3.2.2 With relative velocity

Most merry-go-rounds have signs posted which caution riders to remain in their seats once the ride begins. This is a good and prudent rule, of course. But if our goal is to get a feel for the Coriolis force then we may decide to go for a (very cautious) walk on the merry-go-round. We will presume that the relative velocity, i.e., our walking velocity, is specified, and then calculate the contact force that must be exerted by the merry-go-round upon us as a consequence.

Azimuthal relative velocity: Let's assume that we walk azimuthally so that $r = 6$ m and constant. A reasonable walking pace under the circumstance is about $U_w = 1.5$ m s⁻¹, which corresponds to a relative rotation rate $\omega' = 0.25$ rad s⁻¹, and recall that $\Omega = 0.5$ rad s⁻¹. Let's also assume that we walk in the direction of the merry-go-round rotation so that $\omega = \Omega + \omega' = 0.75$ rad s⁻¹.

From the **inertial frame** momentum equation (31) we can readily calculate that the centripetal force required to maintain $r = \text{constant}$ at this greater angular velocity is

$$-r\omega^2 M = -r(\Omega + \omega')^2 M = F_r \approx -253 \text{ N},$$

or roughly twice the force required when you were seated. If we then reverse direction and walk at the same speed against the rotation of the merry-go-round, F_r is reduced to about -28 N. This pronounced variation of F_r with ω' is a straightforward consequence of the quadratic dependence of centripetal acceleration upon the rotation rate, ω .

When this motion is viewed from the **rotating frame** of the merry-go-round, we distinguish between the rotation rate of the merry-go-round, Ω , and the relative rotation rate, ω' , due to our walking speed. The radial component of the rotating frame momentum equation reduces to

$$-r'\omega'^2 M = (r'\Omega^2 + 2r'\Omega\omega')M + F'_r. \quad (35)$$

The term on the left is the comparatively small centripetal acceleration; the first term on the right is the usual centrifugal force, and the second term on the right, $2r'\Omega\omega'$, is the Coriolis force. The Coriolis force is substantial, $2r'\Omega\omega' M \pm 112 \text{ N}$, with the sign determined by the direction of our motion relative to Ω . If $\Omega > 0$ and $\omega' > 0$ then the Coriolis force is positive and radial and to the right of and normal to the azimuthal relative velocity. Given what we found in the previous paragraph, it is tempting to identify the Coriolis force as the (relative)velocity-dependent part of the centrifugal force. This is, however, somewhat loose and approximate; loose because the centrifugal force is defined to be dependent upon rotation rate and position only and approximate because this ignores the small centripetal acceleration term.

Radial relative velocity: If we are still able, let's now consider a (very cautious) walk in the radial direction. To isolate the effects of radial motion we will presume that our radial speed is constant at $dr'/dt = 1 \text{ m s}^{-1}$ and that we walk along a radial line so that our rotation rate also remains constant at $\omega = \Omega$. (In practice this is very difficult to do for more than a few steps, but that will suffice.) The resulting contact force \mathbf{F} is then in the azimuthal direction, and its magnitude and sense can most easily be interpreted in terms of the balance of angular momentum, $A = \omega r'^2 M$. In this circumstance the rate of change of angular momentum A has been fully specified,

$$\frac{dA}{dt} = 2\Omega r' \frac{dr'}{dt} M = r' F_\theta,$$

and must be accompanied by an azimuthal torque, $r'F_\theta$, exerted by the merry-go-round.

Viewed from an **inertial frame**, the azimuthal component of the momentum balance, Eqn. (31), reduces to

$$2\Omega \frac{dr}{dt} M = F_\theta, \quad (36)$$

where $F_\theta \approx -75$ N for the given data. The azimuthal contact force F_θ has the form of the Coriolis force, but remember that we are viewing the motion from an inertial frame so that there is no Coriolis force. If the radial motion was inward so that $dr/dt < 0$, then F_θ must be negative, or opposite the direction of the merry-go-round rotation, since our angular momentum is necessarily becoming less positive. (Be sure that these signs are clear before going on to consider this motion from the rotating frame.)

From within the **rotating frame**, the momentum equation reduces to an azimuthal force balance

$$0 = -2\Omega \frac{dr'}{dt} M + F'_\theta, \quad (37)$$

where $-2\Omega \frac{dr'}{dt} M$ is the Coriolis force and $F'_\theta = F_\theta$ as before. The contact force exerted by the merry-go-round, F'_θ , is balanced by an inertial force, the Coriolis force, in the direction opposed to F'_θ . For example, if our radial motion is inward, $\frac{dr'}{dt} \leq 0$, then the Coriolis force, $-2\Omega \frac{dr'}{dt} M \geq 0$, is to the right of and normal to our relative velocity, just as we would have expected from the vectorial Coriolis force. This interpretation of a Coriolis force is exactly parallel to the interpretation of centrifugal force in the example of steady, circular motion and Eqn. (34): an acceleration seen from an inertial frame appears to be an inertial force when viewed from within the rotating frame.

Be careful! If you have a chance to do this experiment you will learn with the first step whether the Coriolis force is better described as a real force or as a fictitious correction force. Be sure to ask permission of the operator before you start walking around, and exercise genuine caution. The Coriolis force is an inertial force and so is distributed throughout your body, unlike the contact force which acts only where you are in contact with the merry-go-round, i.e., through the soles of your sneakers. It is therefore essential to maintain a secure hand grip at all times. The radial Coriolis force associated with azimuthal motion is much like an increase or slackening of the centrifugal force and so is not particularly difficult to compensate. However, you are likely to find that the azimuthal Coriolis force associated with radial motion is quite surprising, even presuming that you are the complete master of the present analysis. If you do not have access to a merry-go-round or if you feel that this experiment is unwise, then see Stommel and Moore⁹ for alternate ways to accomplish some of the same things.

3.3 An elementary projectile problem

A very simple projectile problem can reveal some other aspects of rotating frame dynamics. Assume that a projectile is launched at a speed U_0 and at an angle to the ground β from a location $[x \ y] = [0 \ y_0]$. The only force presumed to act on the projectile after launch is the downward force of gravity, $-gM\mathbf{e}_3$, which is the same in either reference frame.

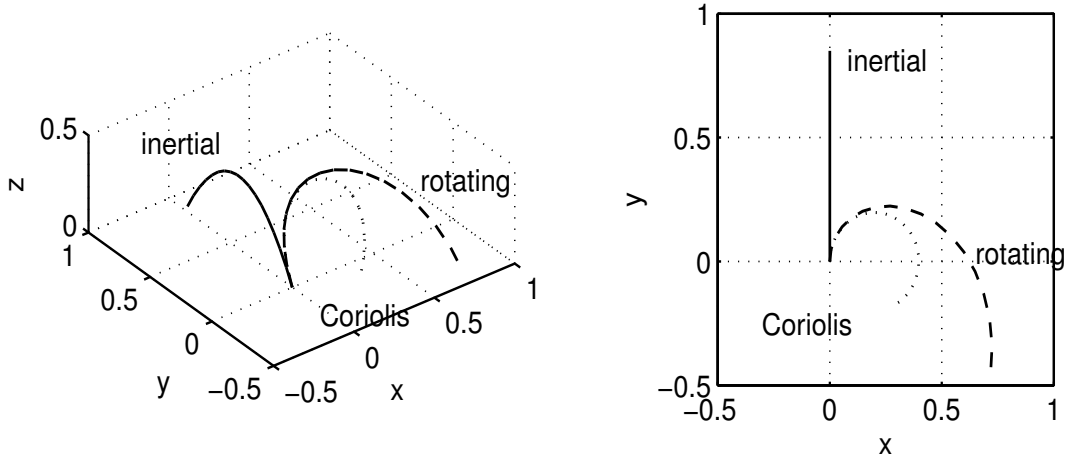


Figure 10: Trajectory of a parcel launched with a horizontal velocity in the positive y -direction as seen from an inertial reference frame (solid line, displaced in the y -direction only), and as seen from a rotating frame (dashed, curves lines). The left and right panels are 3-dimensional and plan views. The dotted curve is with the Coriolis force only (the motivation for this is in Section 4). This trajectory has the form of a circle, and if the projectile had not returned to the surface, $z = 0$, it would have made a complete loop back to the starting point.

3.3.1 From the inertial frame

The equations of motion and initial conditions in Cartesian components are linear and uncoupled;

$$\frac{d^2x}{dt^2} = 0; \quad x(0) = 0, \quad \frac{dx}{dt} = 0, \quad (38)$$

$$\frac{d^2y}{dt^2} = 0; \quad y(0) = y_0, \quad \frac{dy}{dt} = U_0 \cos \beta,$$

$$\frac{d^2z}{dt^2} = -g; \quad z(0) = 0, \quad \frac{dz}{dt} = U_0 \sin \beta,$$

where M has been divided out. The solution for $0 < t < \frac{2U_0 \sin \beta}{g}$, the time the parcel is in the air, is

$$\begin{aligned} x(t) &= 0, \\ y(t) &= y_0 + tU_0 \cos \beta, \\ z(t) &= t(U_0 \sin \beta - \frac{1}{2}gt) \end{aligned} \quad (39)$$

is in Fig. (10).

3.3.2 From the rotating frame

How would this same motion look when viewed from a rotating reference frame? And, how could we compute the motion from within a rotating reference frame?

The first question can be answered most directly by rotating the trajectory, Eqn. (39), via the rotation matrix, Eqn. (12), $\mathbb{X}' = \mathbb{R}\mathbb{X}$ with $\theta = \Omega t$, and with the result

$$\begin{aligned}x'(t) &= (y_0 + tU_0 \cos \beta) \sin(\Omega t), \\y'(t) &= (y_0 + tU_0 \cos \beta) \cos(\Omega t), \\z'(t) &= z = t(U_0 \sin \beta - \frac{1}{2}gt),\end{aligned}\tag{40}$$

valid over the time interval as before. The z component is unchanged in going to the rotating reference frame since the rotation axis was aligned with z . This is quite general; motion that is parallel to the rotation vector Ω is unchanged, just as we would expect from the three-dimensional vector Coriolis force. On the other hand, motion in the (x, y) -plane perpendicular to the rotation vector can be altered quite substantially, depending upon the phase Ωt . In the case shown in Fig. (10), the change of phase is 2.0 at the end of the trajectory, so that rotation effects are prominent.²² One important aspect of the trajectory is not changed, however, the (horizontal) radius,

$$\sqrt{x'^2 + y'^2} = \sqrt{x^2 + y^2},$$

since the coordinate systems have coincident origins (Fig. 11a)

How could we compute the trajectory in the rotating frame? The Cartesian component equations in the rotating frame are a bit awkward (the x-component only):

$$\frac{d^2 x'}{dt^2} = 2\Omega \frac{dy'}{dt} + \Omega^2 \frac{x'^2}{\sqrt{x'^2 + y'^2}}.$$

An elementary problem in the inertial frame transforms into a pair of coupled, nonlinear equations in the rotating frame ($z' = z$). We can always solve these equations numerically, but we are better off in this and many problems involving rotation to use cylindrical polar coordinates where we can take advantage of what we have already learned about the rotating frame solution. We know that

$$r' = r = y_0 + tU_0 \cos \beta,$$

²²A well-thrown baseball travels at about 45 m s⁻¹. How much will it be deflected as it travels over a distance of 30 m? Use Earth's rotation rate given by Eqn. (23)(as we will see in Section 4.2 this is appropriate for the north pole). A long-range artillery shell has an initial speed of about 700 m s⁻¹. Assuming the shell is launched at angle to the ground of 30 degrees, how much will it be deflected over its trajectory (ignoring air resistance)?

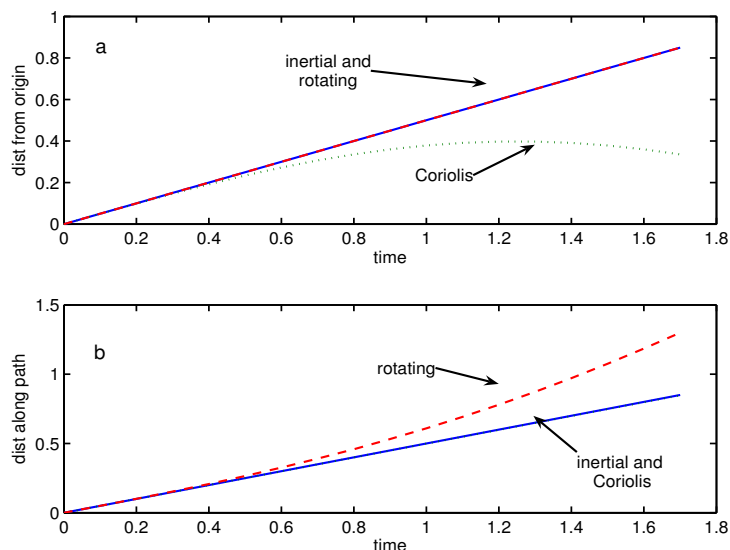


Figure 11: (a) The distance from the origin in the horizontal plane for the trajectories of Fig. (10). The distance from the origin is identical for the inertial and rotating trajectories, and reduced for the Coriolis trajectory (discussed in Section 4). (b) The distance along the path in the horizontal plane for the same trajectories. The slope gives the speed of the parcel. The inertial and Coriolis frame trajectories retain their initial speed and are identical; the rotating frame trajectory accelerates due to the centrifugal force.

and that the angle in the inertial frame, θ , is constant in time since the motion is purely radial and for the specific case considered, $\theta = \pi/2$. The rotation rates are related by $\omega' = -\Omega$, and thus

$$\theta' = \pi/2 - \Omega t.$$

Both the radius and the angle increase linearly in time, and the horizontal trace of the trajectory as seen from the rotating frame is Archimedes spiral (Fig. 10, lower).

When viewed from the rotating frame, the projectile is obviously deflected to the right, and from the azimuthal component of Eqn. (31) we readily attribute this to the Coriolis force,

$$2\omega' \frac{dr'}{dt} M = -2\Omega \frac{dr'}{dt} M,$$

since $\omega' = \Omega$. Notice that the horizontal speed and thus the kinetic energy increase with time (Fig. 11, lower). The rate of increase of rotating frame kinetic energy (per unit mass) is

$$\frac{d\mathbf{V}'^2/2}{dt} = \frac{d(U_0^2 + r'^2\Omega^2)/2}{dt} = \frac{dr'}{dt} r' \Omega^2$$

where the term on the right side is the work done by the centrifugal force, $r'\Omega^2$, on the radial velocity, dr'/dt . If the projectile had not returned to the ground, its speed (observed from the rotating reference frame) would have increased without limit so long as the radius increased.²³

²³In the previous example, walking around on a merry-go-round, we indicated that you would be able to feel the Coriolis force directly. Imagine that you are riding along on this projectile (don't try this one at home) — would you be able to feel the Coriolis force?

3.4 Appendix to Section 3: Circular motion and polar coordinates.

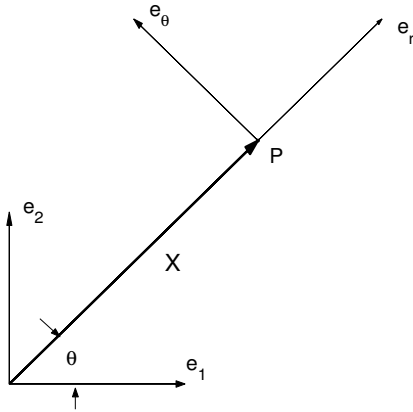


Figure 12: The unit vectors $\mathbf{e}_1, \mathbf{e}_2$ define a stationary reference frame. The unit vectors for a polar coordinate system, \mathbf{e}_r and \mathbf{e}_θ , are defined at the position of a given parcel, P. These unit vectors are time-dependent since the angle θ is time-dependent.

Rotational phenomena are often analyzed most efficiently with cylindrical polar coordinates, reviewed here briefly. The vertical coordinate is exactly the z or x_3 of Cartesian coordinates, and we need consider only the horizontal (two-dimensional) position, which can be specified by a distance from the origin, r , and the angle, θ between the radius vector and (arbitrarily) the x_1 axis (Fig. 12). The corresponding unit vectors are given in terms of the time-independent Cartesian unit vectors that define the stationary frame by

$$\mathbf{e}_r = \cos(\theta)\mathbf{e}_1 + \sin(\theta)\mathbf{e}_2 \quad \text{and} \quad \mathbf{e}_\theta = -\sin(\theta)\mathbf{e}_1 + \cos(\theta)\mathbf{e}_2. \quad (41)$$

The position vector in this system is

$$\mathbf{X} = r\mathbf{e}_r,$$

and hence the velocity is

$$\frac{d\mathbf{X}}{dt}M = \frac{dr}{dt}\mathbf{e}_rM + r\frac{d\mathbf{e}_r}{dt}M = \frac{dr}{dt}M\mathbf{e}_r + r\omega M\mathbf{e}_\theta, \quad (42)$$

where we have taken account of the time-dependence of \mathbf{e}_r and $\omega = d\theta/dt$. Continuing, the equation of motion is

$$\frac{d^2\mathbf{X}}{dt^2}M = \left(\frac{d^2r}{dt^2} - r\omega^2\right)M\mathbf{e}_r + \left(2\omega\frac{dr}{dt} + r\frac{d\omega}{dt}\right)M\mathbf{e}_\theta \quad (43)$$

$$= F_r\mathbf{e}_r + F_\theta\mathbf{e}_\theta. \quad (44)$$

Notice that there are acceleration terms, $r\omega^2$ and $2\omega\frac{dr}{dt}$, that look just like the centrifugal and Coriolis forces (and are sometimes deemed to be such, even by otherwise very careful authors, e.g., Boas,¹² p. 399), though this equation holds in an inertial frame where centrifugal and Coriolis forces (or accelerations) *do not arise*.

To find the rotating frame equation of motion is straightforward; the radius is identical in the rotating frame, $r' = r$, since the origins are assumed coincident. The unit vectors are identical since they are defined at the location of the parcel, $\mathbf{e}'_r = \mathbf{e}_r$ and $\mathbf{e}'_\theta = \mathbf{e}_\theta$; the force components are thus also identical. The only thing different is that the angular velocity ω is decomposed into a time mean and a relative angular velocity, $\omega = \omega' + \Omega$. Substituting this into the inertial frame equation of motion Eqn. (44), and rearrangement to move terms containing Ω to the right hand side yields the formidable-looking rotating frame equation of motion for polar coordinates,

$$\begin{aligned} \frac{d^2 \mathbf{X}'}{dt^2} M &= \left(\frac{d^2 r'}{dt^2} - r' \omega'^2 \right) M \mathbf{e}'_r + \left(2\omega' \frac{dr'}{dt} + r' \frac{d\omega'}{dt} \right) M \mathbf{e}'_\theta \\ &= \left(r' \Omega^2 M + 2\Omega \omega' r' M + F'_r \right) \mathbf{e}'_r + \left(-2\Omega \frac{dr'}{dt} M + F'_\theta \right) \mathbf{e}'_\theta. \end{aligned} \quad (45)$$

Notice that there are genuine centrifugal and Coriolis force terms on the righthand side of Eqn. (45) and that we have derived these terms for the third time now; for Cartesian coordinates, Eqn. (26), for vectors, Eqn. (27), and here for cylindrical polar coordinates. You should be sure to verify this, as it is perhaps the most direct derivation of the Coriolis force, and most easily shows how or where the factor of 2 arises.

4 A reference frame attached to the rotating Earth.

The equations of motion appropriate to the atmosphere and ocean differ from the general rotating frame equations considered up to now in two significant ways. First, it isn't just the reference frame that rotates, but the entire Earth, ocean and atmosphere, aside from the comparatively small (but very important!) relative motion that we call winds and ocean currents. A major consequence is that the horizontal component of the centrifugal force on a stationary parcel is exactly canceled by a component of the gravitational mass attraction. Thus the centrifugal force does not appear in the rotating frame dynamical equations for the atmosphere and oceans, a very welcome simplification (Section 4.1). Second, because the Earth is nearly spherical, the rotation vector is not perpendicular to the plane of horizontal motions except at the poles. This causes the horizontal component of the Coriolis force to vary with latitude (Section 4.2). Lastly, we will compare inertial and rotating frame descriptions of a simple geophysical phenomenon (Section 4.3), and explain why we persist in using the rotating frame equations.

4.1 Cancellation of the centrifugal force

To understand how the centrifugal force is canceled we consider briefly the balance of gravitational mass attraction and centrifugal forces on a rotating Earth. To be sure, the details of this first subsection

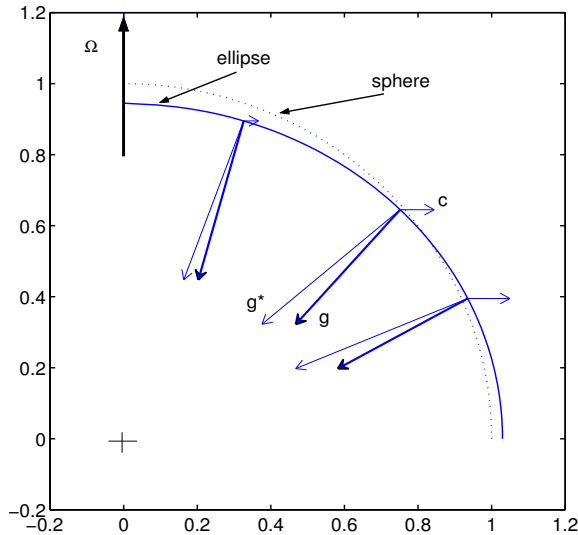


Figure 13: Cross-section through a hemisphere of a gravitating and rotating planet. The gravitational acceleration due to mass attraction is shown as the vector g^* that points to the center of a spherical, homogeneous planet. The centrifugal acceleration, C , associated with the planet's rotation is directed normal to and away from the rotation axis. The combined gravitational and centrifugal acceleration is shown as the heavier vector, g . This vector is in the direction of a plumb line, and defines vertical. A surface that is normal to g similarly defines a level surface, and has the approximate shape of an oblate spheroid (the solid curve). The ellipse of this diagram has a flatness $F = 0.1$ that approximates Saturn; for Earth, $F = 0.0033$.

are a bit beyond the minimum discussion needed for our purpose, but are inherently interesting. A more compact though more abstract way to come to the same result is to consider the definition and measurement of vertical and level in an accelerated fluid environment, Section 4.1.2.

4.1.1 Earth's (slightly chubby) figure

If Earth was a perfect, homogeneous sphere, the gravitational mass attraction at the surface, g^* , would be directed towards the center (Fig. 13). Because the Earth is rotating, every parcel on the surface is also subject to a centrifugal force of magnitude $\Omega^2 R \sin \theta$, where R_e is the nominal Earth's radius, and θ is the colatitude ($\pi/2$ - latitude). This centrifugal force has a component parallel to the surface (a shear stress)

$$C_\theta = \Omega^2 R_e \sin \theta \cos \theta \quad (46)$$

that is directed towards the equator (except at the equator where it is vertical).²⁴ C_θ is not large compared to g^* , $C_\theta/g^* \approx 0.002$ at most, but it has been present since the Earth's formation. A fluid can not sustain a shear stress without deforming, and over geological time this holds as well for the Earth's interior and crust. Thus it is highly plausible that the Earth long ago settled into an equilibrium configuration in which this C_θ is exactly balanced by a component of the gravitational (mass) attraction that is parallel to the displaced surface and poleward.

²⁴Ancient critics of the rotating Earth hypothesis argued that loose objects on a spinning sphere should fly off into space, which clearly does not happen. Even so, given this persistent centrifugal force, why don't we drift towards the equator? Alfred Wegner proposed this as the motive force of Earth's moving continents (see D. McKenzie, 'Seafloor magnetism and drifting continents', in *A Century of Nature*, 131-137. Ed. by L. Garwin and T. Lincoln, The Univ. of Chicago Press, Chicago, IL, 2003.).

To make what turns out to be a rough estimate of the displaced surface, η , we will assume that the gravitational mass attraction remains that of a sphere and that the meridional slope times the gravitational mass attraction is in balance with the tangential component of the centrifugal force,

$$\frac{g^*}{R_e} \frac{d\eta}{d\theta} = \Omega^2 R_e \sin \theta \cos \theta. \quad (47)$$

This may then be integrated with latitude to yield the equilibrium displacement

$$\eta(\theta) = \int_0^\theta \frac{\Omega^2 R_e^2}{g^*} \sin \theta \cos \theta d\theta = \frac{\Omega^2 R_e^2}{2g^*} \sin^2 \theta + constant. \quad (48)$$

When this displacement is added onto a sphere the result is an oblate (flattened) spheroid, (Fig. 13), which is consistent with the observed shape of the Earth.²⁵ A convenient measure of flattening is $F = (R_{eqt} - R_{pol})/R_{eqt}$, where the subscripts refer to the equatorial and polar radius. Earth's flatness is $F = 0.0033$, which seems quite small, but is nevertheless highly significant in ways beyond that considered here.²⁶ The flatness of a rotating planet is given roughly by $F \approx \Omega^2 R/g$. If the gravitational acceleration at the surface, g , is written in terms of the planet's mean radius, R , and density, ρ , then $F = \Omega^2 / (\frac{4}{3}\pi G\rho)$, where $G = 6.67 \times 10^{-11} \text{ m}^3 \text{ kg}^{-1} \text{ s}^{-2}$ is the universal gravitational constant. The rotation rate and the density vary a good deal among the planets, and consequently so does F . The gas giant, Saturn, has a rotation rate a little more than twice that of Earth and a very low mean density, about one eighth of Earth's. The result is that Saturn's flatness is large enough, $F \approx 0.10$, that it can be discerned through a good backyard telescope (Fig. 13).

4.1.2 Vertical and level in an accelerating reference frame

Closely related is the notion of 'vertical'. When we measure vertical we do so by means of a plumb bob; the plumb line is, by definition, the direction vertical. Following the discussion above we know that the time-independent, acceleration field of the Earth is made up of two contributions, the first and

²⁵The pole-to-equator rise given by Eqn. (48), is about 11 km. Precise observations show that Earth's equatorial radius, $R_{eqt} = 6378.2$, is greater than the polar radius, $R_{pol} = 6356.7$ km, by about 21.5 km. This simple model underestimates Earth's equatorial bulge because the mass displaced from the pole towards the equator causes a small equatorward mass attraction that is sufficient to compensate for about half of the meridional tilt effect; thus still more mass must be displaced towards the equator in order to achieve a gravitational/rotational equilibrium. The net result is about a factor two greater amplitude than Eqn. (48) indicates.

A comprehensive source for physical data on the planets is by C. F. Yoder, 'Astrometric and geodetic data on Earth and the solar system,' Ch. 1, pp 1–32, of *A Handbook of Physical Constants: Global Earth Physics (Vol. 1)*. American Geophysical Union (1995).

²⁶To note just two: 1) Earth's ellipsoidal shape must be accounted for in highly precise, long range navigation systems (GPS), while shorter range or less precise systems can approximate the Earth as spherical. 2) Because the Earth is not perfectly spherical, the gravitational tug of the Sun, Moon and planets can exert a torque on the Earth and thereby perturb Earth's rotation vector.¹⁷

by far the largest being mass attraction, \mathbf{g}^* , and the second being the centrifugal acceleration associated with the Earth's rotation, \mathbf{C} , Fig. (13). Just as on the merry-go-round, this centrifugal acceleration adds with the gravitational mass attraction to give the net acceleration, called 'gravity', $\mathbf{g} = \mathbf{g}^* + \mathbf{C}$, a vector (field) whose direction and magnitude we can measure with a plumb bob and by observing the period of a simple pendulum. A surface that is normal to the gravitational acceleration vector is said to be a level surface in as much as the acceleration component parallel to that surface is zero. A level surface can be defined in practice by observing the free surface of a water body that is at rest in the rotating frame, since a resting fluid can sustain only normal stresses, i.e., pressure but not shear stress. Thus the measurements of vertical or level that we can readily make necessarily include the centrifugal force due to Earth's rotation summed with gravitational mass attraction. The happy result is that the rotating frame equation of motion applied in an Earth-attached reference frame, Eqn. (2), does not include the centrifugal force associated with Earth's rotation (and neither do we tend to roll towards the equator!).

4.1.3 The equation of motion for an Earth-attached frame

The inertial and rotating frame momentum equations are listed again for convenience using velocity in place of the previous time rate change of position,

$$\frac{d\mathbf{V}}{dt}M = \mathbf{F} + \mathbf{g}^*M, \quad \text{and,} \quad (49)$$

$$\frac{d\mathbf{V}'}{dt}M = -2\boldsymbol{\Omega} \times \mathbf{V}'M - \boldsymbol{\Omega} \times \boldsymbol{\Omega} \times \mathbf{X}'M + \mathbf{F}' + \mathbf{g}'_*M, \quad (50)$$

and note that the inertial frame velocity of Eqn. (49) may be written in terms of the relative velocity as

$$\mathbf{V} = \mathbf{V}_\Omega + \mathbf{V}', \quad (51)$$

where

$$\mathbf{V}_\Omega = -\boldsymbol{\Omega} \times \mathbf{X}$$

is the planetary velocity due to the solid body rotation of the Earth (Section 2.2). Now we are going to assume the result from above, that there exists a tangential component of gravitational mass attraction that exactly balances the centrifugal force due to Earth's rotation and that we define vertical in terms of the measurements that we can readily make; thus $\mathbf{g} = \mathbf{g}^* + \boldsymbol{\Omega} \times \boldsymbol{\Omega} \times \mathbf{X}$.²⁹ The equations of motion are then, for the inertial frame,

$$\frac{d\mathbf{V}}{dt}M = \boldsymbol{\Omega} \times \boldsymbol{\Omega} \times \mathbf{X}M + \mathbf{F} + \mathbf{g}M \quad (52)$$

and for the rotating frame,

$$\frac{d\mathbf{V}'}{dt}M = -2\boldsymbol{\Omega} \times \mathbf{V}'M + \mathbf{F}' + \mathbf{g}M. \quad (53)$$

Finally we have come to Eqn. (2), which we now see is the rotating frame equivalent of Eqn. (52) (and we will return to these equations in Section 4.3).²⁷

4.2 Coriolis force on motions in a thin, spherical shell

Application to geophysical flows requires one further small elaboration because the rotation vector makes a considerable angle to the vertical except at the poles. An Earth-attached, rectangular coordinate system is usually envisioned to have \mathbf{e}_x in the east direction, \mathbf{e}_y in the north direction, and horizontal is defined by a tangent plane to Earth's surface. The vertical direction, \mathbf{e}_z , is thus radial with respect to the (approximately) spherical Earth. The rotation vector $\boldsymbol{\Omega}$ thus makes an angle ϕ with respect to the local horizontal x', y' plane, where ϕ is the latitude of the coordinate system and thus

$$\boldsymbol{\Omega} = 2\Omega \cos(\phi)\mathbf{e}_y + 2\Omega \sin(\phi)\mathbf{e}_z.$$

If $\mathbf{V}' = u'\mathbf{e}_x + v'\mathbf{e}_y + w'\mathbf{e}_z$, then the Coriolis force (divided by the mass, M) is

$$-2\boldsymbol{\Omega} \times \mathbf{V}' = (2\Omega \cos(\phi)w' - 2\Omega \sin(\phi)v')\mathbf{e}_x + 2\Omega \sin(\phi)u'\mathbf{e}_y - 2\Omega \cos(\phi)u'\mathbf{e}_z. \quad (54)$$

Large scale geophysical flows are very flat in the sense that the horizontal components of wind or current are very much larger than the vertical component, $u' \propto v' \gg w'$, simply because the oceans and the atmosphere are quite thin, having a depth to width ratio of about 0.001. The ocean and atmosphere are stably stratified in the vertical, which still further inhibits the vertical component of motion. For these large scale (in the horizontal) flows, the Coriolis term multiplying w' in the x component of Eqn. (54) is thus very much smaller than the terms multiplied by u' or v' and as an excellent approximation may be ignored, often with no mention. The Coriolis term that appears in the vertical component is usually much, much smaller than the gravitational acceleration, and it too is almost always dropped

²⁷This notion of vertical and level turned out to have considerable practical importance beginning on a sweltering September afternoon when the University Housing Office notified your dear younger brother, Gustave-Gaspard (GG), that because of an unexpectedly heavy influx of freshmen, his old and comfortable dorm room was not going to be available. As a consolation they offered him the use of the merry-go-round (the one in Section 3.3, and still running) at the local, failed amusement park that the University had just gobbled up. With your encouragement, he accepts. The centrifugal force, amusing at first, was soon a huge annoyance; GG suffered from recurring nightmares of sliding out of bed and over a cliff. To counteract this you decide to build up the floor of the merry-go-round so that the tilt of the floor, combined with gravitational acceleration, would be just sufficient to balance the centrifugal force, as in Eqn. (47). A quick calculation and you find that a parabolic displacement, $\eta \propto r^2$, would be just the thing. A plumb line will then be normal to the new floor at every point, and hence the new floor will be a level surface in the acceleration field of the rotating dorm room. Make sure that we have this right, and specifically, how much does the outside edge ($r = 6$ m, $\Omega = 0.5$ rad s^{-1}) have to be built up to achieve this? Given that GG's bed is 2 m long and flat, what is the axial traction (or tidal force)? How is the calibration of a bathroom scale effected? Visitors are always very impressed with the rotating, parabolic dorm room, and to make sure they have the full experience, GG likes to sends them to the refrigerator for another cold drink. Describe what happens next using Eqn. (53). Is their route relevant?

without mention. The result is the thin fluid approximation of the Coriolis force in which only the horizontal Coriolis force due to horizontal motions is retained,

$$\boxed{-2\boldsymbol{\Omega} \times \mathbf{V}' \approx -\mathbf{f} \times \mathbf{V}' = -fv'\mathbf{e}_x + fu'\mathbf{e}_y} \quad (55)$$

The vector $\mathbf{f} = fe_{\mathbf{z}}$, where f is the very important Coriolis parameter,

$$\boxed{f = 2\Omega \sin(\phi)} \quad (56)$$

and ϕ is the latitude. Notice that f varies with the sine of the latitude, having a zero at the equator and maxima at the poles; $f < 0$ in the southern hemisphere.²⁸

For problems that involve parcel displacements, L , that are very small compared to the radius of the Earth, R , a simplification of f is often appropriate. The Coriolis parameter may be expanded in a Taylor series about a central latitude, y_0 ,

$$f(y) = f(y_0) + (y - y_0) \left. \frac{df}{dy} \right|_{y_0} + HOT \quad (57)$$

and if the second term is demonstrably much smaller than the first term, which follows if $L \ll R_e$, then the second and higher terms may be dropped to leave $f = f(y_0)$, a constant. Under this so-called f -plane approximation the period of inertial motions, $2\pi/f$, is just a little bit less than 12 hrs at the poles, a little less than 24 hrs at 30 N or S, and infinite at the equator. The period of inertial motions is sometimes said to be half of a 'pendulum day', the time required for a Foucault pendulum to precess through 2π radians.²⁹

²⁸The Coriolis parameter f vanishes at the equator as does the horizontal component of the Coriolis force. However, as we noted in the discussion of Fig. 5, the three-dimensional (vector) Coriolis force is independent of the location of the velocity and the rotation vectors. To appreciate the significance of this, consider relative velocities that are eastward and northward, and sketch the resulting (three-dimensional) Coriolis force vector $\propto -2\boldsymbol{\Omega} \times \mathbf{V}'$ at several latitudes that span pole-to-pole. Except at the poles, the three-dimensional Coriolis force has a vertical component that is negligible for most atmospheric and oceanic dynamics, but is very important in the context of ship-based gravimetric studies where it is termed the Eotvos effect, see http://en.wikipedia.org/wiki/Eotvos_effect (you may have to type this into your web browser).

²⁹The effect of Earth's rotation on the motion of a simple (one bob) pendulum, called a Foucault pendulum in this context, is treated in detail in many physics texts, e.g. Marion¹¹, and need not be repeated here. Here are a few questions, however. Can you calculate the Foucault pendulum motion by rotating the inertial frame solution for a simple pendulum? How does the time required for precession through 360 degrees depend upon latitude? What happens when the pendulum's natural frequency (in the absence of Earth's rotation) equals the Earth's rotation rate? Given the rotated trajectory, can you show that the acceleration of the bob for very short times is consistent with the rotating frame equations of motion?

Foucault pendulums are commonly displayed in science museums, though seldom to large crowds (for a more enthusiastic view see *The Prism and the Pendulum* by R. P. Crease). Much better is to make and observe your very own Foucault pendulum, a simple pendulum having two readily engineered properties. First, the e-folding time of the motion due to frictional dissipation must be long enough, at least 20-30 min, that the precession will become apparent. This can be most easily achieved by using a dense, smooth and symmetric bob having a weight of about half a kilogram or more, and suspended on a fine, smooth monofilament line. It is helpful if the length can be made several meters or more. Second, the pendulum

4.3 Why do we insist on the rotating frame equations?

We have emphasized that the rotating frame equation of motion has some inherent awkwardness, viz., the loss of Galilean invariance and global momentum conservation. Why, then, do we insist upon using the rotating frame equations for nearly all of our analyses of geophysical flow? The reasons are several, any one of which would be compelling, but beginning with the fact that the definition and implementation of an inertial frame (outside of the Earth) is simply not a viable option; whatever simplicity we might gain by omitting the Coriolis force would be lost to difficulty with observation. Consider just one aspect of this: the inertial frame (or absolute) velocity (Eqn. 51), $\mathbf{V} = \mathbf{V}_\Omega + \mathbf{V}'$, is dominated by the planetary velocity due to the solid-body rotation $V_\Omega = \Omega R_e \cos(\text{latitude})$, where R_e is earth's nominal radius, 6365 km, and thus $V_\Omega \approx 400 \text{ m s}^{-1}$ near the equator. By comparison, a large wind speed at mid-level of the atmosphere is $V' \approx 50 \text{ m s}^{-1}$ and a large ocean current is $V' \approx 2 \text{ m s}^{-1}$. The very large planetary velocity \mathbf{V}_Ω is accelerated centripetally by a tangential (almost) component of gravitational mass attraction associated with the ellipsoidal shape of the Earth discussed in Section 4.1 that is larger than the Coriolis force in the ratio V_Ω/V' that is $O(10)$ for the atmosphere, or much more for ocean currents. The inertial frame equations have to account for \mathbf{V}_Ω and this very large centripetal force explicitly, and yet our interest is almost always the small relative motion of the atmosphere and ocean, \mathbf{V}' , since it is the relative motion that transports heat and mass over the Earth. In that important regard, the planetary velocity \mathbf{V}_Ω is invisible to us Earth-bound observers, no matter how large it is. To say it a little differently — it is the relative velocity that we measure when observe from Earth's surface, and it is the relative velocity that we seek for almost every practical purposes — the Coriolis force follows.

4.3.1 Inertial oscillations from an inertial frame

Given that our goal is the relative velocity, then the rotating frame equation of motion is generally much simpler and more appropriate than is the inertial frame equation of motion. To help make this point we will analyze the free oscillations of Eqs. (52) and (53), i.e., $\mathbf{F} = \mathbf{F}' = 0$, usually called inertial oscillations, that are interesting in their own right. The domain is presumed to be a small region centered on the pole so that latitude = 90 degrees, and the domain is, in effect, flat. We will consider only horizontal motions, and assume the realistic condition that the motion will be a small perturbation away from the solid body rotation, $\mathbf{V}' \ll \mathbf{V}_\Omega$. The motion viewed from the inertial frame is thus almost circular and it is appropriate to use the cylindrical coordinate momentum equation, Eqn. (31) (dividing

should not interact appreciably with its mounting. This is harder to evaluate, but generally requires a very rigid support, and a bearing that can not exert torque, for example a needle bearing. The rotation effect is proportional to the rotation rate, and so you should plan to bring a simple and rugged pocket pendulum on your merry-go-round ride (Section 3.2). How do your observations (even if qualitative) compare with your solution for a Foucault pendulum? (Hint - consider the initial condition.)

out the constant M):

$$\frac{d^2r}{dt^2} - r\omega^2 = -\Omega^2r, \quad (58)$$

$$2\omega \frac{dr}{dt} + r \frac{d\omega}{dt} = 0. \quad (59)$$

Notice that when $\omega = \Omega$ and $dr/dt = 0$, the motion is balanced in the sense that $d^2r/dt^2 = 0$ and r remains constant. We are going to assume an initial condition that is a small radial perturbation away from such a balanced state, $r = R_o$ and $\omega = \Omega$. Since there is no tangential force, Eqn. (59) may be integrated,

$$\omega r^2 = \Omega R_o^2 = A, \quad (60)$$

which shows that the angular momentum, A , is a conserved quantity. Eqn. (60) can then be used to eliminate ω from Eqn. (58) to yield an equation for $r(t)$ alone,

$$\frac{d^2r}{dt^2} - \frac{A^2}{r^3} = -\Omega^2r. \quad (61)$$

To solve this equation it is convenient to move the centripetal acceleration term A^2/r^3 to the right side where it will be summed with the centripetal force,

$$\frac{d^2r}{dt^2} = \frac{A^2}{r^3} - \Omega^2r, \quad (62)$$

yielding what looks just like an equation of motion. However, it is important to understand that d^2r/dt^2 is *not* the radial component of acceleration that is observed in either an inertial or a rotating reference frame (cf. Eqs. 31 and 31) and to acknowledge this explicitly, the right hand side of Eqn.(62) will be called a *pseudo* (or false) force. None of this effects the solution *per se*, but only the words we use and the inferences we might then draw. And specifically, if you measured the radial force/ M on the parcel you wouldn't find $A^2/r^3 - \Omega^2r$, but rather $-\Omega^2r$, the right hand side of Eqn. (61).

Eqn. (62) is a well-known, nonlinear oscillator equation and is not difficult to solve. However, because our interest is in the case of small displacements away from the balanced state, $r = R_o$, a simplification is appropriate. To clarify what is meant by small displacement it is helpful to write the radius as

$$r(t) = R_o(1 + \delta(t)).$$

The meaning of 'small displacement' is that δ should be small compared to 1. Substitution into Eqn. (62) and rearrangement yields

$$\frac{d^2\delta}{dt^2} = \Omega^2(1 + \delta)^{-3} - \Omega^2(1 + \delta). \quad (63)$$

When we plot the right side of Eqn. (63) it is evident that the net pseudo force is a nearly linear function of δ provided $\delta \leq 0.1$. To exploit this we can expand the nonlinear term of Eqn.(63) in Taylor series

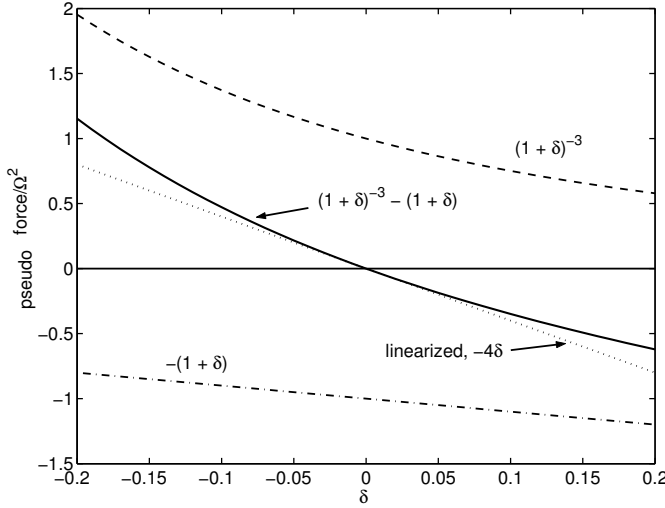


Figure 14: The terms of the right side of Eqn. (63), dubbed *pseudo forces* and normalized by Ω^2 , shown as a function of δ . Note that the net pseudo force (solid line) is nearly linear in δ when δ is small, roughly $\delta \leq 0.1$.

about $\delta = 0$,

$$\begin{aligned} \frac{d^2\delta}{dt^2} &= \Omega^2(1 - 3\delta + 6\delta^2 + HOT) - \Omega^2(1 + \delta) \\ &\approx -4\Omega^2\delta, \end{aligned} \quad (64)$$

where *HOT* are terms that are higher order in δ . For small displacements the quadratic and higher order terms may be neglected, leaving a simple harmonic oscillator equation, Eqn. (64), at a frequency 2Ω .

If the initial condition is a radial impulse that gives a radial velocity V_0 , then the initial condition for Eqn. (64) is

$$\frac{d\delta}{dt}(t=0) = (V_0/R_o) \cos 2\Omega t.$$

The solution for δ is

$$\delta(t) = (V_0/2\Omega) \sin(2\Omega t)$$

and the radius is then

$$r(t) = R_o(1 + \delta_0 \sin(2\Omega t)), \quad (65)$$

where $\delta_0 = V_0/2\Omega$. The corresponding angular rotation rate can be found by using Eqn. (65) together with the angular momentum conservation Eqn. (60),

$$\omega(t) = \frac{\Omega}{(1 + \delta_0 \sin(2\Omega t))^2} \approx \Omega(1 - 2\delta_0 \sin(2\Omega t)). \quad (66)$$

When graphed, these show that the parcel moves in an ellipsoidal orbit, Fig. (15, left panels), that crosses the (balanced) radius $r = R_o$ four times per complete orbit. The rotating frame turns through 180 degrees just as the parcel returns to $r = R_o$ the second time, after completing a full cycle of the oscillation. When viewed from the rotating frame (Fig. 15, right panels), the parcel appears to be moving in a clockwise-orbiting, circular path, with a frequency 2Ω .

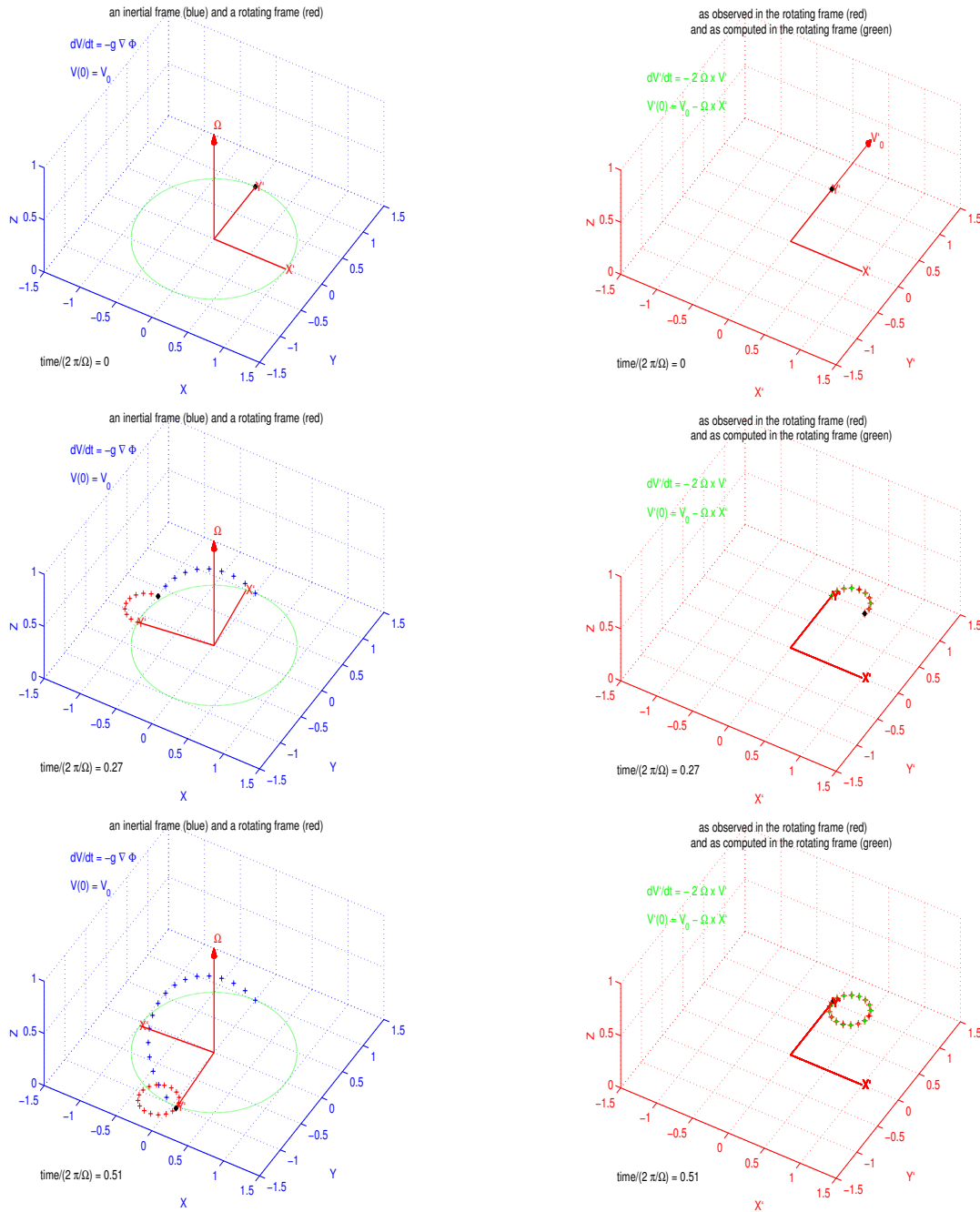


Figure 15: The two-dimensional trajectory of a parcel subject to a centripetal force, $-r\Omega^2$, as if it were on a frictionless parabolic surface. The initial velocity was a solid body rotation in balance with the centripetal force, and a small radial impulse was then superimposed. In this case the ratio $V'/V_\Omega \approx 0.2$, which is far larger than actually occurs in the ocean or atmosphere. The left column shows the resulting ellipsoidal trajectory as seen from an inertial frame, along with the circular trajectory that is seen from a rotating frame (indicated by the rotating, solid unit vectors). The right column shows the trajectory as seen from the rotating frame only, along with the solution computed in the rotating frame (shown as green dots). These lie exactly on top of the 'observed' trajectory and are very difficult to discern if color is not displayed; try the Matlab script coriolis.m (Section 9) that includes this and a number of other cases.

4.3.2 Inertial oscillations from the rotating frame

It is convenient to expand the rotating frame equation of motion (53) in Cartesian coordinates. Since we have restricted the analysis above to small displacements we can utilize the f-plane approximation that takes f as a constant. Thus the horizontal components u' , v' follow

$$\frac{d}{dt} \begin{bmatrix} u' \\ v' \end{bmatrix} = f \begin{bmatrix} -v' \\ u' \end{bmatrix}. \quad (67)$$

Given that the initial condition is an impulse causing a small velocity V_0 in the y-direction then the solution for velocity and displacement is just

$$\begin{bmatrix} u' \\ v' \end{bmatrix} = V_0 \begin{bmatrix} \sin(ft) \\ \cos(ft) \end{bmatrix} \quad \text{and} \quad \begin{bmatrix} X' \\ Y' \end{bmatrix} = \delta_0 \begin{bmatrix} 1 - \cos(ft) \\ \sin(ft) \end{bmatrix}. \quad (68)$$

The velocity of the parcel seen from the rotating frame, \mathbf{V}' , rotates at a rate of $f = 2\Omega$ in a direction opposite the rotation of the reference frame, Ω .³⁰ This is exactly the result found in the inertial frame analysis but was far simpler to obtain because we did not have to account for the absolute velocity, $\mathbf{V} = \mathbf{V}_\Omega + \mathbf{V}'$, but the relative velocity only. From the rotating frame perspective, Eqn. (53), the rotation of the velocity vector is attributable to deflection by the Coriolis force.³¹ This kind of motion, termed an inertial oscillation,³² is frequently observed in the upper ocean following a sudden shift in the wind speed or direction (Fig. 16).

³⁰Two questions for you: 1) How does this compare with the momentum balance and motion described by Eqn. (32)? 2) Suppose that the impulse was in the azimuthal direction, what would change?

³¹We noted in Section 3.4 that the rotating frame equations of motion does not support global momentum conservation or Galilean invariance. The former can be seen by noting that if all forces except Coriolis were zero, and the initial condition included a velocity, then that velocity would be continually deflected and change direction (as an inertial oscillation) with nothing else showing a reaction force; i.e., global momentum would not be conserved. This evident nonconservation is ignorable in most practical analyses. And too, when a central force \mathbf{F} produces a change of momentum in our parcel, the corresponding reaction force $-\mathbf{F}$ generates the complementary change of momentum in the (global) environment that would then undergo a compensating Coriolis deflection.

The Coriolis force is isomorphic to the Lorentz force, $q\mathbf{V} \times \mathbf{B}$, on a moving, charged particle in a magnetic field \mathbf{B} . Thus a charged particle moving through a uniform magnetic field will be deflected into a circular orbit with the cyclotron frequency, qB/M , analogous to an inertial oscillation at the frequency f . General Relativity predicts that a rotating (massive) object is accompanied by a 'gravitomagnetic' field analogous to a magnetic field, and that gives rise to a Coriolis-like force on moving objects. The Gravity Probe B satellite mission seeks to test this aspect of General Relativity; <http://einstein.stanford.edu/index.html>

³²The name 'inertial oscillation' is very widely accepted but is not highly descriptive of the dynamics in either the rotating or inertial reference frame. For the rotating frame, 'Coriolis oscillation' might be more appropriate, and for the inertial frame see D. R. Durran, 'Is the Coriolis force really responsible for the inertial oscillation?' *Bull. Am. Met. Soc.*, **74**(11), 2179–2184 (1993).

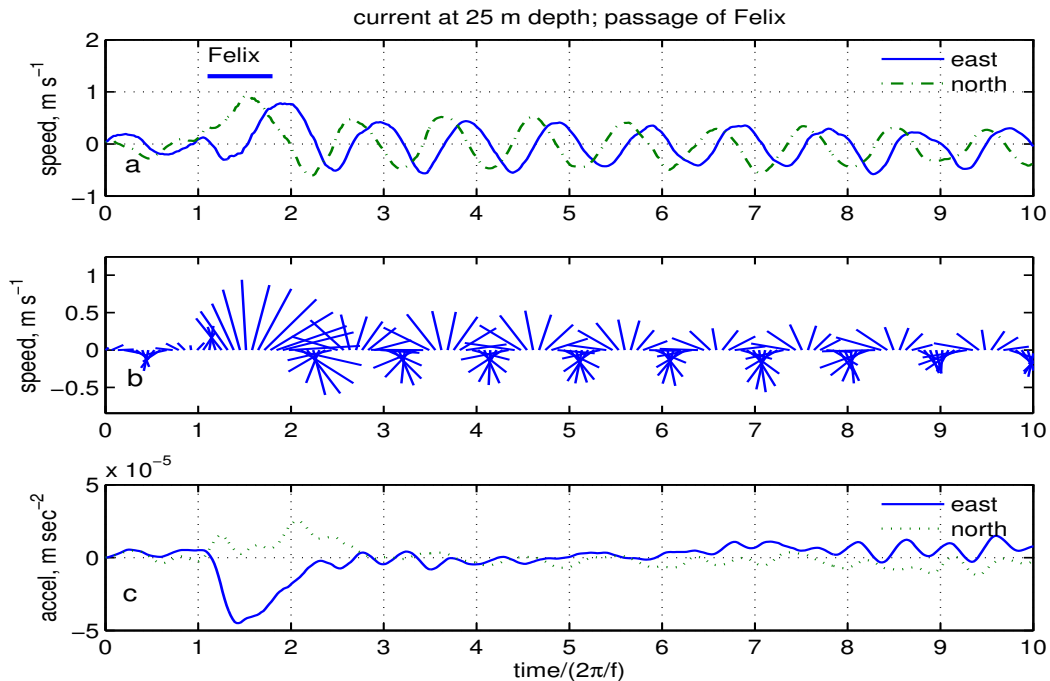


Figure 16: (a and b) Ocean currents at a depth of 25 m, measured by a current meter deployed southwest of Bermuda. The time scale is inertial periods, $2\pi/f$, which are nearly equal to days at this latitude. Hurricane Felix passed over the current meter mooring at the time noted at upper left, and the strong and rapidly changing wind stress produced energetic, clockwise rotating currents within the upper ocean. To a first approximation these are inertial oscillations. They differ from pure inertial oscillations in that their frequency is roughly 5% percent higher than f and their amplitude e-folds over about 10 days (by inspection of these data). These small departures from pure inertial motion are indicative of wave-like dynamics considered in Section 7.2. (c) Acceleration estimated from the current meter data as $d\mathbf{V}'/dt + 2\boldsymbol{\Omega} \times \mathbf{V}'$, as if the measurements were made on a specific parcel. The large acceleration to the west northwest corresponds in time to the passage of Felix. The direction of the estimated acceleration is roughly parallel to the observed winds (not shown here). Notice the much smaller oscillations having a period of about 0.5 inertial periods (especially for $t > 8$). These are very likely due to pressure gradients associated with the semidiurnal tide. This is a small part of the data described in detail by Zedler, S.E., T.D. Dickey, S.C. Doney, J.F. Price, X. Yu, and G.L. Mellor, 'Analysis and simulations of the upper ocean's response to Hurricane Felix at the Bermuda Testbed Mooring site: August 13-23, 1995', *J. Geophys. Res.*, **107**, (C12), **25-1 - 25-29**, (2002), available online at <http://www.opl.ucsb.edu/tommy/pubs/SarahFelixJGR.pdf>.

5 A dense parcel on a slope.

The next problem is to model the motion of a dense parcel that is released onto a sloping sea floor. The Coriolis force will be calculated using the constant f approximation. The vertical buoyancy force (per unit mass) is $g' = g \frac{\delta\rho}{\rho_0}$, where $\delta\rho$ is the density anomaly of the parcel with respect to its surroundings (assumed constant), and ρ_0 is a nominal sea water density, 1030 kg m^{-3} . Because the sea floor is sloping, there is a component of the buoyancy force parallel to the sea floor, $g'\alpha$ where α is the bottom slope, presumed to have a y component only. If the parcel is in contact with a sloping bottom, then it is plausible that the momentum balance should include a frictional term due to bottom drag. The task of estimating an accurate bottom drag for a specific case is beyond the scope here, and we will represent bottom drag by the simplest linear (or Rayleigh) drag law in which the drag is presumed to be proportional to and antiparallel to the velocity difference between the current and the bottom, i.e., bottom drag = $-r(\mathbf{V} - \mathbf{V}_{\text{bot}})$.³³ The ocean bottom is at rest in the rotating frame and hence $\mathbf{V}_{\text{bot}} = 0$ and omitted from here on. From observations of ocean currents we can infer that a reasonable value of r for a density-driven current on a continental shelf is $r = O(10^{-5}) \text{ s}^{-1}$. Thus r is roughly an order of magnitude smaller than a typical mid-latitude value of f . Since r appears in the momentum equations in the same way that f does we can anticipate that rotational effects will be dominant over frictional effects. The equations of motion are then:

$$\begin{aligned}\frac{du}{dt} &= fv - ru, \\ \frac{dv}{dt} &= -fu - rv + g'\alpha,\end{aligned}\tag{69}$$

and we assume initial conditions $u(0) = 0, v(0) = 0$. The depth of the parcel can be computed diagnostically from the y position and the known slope. Notice that we have dropped the superscript prime that had previously been used to indicate the rotating frame variables and we have used the thin fluid approximation for the Coriolis force terms. We also use the f -plane approximation that $f = \text{constant}$ since typical parcel displacements are very small compared to the Earth's radius (more on this below). The solution of this linear model is not complex by the standards of fluid dynamics,

$$\begin{aligned}u(t) &= \frac{g'\alpha}{r^2 + f^2} [f - \exp(-tr)(f \cos(ft) - r \sin(ft))], \\ v(t) &= \frac{g'\alpha}{r^2 + f^2} [r - \exp(-tr)(f \sin(ft) + r \cos(ft))],\end{aligned}\tag{70}$$

³³A linear drag law of this sort is most appropriate as a model of viscous drag in a laminar boundary layer within which $\tau = \mu \frac{\partial U}{\partial z}$, where μ is the viscosity of the fluid. The boundary layer above a rough ocean bottom is almost always fully turbulent above a very thin, $O(10^{-3} \text{ m})$, laminar sublayer that is in contact with the bottom. If the velocity used to estimate drag is measured or computed for a depth that is within the fully turbulent boundary layer, as it is bound to be, then the appropriate drag law can be approximated as independent of the viscosity and is quadratic in the velocity, $\tau \propto \rho U^2$. Our use of a linear drag law is purely expedient.

but it does contain three parameters along with the time, and so has a fairly large parameter space. Our interest is not so much any one specific solution but rather to understand the quantitative effects of rotation and friction over the entire family of solutions. How can we display the solution to this end?

One approach that is very widely applicable is to rewrite the governing equations and (or) the solution using nondimensional variables. This will serve to reduce the number of parameters to the fewest possible while retaining everything that was present in the dimensional equations. To define these nondimensional variables we begin by noting that there are three external parameters in the problem (external in that they do not vary with a dependent variable): the buoyancy and bottom slope, $g'\alpha$, which always occur in this combination and so count as one parameter, an acceleration; the Coriolis parameter, f , an inverse time scale, and the bottom friction coefficient, r , also an inverse time scale. To define a nondimensional time we need an external time scale and choose the inverse of the Coriolis parameter, $t_* = tf$, rather than r^{-1} , since we expect that rotational effects will dominate frictional effects in most cases of interest. To form a nondimensional velocity we make an estimate of the velocity scale as the product of the acceleration and the time scale f^{-1} as $U_{geo} = (g'\alpha)/f$ and thus the nondimensional velocity is just $u_* = u/(g'\alpha/f) = u/U_{geo}$ and similarly for the v component. We will explain the subscript geo(strophic) shortly. Rewriting the governing equations in terms of these nondimensional variables gives

$$\begin{aligned}\frac{du_*}{dt_*} &= v_* - Eu_*, \\ \frac{dv_*}{dt_*} &= -u_* - Ev_* + 1,\end{aligned}\tag{71}$$

where E is the Ekman number,

$$E = \frac{r}{f}$$

the nondimensional ratio of the linear friction parameter to the Coriolis parameter (more on E below). The initial conditions are $u_*(0) = 0$, $v_*(0) = 0$. The solution to these equations is

$$\begin{aligned}u_*(t_*) &= \frac{1}{1+E^2} [1 - \exp(-Et_*)(\cos(t_*) - E \sin(t_*))], \\ v_*(t_*) &= \frac{1}{1+E^2} [E - \exp(-Et_*)(\sin(t_*) + E \cos(t_*))],\end{aligned}\tag{72}$$

and for completeness;

$$u_* = \frac{u}{g'\alpha/f}, \quad v_* = \frac{v}{g'\alpha/f}, \quad \text{and} \quad t_* = tf.$$

The geostrophic velocity scale $g'\alpha/f$ appears with the velocity only, and thus the single nondimensional parameter E serves to define the parameter space of this problem. There are other forms of the Ekman number depending upon the way that friction is parameterized. They all have in

common that small E indicates small friction compared to rotation.³⁴ Trajectories computed from Eqn. (72) for several values of E are in Fig. (17 left). Trajectories having larger E show both a more rapid damping of the inertial oscillations and a steeper descent of the slope, i.e., greater frictional effects than do the solutions with small E . In place of 'large friction' or 'large rotation', we have instead large or small E , which takes account of variation of both r and f . Thus, for a given r , we would expect that frictional effects are greater at low latitudes than at higher latitudes.

5.1 Inertial and geostrophic motion

The solution Eqn. (72) can be envisioned as the sum of two distinct modes of motion, a time-dependent, oscillatory motion, the now familiar inertial oscillation,

$$\begin{bmatrix} u_* \\ v_* \end{bmatrix} \propto \exp(-Et_*) \begin{bmatrix} \cos(t_*) \\ \sin(t_*) \end{bmatrix},$$

here damped by friction, and a time mean motion that is the single parcel equivalent of geostrophic motion

$$\begin{bmatrix} u_* \\ v_* \end{bmatrix} \propto \begin{bmatrix} 1 \\ E \end{bmatrix},$$

also modified by friction. In this linear model the amplitude of either mode³⁵ is directly proportional to the velocity scale, $U_{geo} = g'\alpha/f$. For a dense water parcel on a continental slope (Fig. 18) rough values are $g' = g(\delta\rho)/\rho_0 \approx g0.5/1000 = 10^{-2} \text{ m s}^{-2}$, $\alpha = 1.3 \times 10^{-2}$, and f at latitude 62 N is $1.3 \times 10^{-4} \text{ s}^{-1}$. This gives a geostrophic speed $U_{geo} \approx 0.5 \text{ m s}^{-1}$, cf. Fig. (18).

The inertial oscillations found in this solution are the consequence of starting from a state of rest and the imposition of what amounts to an impulsively started external force (the buoyancy force). This is not an especially realistic model of a density current released onto a continental slope, but it does serve as a first approximation of the rapidly changing wind stress exerted upon the upper ocean during the passage of a storm (Fig. 16). A pure inertial oscillation, that is, an exact two term balance between

³⁴If this is one of your first encounters with dimensional analysis then this procedure is likely to seem arbitrary and esoteric. You will come to appreciate the benefits of dimensional analysis with experience, mainly, but an attempt to help is 'Dimensional analysis of models and data sets', by J. Price, *Am. J. Phys.*, **71**(5), 437–447 (2003) and available online from <http://www.whoi.edu/science/PO/people/jprice/class/DA-AJP.pdf> Any specific dimensional analysis may indeed be somewhat arbitrary, as there are usually several plausible forms. For example, in this problem we could have used $1/r$ to measure (or nondimensionalize) the time. How would this change the solution, Eqn. (72)?

³⁵This usage of 'mode' may be a little unusual; the intent is to identify a possible two term balance within the equation of motion, i.e., between a pressure gradient and the Coriolis force, for example. By this we are not asserting that such a balance necessarily holds strictly even within our very simple models but rather that modes are a kind of vocabulary useful for describing the complex balances that actually do occur. When the equations or physical phenomena are nonlinear, as they usually are, then the actual solution or flow will not be a sum over the modes computed individually. Beyond those already noted, what other modes could be present in Eqs. (72)?

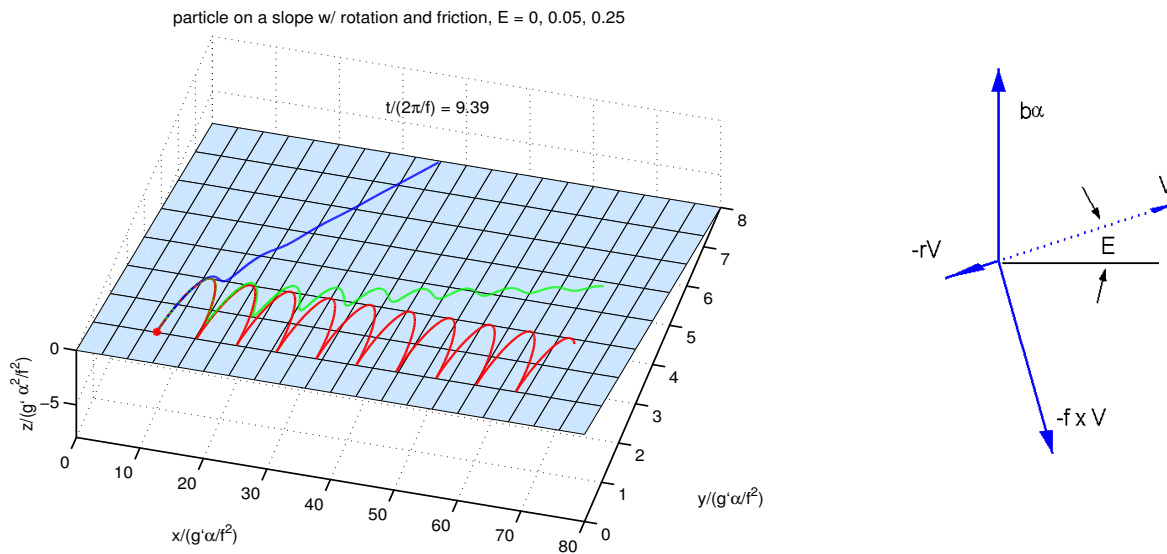


Figure 17: (left) Trajectories of dense parcels released from rest onto a sloping bottom computed by integrating the horizontal velocity, Eqn. (72). The elapsed time in units of inertial periods, $2\pi/f$, is at upper left. The buoyancy force is toward positive y and the Ekman number, E , has the values shown. Notice that for values of $E \ll 1$ (red trajectory), the long-term displacement is nearly at right angles to the imposed force, indicative of geostrophic balance. The along- and across-slope distance scales are distorted by a factor of almost 10, so that the blue trajectory having $E = 0.25$ makes a shallower descent of the slope than it first appears here. Click on this panel to start an animation. (right) The force balance (solid arrows) and the time-mean motion (the dashed vector) for the case $E = 0.25$. The angle of the velocity with respect to the isobaths is $E = r/f$, the Ekman number. The Coriolis force (M) is labeled $-\mathbf{f} \times \mathbf{V}$ where \mathbf{f} is f times a vertical unit vector. Simulations of this sort are carried out by the script `partslope.m` (Section 9).

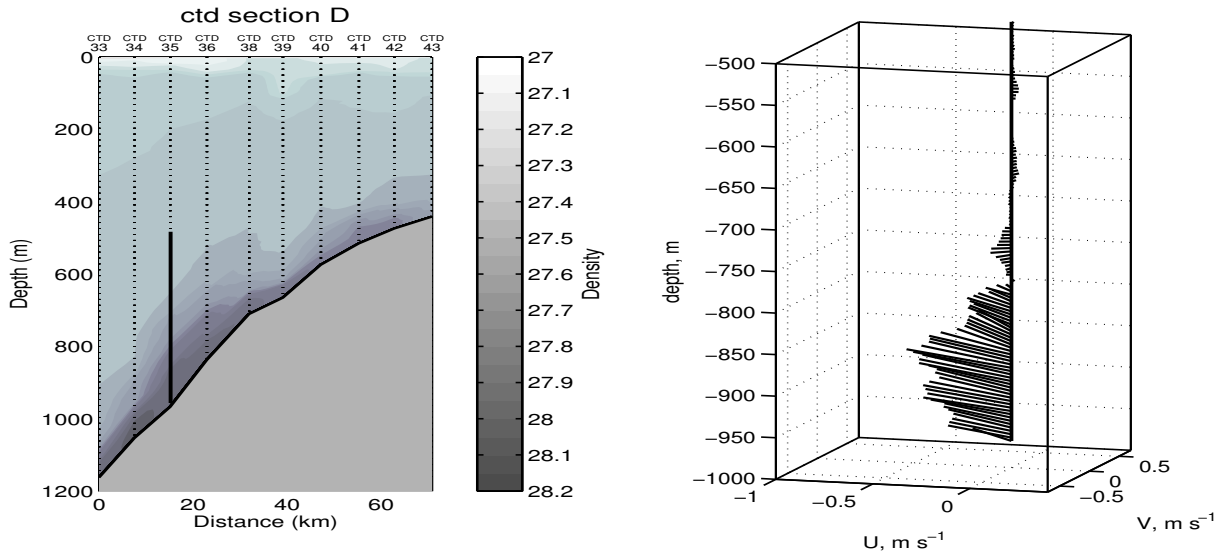


Figure 18: Observations of density and currents along the southern flank of the Scotland-Iceland Ridge, about 90 km west of the Faroe Islands. The dense water found along the bottom is an outflow from the Norwegian-Greenland Sea that has come through the narrow Faroe Bank Channel (about 15 km width, at latitude 62 North) and that will eventually settle into the deep North Atlantic. The units of density are kg m^{-3} , and 1000 has been subtracted away. Currents were measured at the thick vertical line shown on the density section. The density section is aligned normal to the isobaths and the current appeared to be flowing roughly along the isobaths, but the direction was temporally varying. What is clearer is that the core of the dense water has descended roughly 200 m between this site and the narrow Faroe Bank Channel, about 90 km upstream from this site. A question: which trajectory of Fig. (17) is analogous to this current? Said a little differently, what is the approximate Ekman number of this current?

the time rate of change and the Coriolis force (Eqn. 67), would not evolve with time; the amplitude would remain constant and the frequency = f for all time. The amplitude of the (near) inertial oscillations seen in the field data of Fig. (16) and the model solution of (17) decrease with time; the model-computed oscillations decay as $\exp(-Et_*)$ on account of bottom drag.³⁶

³⁶A couple of questions for you: 1) Can you devise an initial condition for this problem that would eliminate the inertial oscillations? Could you make the inertial oscillations larger than those shown in Fig. (17, left)? To test your hypothesis you might try experimenting with the Matlab script partslope.m 2) Draw the vector force balance for inertial oscillations (include the acceleration) with and without bottom drag as in Fig. (17, right). 3) We have pointed out that the value of the bottom drag coefficient r is not well known *a priori* and so we might regard r as an adjustable parameter. What value of r is required to mimic the observed decay of near-inertial oscillations of Fig. 16? Does the same model solution also account for the small, super-inertial frequency shift noted in the field data?

5.2 Energy budget

The energy budget can make an interesting diagnostic of a phenomenon (provided that there are not large, unknown dissipation terms). In this case we know the dissipation exactly, and with a little thought it is clear that the only source of energy in this problem is the potential energy associated with the dense parcel sitting on a sloping bottom. If the parcel descends the slope, it will release potential energy. To go further we need to derive and evaluate the energy budget (per unit mass) of our single parcel; we multiply the x -component momentum equation by u_* and the y -component equation by v_* and add:

$$\frac{d(u_*^2 + v_*^2)/2}{dt_*} = v_* - E(u_*^2 + v_*^2). \quad (73)$$

Notice that the Coriolis force *per se* drops out of the energy budget since it is normal to the current and does no work. The term at left is kinetic energy, and the second term on the right is work by friction. The first term on the right is the rate of work by the buoyancy force which can also be interpreted as the rate of release of potential energy, $PE = g'(z - z_0) = g'\alpha(y - y_0)$,

$$v_* = \frac{vf}{(g'\alpha)^2} = \frac{dz}{dt} g'\alpha \frac{f^2}{(g'\alpha)^2} = \frac{-dPE}{dt} \frac{1}{U_{geo}^2}.$$

Potential energy is the only energy source in this problem, and the reference depth, z_0 , is arbitrarily set at the initial depth. It can be helpful to integrate with time to see energy changes from the initial state:

$$\begin{aligned} (u_*^2 + v_*^2)/2 - \int_0^t v_* dt_* &= - \int_0^t E(u_*^2 + v_*^2) dt_* \\ KE + PE &= FW \end{aligned} \quad (74)$$

where KE is the kinetic energy, PE is the change in potential energy as the parcel moves up and down the slope, and FW is the work by the bottom friction (Fig. 19).

After the parcel was released from a state of rest, it first descended the slope, converting potential energy into kinetic energy, though with some loss to friction. The Coriolis force then turned the moving parcel to the right and by about $t = 1/f$ or $t_* = 1/(2\pi)$, the parcel had been turned significantly, 1 radian or about 50° , with respect to the buoyancy force. The time scale for the Coriolis force to have an appreciable effect on a moving object is thus $1/f$, a very important time scale that we will see again. The Coriolis force continued to turn the parcel to the right, and by about $t_* = 1/2$ had turned the parcel back up the slope, converting kinetic energy back into potential energy. This parcel did not quite reach it's initial height because of frictional losses, i.e., energy was not conserved.

Though the Coriolis force does not appear directly in the energy budget it nevertheless has a profound effect on the energy budget overall in as much as it inhibits the release of potential energy. If there is some friction, as there was in the case shown, then the cross-isobath component of the motion (which carries the parcel to greater bottom depth and thus releases potential energy) is proportional to

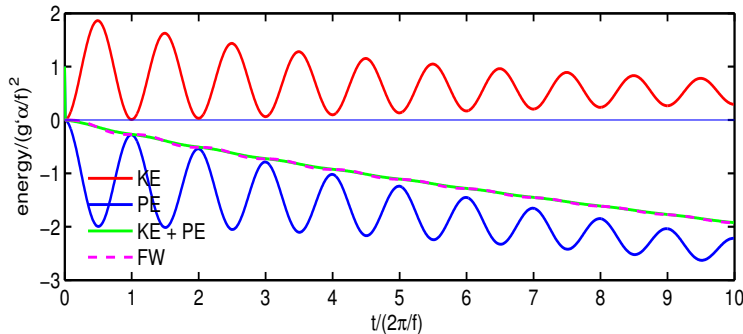


Figure 19: The energy budget for the trajectory of Fig. (17) having $E = 0.2$. These data are plotted in a nondimensional form in which the energy or work is normalized by the square of the velocity scale, $U_{geo} = g'\alpha/f$, and time is nondimensionalized by the inertial period, $2\pi/f$. Potential energy was assigned a zero at the initial depth of the parcel. Note the complementary inertial oscillations of PE and KE, and that the decrease of total energy was due to work against bottom friction (the green and dashed red lines overlay one another).

the Ekman number, from Eqn. (72), $v_*/u_* = E$, and thus inversely proportional to f for a given frictional coefficient, r . Whether friction or rotation is dominant, and thus whether circulations are rapidly dissipated or long-lived, depends solely upon the Ekman number in this highly simplified system (Fig. 17b). In the limit that $E \rightarrow 0$, the time-averaged motion becomes perpendicular to the buoyancy force and the parcel simply coasts along isobaths with no temporal evolution in velocity (or depth) and no energy exchanges, the energy budget consequence of an exact geostrophic balance.³⁷

6 Part II: Geostrophic adjustment and potential vorticity.

In this second part of the essay we will consider several problems that are variants on geostrophic adjustment — a thickness anomaly on a dense fluid layer will be released from a state of rest and allowed to flow under the influence of gravity and the Coriolis force (friction, too, in the homework). The general aim is to understand how Earth's rotation effects the resulting motions, and specifically to understand how the Coriolis force will, under common conditions, lead to a steady (or quasi-steady) motion in geostrophic balance, e.g., the westerlies of Fig. 1 and the eddies and ocean gyres of Figs. 2

³⁷Some questions for you to consider: (1) This parcel oscillating on a slope is reminiscent of a viscous pendulum started from rest with a displaced bob. Can you describe an analogy between the Coriolis force and the tension in the line of the pendulum? (2) Assuming small Ekman number, how long does it take for a geostrophic balance to arise? (3) Are the time-averaged solutions of the single parcel model the solutions of the time-averaged model equations? Suppose the model equations were not linear, say that friction is $\propto U^2$, then what? (4) Inertial oscillations do not contribute to the long-term displacement of the parcel, though they can dominate the instantaneous velocity. Can you find an initial condition on the parcel velocity that prevents these pesky inertial oscillations? For this you may want to use partslope.m (Section 9). (5) Suppose the parcel is moving parallel to the isobaths, but at a speed that is a little less than the geostrophic speed - what happens next? (6) Finally, can you explain, in words, why a geostrophic balance (or a near geostrophic balance) is expected, given only small E and sufficient space?

and 3. This is a very important first step toward understanding the large scale atmosphere and ocean, and one that we can fairly claim to take in this essay and via the homework extensions. The next significant step in understanding is to learn how small departures from geostrophy will cause large scale phenomena to evolve in time, i.e., to propagate, change scale, dissipate, etc. By comparison this is an almost open-ended task that makes up a large part of geophysical fluid dynamics; we can make a beginning in Section 7.3.

6.1 The shallow water model

The horizontal structure and variability of winds and currents is of particular interest here, and for this purpose we can utilize a model of a single fluid layer. This layer is presumed to have a nominal thickness, H , that is spatially uniform, and it sits upon a lower, solid boundary (e.g., the sea floor) that is at a depth $z = -H - b(x, y)$ (Fig. 20). The anomaly of layer thickness (above a level surface) is $\eta(x, y, t)$ and will vary with horizontal position and with time. The total thickness of the layer is thus $h = H + b + \eta$. From here until Section 7.3.4 we will take $b = 0$ (flat bottom) for simplicity. The fluid above the layer is taken to have uniform pressure horizontally and no motion, and a uniform density ρ_o . The fluid within the active layer has a greater density, $\rho_o + \delta\rho$ where $\delta\rho$ is a specified constant. The horizontal domain is either one-dimensional (in Sections 7.1 and 7.2) or two-dimensional (Section 7.3). Motion was started from a state of rest by releasing an elevated ridge (Sections 7.1 and 7.2) or circular eddy (Section 7.3) that slumps under gravity and initiates waves and currents.

Compared with the single parcel model of Section 5, this single layer fluid model is a significant step toward a realistic model of large scale flow of the atmosphere and ocean. The principle idealization is that the horizontal velocity \mathbf{V} within the layer is depth-independent. Winds or currents are thus represented by a two component vector field i.e., $\mathbf{V}(x, y, t) = [u(x, y, t), v(x, y, t)]$, vs. $\mathbf{V}(x, y, z, t)$, a bigger help than it may first appear. To be a valid approximation this requires that the horizontal scale of the motion (e.g., a wavelength) must be considerably greater than the layer thickness, H . In that sense the layer is (or should be) shallow compared to the motions of interest, and the resulting single layer model equations are appropriately termed the shallow water system.³⁸

In Section 2 our goal was to learn the origin of the Coriolis force, and so it was appropriate to go through a very deliberate transformation of acceleration into a rotating reference frame and thus to derive the Coriolis force. The goal now is to begin to understand some of the consequences of Earth's rotation in the context of a simple fluid model and a geostrophic adjustment problem. To keep the scope

³⁸If our intent was to utilize the shallow water model to make a realistic simulation of an observed phenomenon, then we would have to argue in favor of three idealizations: 1) that the initial state was free of vertical shear, $\partial\mathbf{V}/\partial z = 0$, 2) that the layer of interest was outside of frictional boundary layers, and 3) that the horizontal density variation within the layer was effectively zero. Most real geophysical flows violate all three of these conditions to some degree, and so may require a number of layers stacked one on top of another to represent vertical shear, boundary layers, stratification, etc. One layer is enough for us, for now.

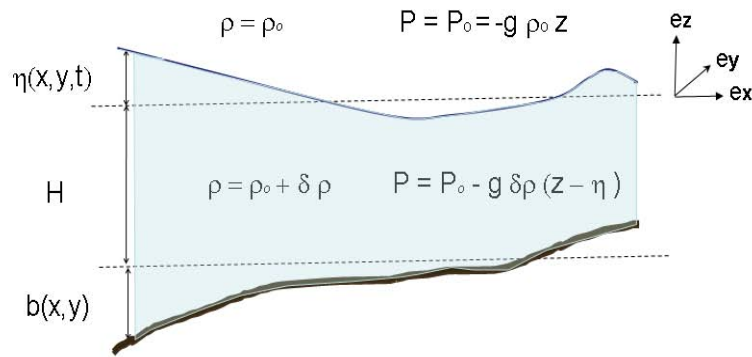


Figure 20: Schematic of a single fluid layer sitting on a variable-depth lower, solid surface. The horizontal dashed lines are level surfaces (perpendicular to gravity). This layer could be a uniform-density (barotropic) ocean, in which case η is the sea surface and the fluid above is the atmosphere and hence $\delta\rho \gg \rho_0$. Or, it could be a relatively dense layer within a (baroclinic) ocean, in which case $\delta\rho \ll \rho_0$.

of this essay under control we are now going to emphasize application over derivation, and jump straight into (the shallow end of) fluid dynamics.³⁹ The momentum balance of a shallow fluid layer including the Coriolis force may be written

$$\frac{D\mathbf{V}}{Dt} = \frac{\partial\mathbf{V}}{\partial t} + \mathbf{V} \cdot \nabla\mathbf{V} = -f\mathbf{k} \times \mathbf{V} - \frac{1}{\rho_0} \nabla P - r\mathbf{V},$$

where the time derivative $D(\)/Dt$ is called the material derivative or the derivative 'following the flow', about which more below. The anomaly of hydrostatic pressure within the layer is

$$P(x, y, z, t) = -g(\rho_0 z + \delta\rho(z + \eta(x, y, t))) \quad (75)$$

and directly proportional to the layer thickness anomaly, η . Thus an elevated layer thickness indicates a high pressure anomaly. The horizontal component of the pressure gradient force that drives the flow is

$$-\nabla P = -g\delta\rho\nabla\eta(x, y, t) \quad (76)$$

and is depth-independent within the layer. Rewriting the momentum balance in terms of η and reduced gravity $g' = g\delta\rho/\rho_0$ gives

$$\boxed{\frac{D\mathbf{V}}{Dt} = \frac{\partial\mathbf{V}}{\partial t} + \mathbf{V} \cdot \nabla\mathbf{V} = -f\mathbf{k} \times \mathbf{V} - g'\nabla\eta - r\mathbf{V}} \quad (77)$$

³⁹The shallow water equations used here are derived in most GFD texts⁸ and in detail in an excellent online source: <http://kiwi.atmos.colostate.edu/group/dave/pdf/ShallowWater.pdf>

The pressure gradient has exactly the form of the buoyancy force on a dense parcel on a slope (Section 5), with the crucial difference that the gradient of the thickness anomaly replaces the fixed, prescribed bottom slope. The thickness anomaly is a part of the flow (a dependent variable) that changes with time and position depending upon the divergence of the velocity times layer thickness,

$$\boxed{\frac{D\eta}{Dt} = \frac{\partial\eta}{\partial t} + \mathbf{V} \cdot \nabla\eta = -h\nabla \cdot \mathbf{V}} \quad (78)$$

often called the continuity equation.

To complete the specification of a problem we have to define the computational domain over which the governing equations will be solved, and specify appropriate boundary conditions on the edges of the domain. For the computational domain, we will take a square region that is 4000 km on a side. In the geostrophic adjustment problems to follow, the only energy source is the eddy near the center of the domain, and hence we can expect that waves will be radiated outward only, i.e., that nothing will come from outside the domain in. A plausible and fairly effective representation of this one-way outward transfer is a radiation boundary condition,

$$\frac{\partial\psi}{\partial t} = -C\frac{\partial\psi}{\partial n} \quad (79)$$

where ψ is any variable, and n is the direction normal and outward from the boundary. The speed C is taken to be the gravity wave speed, $C = \sqrt{g'H}$, the fastest moving wave in the shallow water system (more on this in Section 7.1).

6.2 Solving and diagnosing the shallow water system

Equations (77) and (78) are a coupled set of nonlinear, partial differential equations in three dependent variables, the two components of the horizontal velocity, $\mathbf{V} = [u, v]$, and the thickness anomaly, η . This system is nonlinear because the material derivative, $D(\cdot)/Dt = \partial(\cdot)/\partial t + \mathbf{V} \cdot \nabla(\cdot)$, includes an advection term that is the product of two dependent variables, velocity times the velocity gradient in Eqn. (77), or velocity times thickness gradient in Eqn. (78). These nonlinear advection terms contribute some of the most interesting phenomenon of fluid dynamics and they also stymie analytic solution methods. Solutions of the full shallow water system are necessarily generated by numerical methods: the one-dimensional cases shown here were solved by the Matlab script `geoadj_1d.m`, and the two-dimensional cases by the Fortran code `geoadj_2d.f`, both of which are available from the web site noted in Section 9. In common with any numerical model, these models produce (putative) solutions in the form of huge data files, $u(x_i, y_i, t_j), v(x_i, y_i, t_j), \dots$, where x_i, t_i are discretized position and time, and that's it. To learn something useful from a mass of such numerical data requires as much effort and thought as generating the solution in the first place. To wit, we will 1) diagnose the budgets of energy and vorticity (described below), 2) compare the wave-like properties of the solution with the dispersion

relation of the linear shallow water system, and then 3) form and test conjectures by conducting further numerical experiments (that will be the homework, actually).

6.2.1 Energy balance

The total mechanical energy of the layer, $E = KE + PE$, is the sum of kinetic energy, $KE = \frac{1}{2}\rho_0 h \mathbf{V}^2$ and potential energy, $PE = \frac{1}{2}g'h^2$. To find the rate of change of KE we take the dot product of the momentum equation with the velocity, and the rate of change of PE is found by multiplying the continuity equation by the total thickness. In the absence of external forcing (bottom friction set to zero) the total energy follows the budget equation

$$\frac{DE}{Dt} + \nabla \cdot (g'h^2\mathbf{V}) = 0. \quad (80)$$

that includes a flux term due to pressure work. For example, if the pressure anomaly is positive on the (permeable) boundary of a control volume where the velocity is directed outward, say, then the fluid inside the control volume will be doing pressure work on the fluid outside of the control volume. The total energy within the control volume will thus decline, while the energy outside the control volume will increase. This pressure-work term accounts for the energy transport associated with wave radiation across an open boundary, for example. The fluid flow can also transport energy at the rate \mathbf{V} , a process accounted by the advection term, $\mathbf{V} \cdot \nabla E$, of the total derivative.

6.2.2 Potential vorticity balance

Up to now, our point of view of Earth's rotation has been through the *linear* momentum balance (linear here in the geometric sense), and the Coriolis *force*. That is still entirely relevant in the shallow water model, but there is another and complementary point of view, *angular* momentum balance, that has proven immensely fruitful for the understanding of fluid dynamics generally and geophysical fluid dynamics especially. Two main reasons, to get a little ahead in this short story, are that 1) Earth's rotation provides a very large background angular momentum that is made visible by small changes in the thickness or latitude of a fluid column (described here), and, 2) the angular momentum balance amounts to a kind of filter that serves to highlight the processes that cause departures from geostrophic balance while eliminating gravity wave motions (Section 7).

Back a step or two..... to analyze the motion of a rotating, solid object, say a gyroscope, you might begin by computing the linear momentum balance of the component pieces. Thus would require an accounting of radial accelerations and internal stresses on each piece and would likely be a fairly arduous task. Assuming that the gyroscope is not at risk of breaking up, then at some point you might decide to take the structure for granted, and focus your effort toward analyzing the angular (azimuthal) momentum balance. As a first step you would define a coordinate system that gave the most compact

and least complex accounting of the moment of inertia of the gyroscope and then consider the processes that cause the angular momentum to change with time. The physical content of your angular momentum analysis would not be fundamentally different from the linear momentum description, but it would likely be a great deal simpler in the same way that choosing appropriate variables and an appropriate coordinate system can facilitate any mathematical analysis. The same considerations apply to an analysis of a fluid flow: an angular momentum analysis and description will often be a good deal simpler and so more insightful than is the otherwise equivalent linear momentum analysis.

The fluid flow equivalent of angular velocity is the curl of the fluid velocity,

$$\xi \equiv \nabla \times \mathbf{V},$$

called the vorticity. If the fluid velocity is a three-dimensional vector, then so too is the vorticity. Because the shallow water velocity is two-dimensional, the shallow water vorticity

$$\xi = \nabla \times \mathbf{V} = \left(\frac{\partial V}{\partial x} - \frac{\partial U}{\partial y} \right) \mathbf{z} \quad (81)$$

has a vertical component only and is effectively a scalar. You can visualize vorticity as the rotation of small (but not quite point-like) cylinders, or two-dimensional parcels, that make up the fluid.⁴⁰ The vorticity of a fluid is unlike the angular momentum that we associate with a solid object in that it is defined at every point in a fluid, i.e., we associate a vorticity field with a fluid flow, just as there is a velocity field and a thickness field in the shallow water model.

The governing equation for vorticity may be found by taking the curl of the momentum equation, $\partial/\partial x$ of the y -component minus $\partial/\partial y$ of the x -component. The effect of applying the curl operator is that all of the forces that are derivable from a potential are eliminated, most notably the pressure gradient, i.e., $\partial^2 \eta / \partial x \partial y - \partial^2 \eta / \partial y \partial x = 0$. A divergence term $\partial u / \partial x + \partial v / \partial y$ will arise and may be eliminated using the thickness (continuity) equation, (78). After a little further rearrangement (which you should verify, first with the linear shallow water system of Section 6.3) the result is a conservation law for a scalar called the potential vorticity, q ,

$$q = \frac{f + \xi}{h} \quad \text{and} \quad \frac{Dq}{Dt} = 0 \quad (82)$$

that includes the vorticity, ξ . In this context,

⁴⁰An essential resource for vorticity and much else in fluid mechanics is the collection of fluid mechanics films available online at <http://web.mit.edu/hml/ncfmf.html> Vorticity and potential vorticity are treated in every GFD text⁸, and some of the kinematic aspects of are discussed in Section 6 of the companion essay 'Lagrangian and Eulerian representations...' <http://ocw.mit.edu/ans7870/resources/price/index.htm>

If the sense of the rotation is in the same direction as Earth's rotation, the vorticity is often said to be *cyclonic* (from the Greek *kyklon*, for circular motion). Cyclonic rotation is thus counterclockwise in the northern hemisphere and clockwise in the southern hemisphere. Anticyclonic is the reverse.

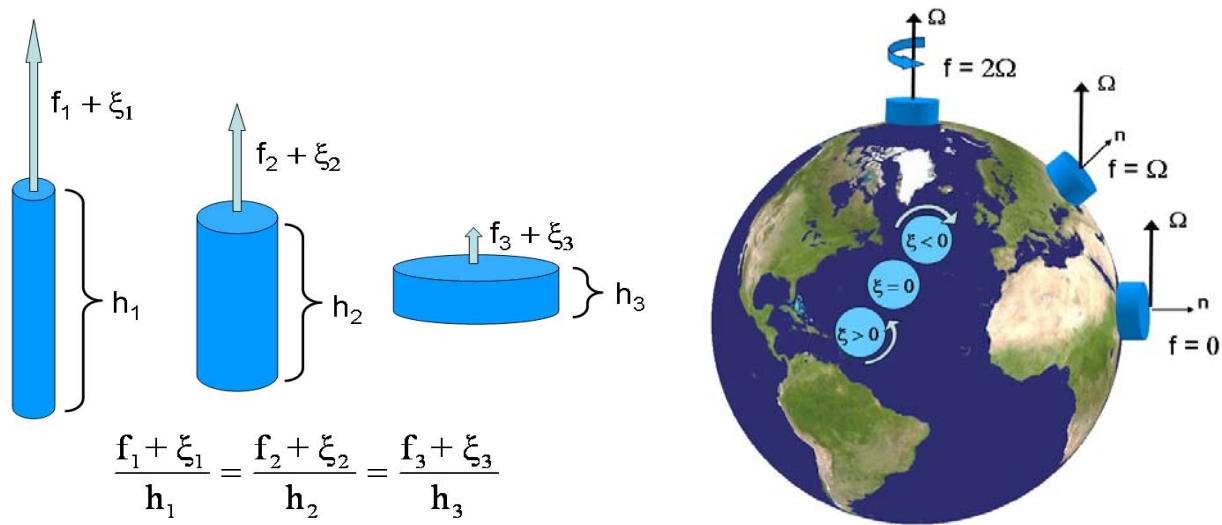


Figure 21: Schematic fluid columns and a rotating Earth. (left) Rotating fluid columns that have a constant volume but variable height, h . Absent external torques, the potential vorticity of the column, $(f + \xi)/h$, will be conserved under changes of thickness. Hence the absolute vorticity, $f + \xi$, will change in proportion to h as indicated by the variable length of the rotation vectors, i.e., $(f_1 + \xi_1)/h_1 = (f_2 + \xi_2)/h_2$ etc. (right) The columns perched at upper and right on the Earth are intended to show that the vorticity (twice the rotation rate) of a fluid column due solely to Earth's rotation is $\nabla \times \mathbf{V}_\Omega = 2\boldsymbol{\Omega} \cdot \mathbf{n} = 2\Omega \sin(\text{latitude}) = f$, where $\mathbf{V}_\Omega = -\boldsymbol{\Omega} \times \mathbf{X}$ is the planetary velocity due to Earth's rotation (Eqn. 51, Section 4.3). The planetary velocity \mathbf{V}_Ω is apparent to an inertial observer, as is the accompanying planetary vorticity, f . An Earth-bound observer will see only the relative velocity of winds and ocean currents, and the accompanying relative vorticity, ξ . The three columns in the North Atlantic are shown end-on to illustrate the sense of the relative vorticity that would be acquired by a q -conserving column that was displaced north or south away from a reference site where $\xi = 0$, all the while maintaining constant thickness (and absent external torques). An inertial observer will report that the column conserved the absolute vorticity, $f + \xi$. An Earth-bound observer will report that the north-south displacement of the column caused the ξ of the column to change in the sense indicated here.

ξ is often termed the *relative* vorticity, since it is the vorticity of the relative velocity, i.e., the winds and currents observed from an Earth-attached reference frame, and the \mathbf{V}' of Eqn. (51), though by now we have dropped the prime superscript on \mathbf{V} ,

f is termed the *planetary* vorticity, and is the vorticity of the planetary velocity due to Earth's rotation, $f = \nabla \times \mathbf{V}_\Omega$, Fig. (21) and Section 4.3,

$f + \xi$ is termed the *absolute* vorticity, since it is the vorticity of the absolute velocity, $\nabla \times (\mathbf{V}_\Omega + \mathbf{V}')$.

q conservation is powerful and useful precisely because it is remarkably simple and yet includes an important part of the velocity field — absent external forcing or friction, q of the shallow water model is conserved following a parcel. There is nothing comparable to the pressure work term found in the energy balance, Eqn. (80), that transmits energy at the speed of gravity waves. Instead, potential vorticity has the conservation property of a dye that, once put into a fluid, remains with the fluid no matter how complex the flow may be. Said a little differently, q is transported with the fluid velocity, and not the gravity wave velocity. But quite unlike a simple dye, the potential vorticity includes an important part (not all) of the velocity field. In some cases it may be sufficient to calculate the evolution of a flow from q -conservation only (the low frequency waves of Section 7.3 are an example), which is a marked simplification over solving the full shallow water system. In other cases, however, q may be irrelevant (the pure gravity wave dynamics of Section 7.1).

Potential vorticity amounts to a generalized angular momentum insofar as it accounts for a variable moment of inertia (thickness) as well as the vorticity f due to the Earth's rotation. The planetary vorticity is extremely important in this regard, because, for most large scale flows, f is considerably larger than is ξ , often by a factor of 10 or more. A fluid column having potential vorticity will exhibit a kind of gyroscopic rigidity in the sense that it will respond to changes in the parcel configuration (thickness) or to changes in latitude and thus f . For example, suppose that a fluid column has absolute vorticity $(f_1 + \xi_1)$ and thickness h_1 in an initial state, and is then squashed from h_1 to h_2 . Assuming only that the squashing occurs without frictional or external torques, then the absolute vorticity of the column will change to $(f_2 + \xi_2) = (f_1 + \xi_1)h_1/h_2$ (Fig. 21). Because $f \gg \xi$, generally, a change in thickness of 10% is often highly significant, as is a change in latitude (and thus f) of only a few degrees.⁴¹

⁴¹Two problems for you: 1) A right cylinder of radius r and height h has a moment of inertia $I = Mr^2/2$ where M is the mass of the cylinder. The angular momentum due to rotation at a rate ω about the central axis is $L = I\omega$. Show that conservation of angular momentum under changes of h and r that are mass (volume) conserving can be summarized with a vorticity conservation law like Eqn. (82). 2) Assume that a fluid column having a radius of 50 km and a thickness of 500 m is moved from 20 °N to 25 °N and that it conserves q . Assuming that all the change in f is accounted by changes in ξ (no thickness change), estimate the magnitude of the resulting current. Now suppose that the change in f is accommodated entirely by a change in thickness.....how much?

The winds or currents that we might infer from a q -conservation argument can always be computed via the full shallow water system and in that regard, q -conservation may seem to be a bit superfluous. However, when it is time to interpret a solution or observations, a potential vorticity-based description will oftentimes be far simpler and more insightful than the corresponding linear momentum description, provided that potential vorticity concepts have been made a part of our fluid dynamics vocabulary. We can make a small start on that here by using potential vorticity balance to help interpret each of the geostrophic adjustment experiments that follow.

6.3 Linearized shallow water equations

There are a few nonlinear (finite amplitude) phenomena that arise here, but our emphasis will be mainly the linear dynamics that shows the effects of Earth's rotation. The amplitude of the initial thickness anomaly was therefore kept small enough, $\eta_0 \ll H$, that the nonlinear advective terms, which are quadratic in the dependent variables, were much smaller than the local time rate of change, which is linear in the dependent variables. Hence $D(\)/Dt \approx \partial(\)/\partial t$ and $\eta \ll H$ are valid approximations for these solutions, which may be diagnosed adequately by means of the linearized shallow water system; in Cartesian components,

$$\frac{\partial u}{\partial t} = fv - g' \frac{\partial \eta}{\partial x}, \quad (83)$$

$$\frac{\partial v}{\partial t} = -fu - g' \frac{\partial \eta}{\partial y}, \quad (84)$$

$$\frac{\partial \eta}{\partial t} = H \left(\frac{\partial u}{\partial x} + \frac{\partial v}{\partial y} \right). \quad (85)$$

Once we have a linear solution and diagnosis in hand, we can then run additional experiments with increased amplitude of η_0 to see what the nonlinear effects may be (generally small here, because the configuration of the initial condition does not promote interaction among neighboring eddies, for example).

7 Models of the Coriolis parameter.

To this point we have presumed that the Coriolis parameter f was a constant for any given problem. But now we are thinking about a spatially extended fluid system and so it is time to acknowledge that f varies in space; from Section 4.2 you may recall that $f = 2\Omega \sin(\phi)$, with ϕ the latitude. Some of the surprising consequences of this are shown in Section 7.3. Before we come to that, it will be very helpful to build some intuition for the shallow water system by first examining a problem in which $f = 0$ so that there is no rotation and gravity waves only (Section 7.1), then allow that $f = \text{constant}$, so that

there are gravity waves, inertial oscillations and geostrophic motion all at once (Section 7.2), and then we will be ready for $f = f(y)$, which, of course, is what actually obtains (Section 7.3). This third model will include all of the phenomena that came before plus a low frequency wave motion.

Our specific goal will be to model some aspects of the baroclinic ocean eddies seen in Fig. 3. We have therefore chosen values for $H = 500$ m, and $\delta\rho = 2 \text{ kg m}^{-3}$ that are representative of the ocean main thermocline. The resulting gravity wave speed (discussed in detail below) $C = \sqrt{g'H} = 3.1 \text{ m s}^{-1}$, is that of an internal (or baroclinic) wave. So far as the shallow water model goes we could have chosen instead the full ocean depth, $H = 4000$ km, and $\delta\rho = 1000 \text{ kg m}^{-3}$, the density difference across the sea surface, in which case $C = 640 \text{ m s}^{-1}$, the speed of an external (or barotropic)⁴² wave, e.g., a tsunami wave or a tidal wave. The width of the initial ridge or eddy thickness anomaly was taken to be 400 km, comparable to the observed eddy diameter, and the amplitude was 20 m, so that $\eta_0 \ll H$, as noted in Section 6.3.

7.1 Case 1, $f = 0$, nonrotating

Immediately after the ridge was released, it began to divide into two equal wave pulses of amplitude $\eta_o/2$ (Fig. 22). These moved steadily outward at the expected gravity wave speed, $\sqrt{g'H} = 3.1 \text{ m s}^{-1}$, as we will discuss further below. The current that accompanied the wave pulses was in the direction of the pulse movement, i.e., toward positive x within the rightward-traveling pulse. This could be said to be a longitudinal wave motion; in Section 7.3 we will find a low frequency wave that is transverse. Aside from these pulses, there was nothing. If you had expected the response to look something like the waves on the surface of a pond or tsunami waves on the ocean, then this solution will seem a little strange. Is there a way to verify that this numerical solution is accurate enough with regard to these features to merit further discussion?

There is a well-known, exact analytic solution for the initial value problem of the elementary wave equation that we can use as a reference. The wave equation of the linear, nonrotating shallow water system (Eqns. 83 - 85) is easily found by eliminating u and v in favor of η ,

$$\frac{\partial^2 \eta}{\partial t^2} = g'H \frac{\partial^2 \eta}{\partial x^2}. \quad (86)$$

Given that the initial data is

$$\eta(x, t = 0) = \eta_o(x) \quad (87)$$

then the D'Alembert solution

$$\eta(x, t) = \frac{1}{2}\eta_o(kx - \omega t) + \frac{1}{2}\eta_o(kx + \omega t), \quad (88)$$

⁴²A barotropic fluid is one in which the density depends upon the pressure only, while in a baroclinic fluid the density may vary otherwise. The single layer model is degenerate in this regard, since density is assumed uniform throughout the active layer. The dimensional values of H and $\delta\rho$ chosen here are consistent with the lowest vertical mode of the baroclinic waves of a more general, multi-layer model.

solves (86) and (87) provided that

$$\omega = k\sqrt{g'H}. \quad (89)$$

The wave frequency is $\omega = 2\pi/(\text{wave period})$, or waves per time, and the wavenumber is $k = 2\pi/(\text{wave length})$, or waves per space interval. The relationship $\omega(k)$ is called the dispersion relation, and is the crucial and distinguishing property of a wave system.⁴³ Gravity waves, and moreover gravity waves that all have the same phase speed, $C_p = (\text{wave length})/(\text{wave period}) = \omega/k = \sqrt{g'H}$, and the same group speed, $C_g = \partial\omega/\partial k = \sqrt{g'H}$, are the only possible nontrivial motion. The derived parameter $\sqrt{g'H}$ arises so often that it is useful to assign a new symbol, just plain $C = \sqrt{g'H}$.⁴⁴

Because all of the waves (that is to say, waves of all wavelengths) have the same phase speed, they retain the relative phase that they were assigned in the initial condition. Thus, the initial shape, $\eta_o(x)$, is retained in the propagating wave pulses, and so the system is said to be nondispersive. It is also isotropic (from Greek *iso* + *tropos*, equal in all directions) and hence by symmetry half of η_o goes in one direction, and half goes the other.⁴⁵

The energy budget was evaluated over a domain ± 1000 km (Fig. 23). Several features of the energy budget are in common with the parcel on a slope. First, the only source of energy in this problem was the potential energy stored in the initial ridge, η_o (and this will be true in all of the geostrophic adjustment problems treated here). Second, after the ridge was released and began to slump, the decrease of PE was accounted for by the increase of kinetic energy, KE. Thus the total energy, KE + PE, was approximately conserved (aside from small losses due to numerical viscosity and to a small but numerically necessary diffusion). Other aspects of the energy budget were quite different: notice that once the outward-going wave pulses were fully separated, $t \geq 0.8$ days, the kinetic energy

⁴³Some important things have gone by rather quickly here. You should verify that 1) any function whose argument is $(kx \pm \omega t)$ satisfies the elementary wave equation provided that $\omega/k = \sqrt{g'H}$, and 2) the initial data is satisfied by Eqn. (88) for any $\eta_o(x)$. However, if $\eta_o \ll H$ does not hold, then the assumption that the system is linear would not be appropriate.

⁴⁴If phase speed and group speed are not familiar, an excellent resource is Chapter 1 and 2 of Pedlosky's 'Waves in the Ocean and Atmosphere'.⁸ For a quick refresher, you might take a look at the script `twowaves.m` (Section 9), which allows you to define an arbitrary dispersion relationship between two waves that are then superimposed. The envelope of the superposition, and thus a wave form or pulse, propagates at the group speed, $C_g = \delta\omega/\delta k$, where δ is the difference between the two waves. This demonstration of group speed is purely kinematic since we specify the dispersion relation for the two waves and then look for the consequences. In a full problem, the dispersion relationship is determined by the physics of the wave medium, and specifically the relationship of restoring force to wavelength.

⁴⁵Our numerical solution (Fig. 22) differs slightly from the D'Alembert solution in that these pulses did not retain the exact shape of the initial ridge. In part this is a finite amplitude effect of advection of thickness anomaly by the current, $u\partial\eta/\partial x$, which was present in the numerical model and numerical solution, but not in the linear shallow water model and the D'Alembert solution. Thickness advection tends to steepen the advancing edge of the wave pulse (where the phase speed and the current are in the same direction) while stretching out the trailing edge. You can investigate finite amplitude effects in the numerical model `geoadj_1d.m` (Section 9) by choosing a much larger value for the initial thickness anomaly, say $\eta_o = 200$ m. Can you show that finite amplitude effects are large or small according to the Mach number, $M = U/C$, where U is the amplitude of the current? The solution shown here was computed with the linear damping set to a very small value so that frictional effects were negligible. What value of r is required to damp the outgoing wave pulse to half initial amplitude as it arrives at $x = 1000$ km? How does the required r vary with the nominal layer thickness, H ?

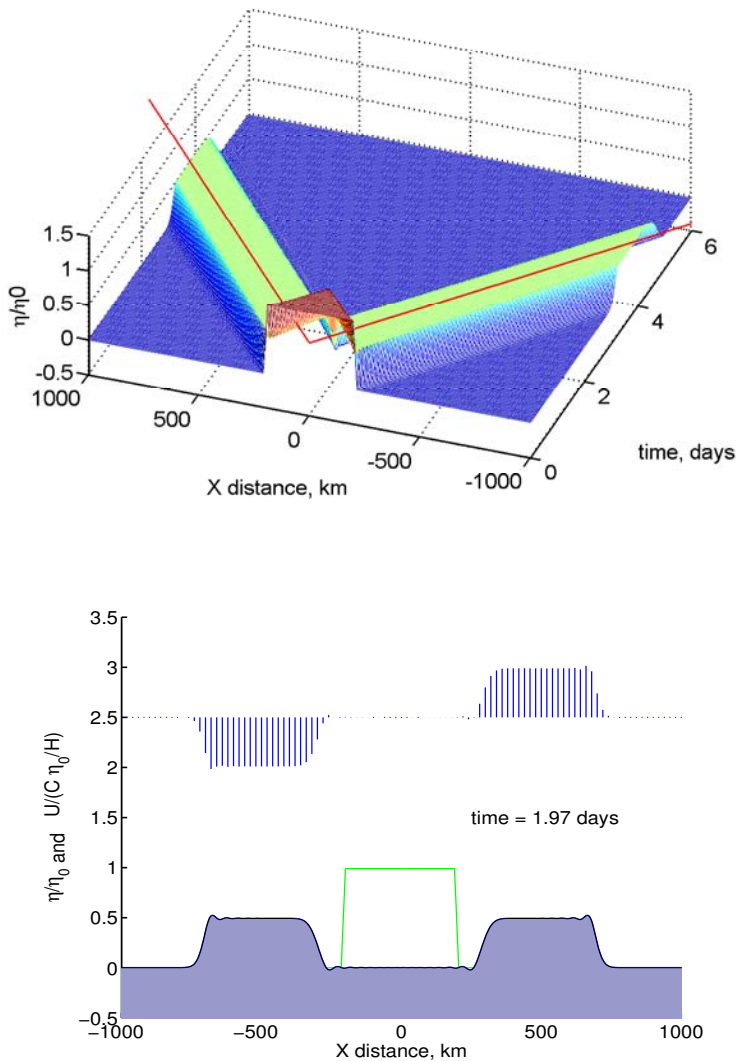


Figure 22: (upper) The layer thickness anomaly, $\eta(x, t)$, of a non-rotating fluid layer following the release of a rectangular ridge. The thin red lines have a slope given by the gravity wave speed, $C = \sqrt{g'H} (= 3.1 \text{ m s}^{-1}$ in this case). This solution was computed by the numerical model, `geoadj_1d.m` (Section 9). (lower) A snapshot of the solution at $t = 2.0$ days. The green line shows the initial thickness anomaly. The current, which is shown by the array of vectors plotted above, is in the x -direction only (left-to-right in this figure), and is scaled with $C\eta_0/H = 0.12 \text{ m s}^{-1}$. A curious feature of the linear, nonrotating shallow water model is that the gravity wave speed, C , is the only intrinsic scale; there is no intrinsic horizontal length scale or time scale (as there will be when rotation is included). We have therefore chosen dimensional units that are convenient for this specific initial condition, kilometers and days. If you are viewing with Acrobat Reader, you may click on the lower panel to start an animation.

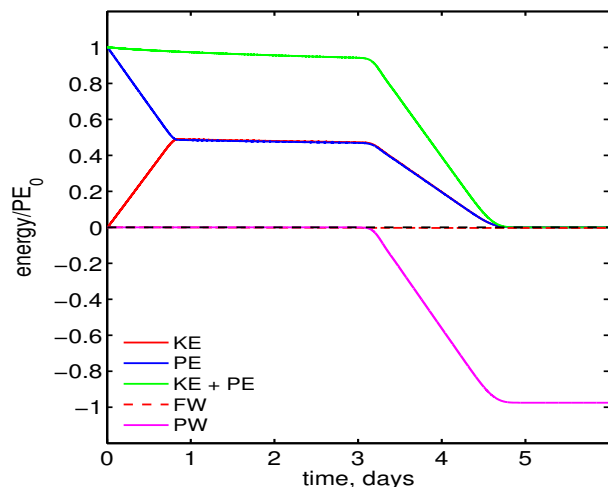


Figure 23: The energy budget for the gravitational adjustment problem of Section 7.1. The energy and work terms are nondimensionalized with the initial potential energy, PE_0 , and time is in days. The first four curves shown here have the same meaning as the curves with the same name (and color) in the parcel on a slope of Section 5.3. FW was vanishingly small since the frictional parameter r was effectively zero in this experiment.

and potential energy were thereafter equal. Energy equipartition is a fundamental characteristic of (nonrotating) gravity wave motion and thus provides a useful check on the numerical solution in the much more common case that an exact analytic solution is not available. At $t \approx 3.1$ days, the wave pulses reached the edge of the control volume, and thereafter energy was lost from the system by outward-going wave radiation represented by the pressure work, PW.⁴⁶

Potential vorticity is interesting, too, but in quite a different way — there isn't any! There was no planetary vorticity since $f = 0$, there was no vorticity in the initial condition since the ridge was at rest, and no vorticity was produced by the subsequent gravity wave processes, which are completely dependent upon the pressure gradient. Potential vorticity budgets can be invaluable for the analysis of low frequency phenomenon (next sections), but we are warned here that potential vorticity is blind to gravity waves.

You probably noticed that geostrophy does not appear to hold in near-equatorial regions of the atmosphere (Fig. 1). In part this is because near-equatorial pressure variations are quite small compared to those at mid-latitudes and so pressure isolines are not always evident in the near-equatorial regions of weather maps. Our experiments with the single parcel model (Section 5.2) may appear at first to offer an explanation for both the small values of the equatorial pressure gradient and the absence of geostrophy: for a given linear frictional parameter k , the Ekman number E will become very large as the latitude goes to zero, and hence geostrophy would not be expected to hold at near-equatorial

⁴⁶A difference between the single parcel energy budget (Section 5.3) and the present single fluid layer budget is that when we had only a single parcel, there was no choice about where to evaluate the energy budget — of course we followed the moving parcel. In a fluid dynamics context we would call that a Lagrangian (material-following) budget. Here we have a fluid continuum, and so we do have choices. We evaluated the energy budget over a fixed control volume that extended ± 1000 km about the center, the part of the model domain that we have plotted, but less than the width of the computational domain. This energy budget is Eulerian, in that the spatial coordinates and the control volume are fixed in space. As one consequence, energy can leave the control volume through the sides, something that could not happen in the single parcel energy budget.

latitudes on account of strong frictional damping. The conclusion is correct as far as it goes, but the reason is not. The single parcel model makes a very poor analogy to the winds and currents of equatorial regions because of things omitted, i.e., gravity wave dynamics. Thus when pressure isolines are shown in the equatorial region, the winds often appear to be almost normal to the pressure isolines, the (longitudinal) pressure/velocity relationship associated with gravity waves. Long before being damped by friction, an equatorial mass and pressure anomaly will disperse into large scale gravity waves that may propagate for thousands of kilometers along the equator. A gravity wave response to distant wind shifts (that includes wave modes not present in this nonrotating model) is a key element of the El Nino/Southern Oscillation phenomenon and of the equatorial atmosphere and oceans generally.

Summary: The nonrotating, shallow water system is truly austere. It is isotropic and it is characterized by just one intrinsic property, the phase and group speed, C , of (nondispersive) gravity waves, the only possible nontrivial motions.

7.2 Case 2, $f = \text{constant}$, an f -plane,

The one-dimensional domain and initial condition were repeated in the next experiment, but the latitude was set to 20 degrees N so that rotation effects would be appreciable. The Coriolis parameter f was taken as constant, an approximation that is often denoted by 'f-plane' (made clearer below). The coefficients in the linearized, shallow water system — f , g' and H — were then constants for a given problem.

Given the previous experiment, we might expect that a significant aspect of the adjustment process will be wave radiation away from the ridge. That is indeed the case, and the wave properties may be told from the dispersion relationship that links the wave frequency ω and the wave number, k . To find the dispersion relation, we postulate a plane wave solution of the form

$u(x, y, t) = U \exp(i(k_x x + k_y y - \omega t))$ and similarly for v and η , where U, V, Υ are the constant but unknown amplitudes of the wave velocity components and η . The k_x and k_y are the components of the wave number vector $K = \sqrt{k_x^2 + k_y^2} = 2\pi/\lambda$. Substituting into the governing equations and rewriting the resulting algebraic, homogeneous equations in a matrix format yields

$$\begin{bmatrix} -\omega & -f & g'k_x \\ f & -\omega & g'k_y \\ Hk_x & Hk_y & -\omega \end{bmatrix} \begin{bmatrix} U \\ V \\ \Upsilon \end{bmatrix} = 0. \quad (90)$$

This homogeneous system will have nontrivial solutions only when the determinant of the coefficients vanishes,

$$\omega^3 - \omega(g'HK^2 + f^2) = 0 \quad (91)$$

and thus the roots are given by (Fig. 24)

$$\omega = 0, \text{ and } \omega^2 = g'HK^2 + f^2. \quad (92)$$

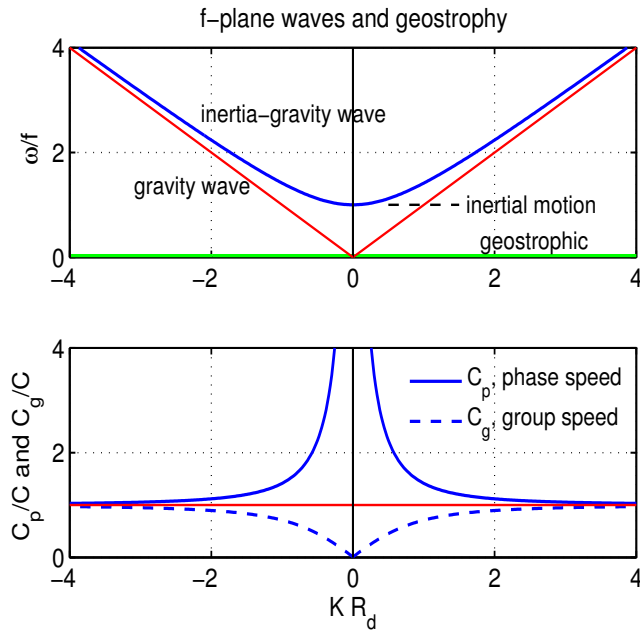


Figure 24: (upper panel) The dispersion relation for plane waves supported by the rotating, single layer model, often called inertia-gravity waves. The dispersion relation is isotropic (depends upon the magnitude of K only) and is symmetric about the ω axis. As discussed in the text, the frequency is normalized by the Coriolis parameter, f , and the wavenumber (an inverse length) by $1/R_d = f/C$, discussed in the text. (lower panel) The phase and group speeds of the inertia-gravity waves. Unlike the pure gravity waves of Section 7.1, these waves are dispersive, i.e., the phase speed varies with K . Note that the group speed goes to zero for very long waves that have frequencies near f , i.e., for near-inertial motions.

Before we plot the dispersion relation we should consider whether there may be a choice of nondimensional variables that makes sense. The Coriolis parameter f is an obvious (inverse) time scale for normalizing the frequency, ω , and when we follow through we find that K is automatically scaled by a length scale,

$$R_d = C/f$$

called the radius of deformation (recall that $C = \sqrt{g'H}$). The resulting nondimensional dispersion relation (Fig. 24) suffices for all values of f , g' and H , i.e., for all shallow water, f -plane models. R_d is the intrinsic horizontal scale of the rotating, shallow water model and will arise again more than once; it has a clear physical interpretation that we will come to just below. For now we will note that the value of R_d depends upon the stratification through C and the latitude through f . In the ocean thermocline at 20°N , $R_d \approx 60$ km. The R_d of the atmosphere at this latitude is much larger, $R_d \approx 1000$ km, because the atmosphere is both thicker than the ocean thermocline, and more strongly stratified. We are not prepared to explain why, but this very large disparity in R_d is reflected directly in the dominant horizontal scales of the variability seen in the atmosphere and ocean (cf. Figs. 1 and 3), i.e., much larger horizontal scales in the atmosphere.

There are three important limits, or modes, evident in the dispersion relation that we have seen before in a simpler guise, Sections 5 and 7.1. The root $\omega = 0$ corresponds to steady, geostrophic motion (the green line of Fig. 24, upper). The non-zero ω root (the blue line) corresponds to gravity waves that are modified by rotation, often called inertia-gravity waves. There is a short and long wave limit of

inertio-gravity waves: as $K R_d$ becomes very large (wavelength very short compared to R_d), inertio-gravity waves asymptote to pure gravity wave motion in which the phase speed is $C = \sqrt{g'H}$, just as in the non-rotating, shallow water model (Section 7.1).⁴⁷ As $K R_d$ becomes very small (wavelength very long compared to R_d) inertio-gravity waves asymptote to pure inertial motion, which occur also in the single parcel model of Section 5.⁴⁸ Plane waves on an f -plane are thus dispersive, meaning that C_p varies with K so that the shape of $\eta_0(x)$ is not, in general, preserved as waves propagate away from a source (cf. the nonrotating, pure gravity wave case of Section 7.1). Instead, the initial form $\eta_0(x)$ will become more or less spread out, or 'dispersed', over time as waves of different wavelengths propagate at different C_p . Notice that there is a low frequency range $0 < \omega < f$ within which there are no free waves possible in this system.

Back to our geostrophic adjustment problem: when the ridge was released in this rotating environment, the result overall was very different from that found when only pure gravity waves were possible (Section 7.1). There were again gravity waves that propagated away from the ridge (Figs. 25 and 26), and the phase speed of the fastest moving wave front was almost equal to the gravity wave speed, $\sqrt{g'H}$, and the current that accompanies the first wave front was polarized in the x-direction. The amplitude of these waves was, however, much less than half the initial thickness of the anomaly as seen in the non-rotating case. As time ran and waves continued to arrive in the far field, the current associated with the waves changed to a nearly circular, clockwise-rotating motion that approximates an inertial oscillation. The frequency of rotation was slightly higher than f (cf. Fig. 16 and which is easiest to see in the animation of Fig. 25). These qualitative features of the wave response were as we would have expected from the dispersion relation for the (linear, plane) waves of the rotating, shallow water system, Fig. (24): pure gravity waves have the fastest group speed and would be expected to arrive first in the far field; inertial motions, once they are generated, are likely to persist for days since they have very low group speed.⁴⁹

After about five days had passed, gravity wave dispersion had been largely completed, though some inertial motion persisted. What remained of the ridge and the associated currents was then in an approximately steady balance between the pressure gradient associated with the sloping layer thickness,

⁴⁷If the wavelength is less than the layer thickness, H , then the wave motion will become a short gravity wave that is surface-trapped. These are the high frequency, wind-generated waves that make up most of the sea state. Their frequency can be high enough that the pressure is nonhydrostatic and so these waves, sometimes called deep-water waves, are not in the domain of the shallow water system.

⁴⁸Go back to the shallow water system Eqns. (77) - (78) and identify which of the terms are relevant in each of these three limits.

⁴⁹One could solve the linear initial value problem via Fourier transform. An example for the non-rotating case is carried out by the script `ftransform.m` (Section 9), which allows for the choice of a dispersion. In the non-rotating case, the initial thickness anomaly η_0 all goes into propagating waves. In the rotating case, a more or less significant fraction of η_0 remains in the geostrophically balanced end-state. The linear dispersion relation is an invaluable guide to the kinds of wave motions that we will find in the geostrophic adjustment process, but does not tell us how much of the initial ridge will appear in waves vs. the balanced geostrophic state. This is an aspect of geostrophic adjustment best treated with potential vorticity conservation, described next.

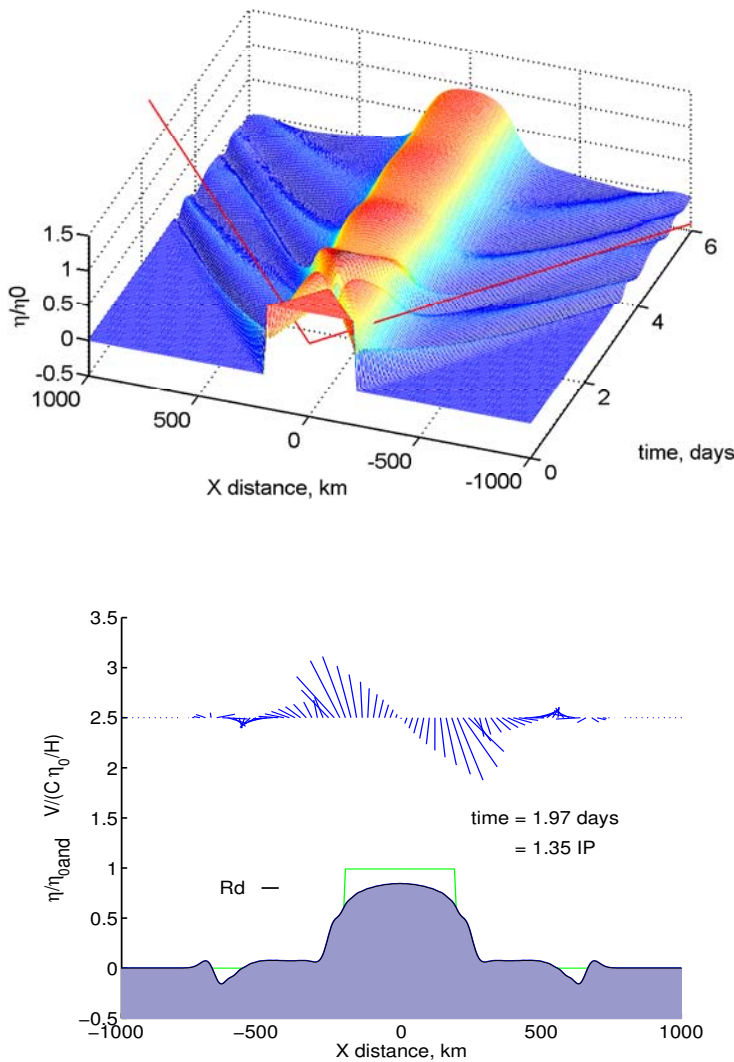


Figure 25: (upper) The layer thickness anomaly, $\eta(x, t)$, of a rotating fluid layer following the release of a rectangular ridge. This solution was computed by the numerical model `geoadj_2d.m`. Time and horizontal distance are shown in days and kilometers to facilitate direct comparison with the nonrotating problem shown in Fig. 22. The thin red lines have a slope given by the gravity wave speed, $C = \sqrt{g'H} = 3.1 \text{ m s}^{-1}$ in this case. (lower) A snapshot of the solution at $t = 2.0$ days. The green line shows the initial displacement η_o . The current, which is shown by the array of vectors plotted above, is scaled with $C\eta_o/H = 0.12 \text{ m s}^{-1}$ for the parameters of this experiment. Note the counter-flowing jets along the flanks of the partially subsided ridge. When the ridge reaches geostrophic balance, the Coriolis force acting on these jets is just sufficient to restrain the ridge from slumping further. If you are viewing with Acrobat Reader you may click on this panel to start an animation.

$\partial\eta/\partial x$, which would tend to spread the ridge further, and the Coriolis force acting on the along-ridge current (normal to the page) which would tend to compress the ridge. When these opposing forces were balanced so that $0 \approx fv - g'\partial\eta/\partial x$ at every point, the ridge was then in a steady, nearly geostrophic balance. An exactly steady, exact geostrophic balance is possible in this system, but our numerical solution didn't quite realize that.

A key result of this experiment is that most of this wide ridge survived the geostrophic adjustment process, e.g., about 80% of the initial potential energy (Fig. 26). In a loose sense, we might say that rotational effects exceeded gravity wave dispersion in this experiment. The conservation law for potential vorticity, $Dq/Dt = 0$, provides significant insight into why this was the case. In words, the q -conservation law Eqn. (82) states that $q(\alpha)$ is unchanged by the process of geostrophic adjustment, where α is a parcel (or column) tag. In this linear case we know even more, that q is conserved in place

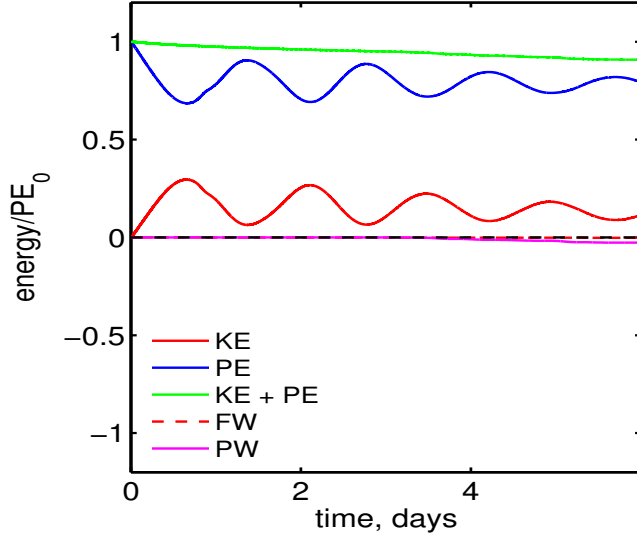


Figure 26: The energy budget for the f -plane geostrophic adjustment problem evaluated over $x = \pm 1000$ km. The energy and work terms are nondimensionalized with the initial potential energy, PE_0 , and time is in days. These data may be compared directly with that of the non-rotating case Fig. (23), and are remarkably different: very little energy was radiated out the sides of the domain, and the final, geostrophically balanced ridge ($t = 6$ days) retained most of the potential energy of the initial state. In other words, in this f -plane case, there was a significant steady state.

in the sense that $q(x) = q_0(x)$ with q_0 the initial state and x is the usual (Eulerian) spatial coordinate. The initial state includes the ridge within which the layer thickness was $H + \eta_0$, and elsewhere the thickness was H . The q distribution in the initial and in the final state was then (recall that $\xi = \nabla \times \mathbf{V} = \partial v / \partial x$ in this one-dimensional problem)

$$q = \frac{f + \partial v / \partial x}{H + \eta} = q_0 = \frac{f}{H + \eta_0} \text{ if } |x| \leq L, \quad (93)$$

and otherwise

$$\frac{f + \partial v / \partial x}{H + \eta} = \frac{f}{H} \text{ if } |x| > L. \quad (94)$$

In addition, we have come to expect that the final state will be in geostrophic balance, and hence we have a relationship between v and η , *viz.*

$$0 = fv - g' \frac{\partial \eta}{\partial x}.$$

If we substitute this geostrophic balance into the q conservation law, say for the region $x \geq L$, Eqn. (94), then with rearrangement we have a constant coefficient, second order ordinary differential equation for $\eta(x)$,

$$\frac{g'H}{f^2} \frac{d^2 \eta}{dx^2} - \eta = 0.$$

The boundary conditions on η may be applied over four segments, for example for the right-most segment $x \geq L$, $\eta(L) = \eta_0/2$ and $\eta(\infty) = 0$ and the solution is then

$$\eta(x) = \frac{\eta_0}{2} \exp\left(-\frac{x-L}{R_d}\right).$$

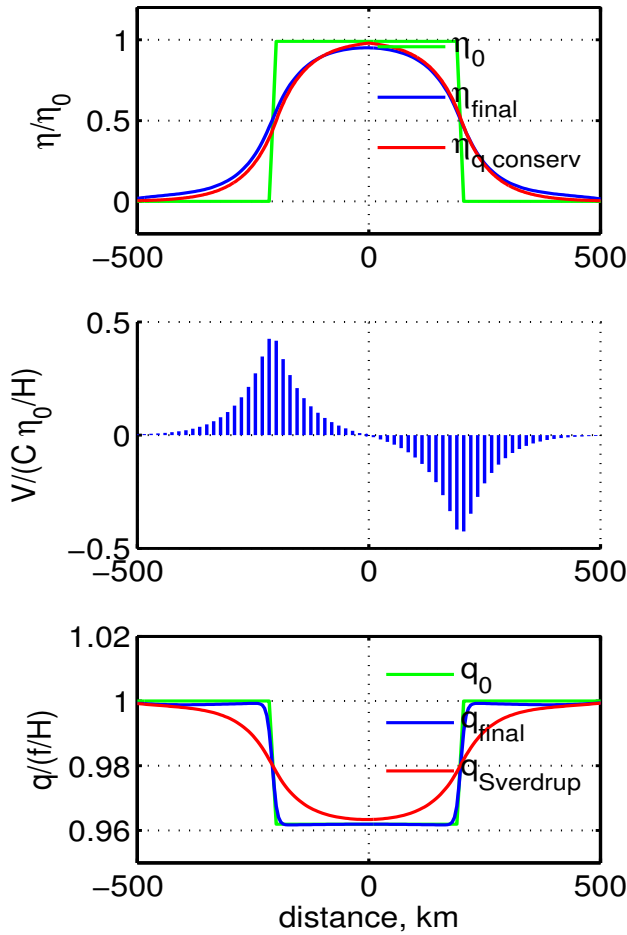


Figure 27: Elements of the potential vorticity balance. (upper) The initial and final ($t = 6$ days) thickness anomaly (green and blue lines) from the numerical solution and $\eta(x)$ computed under the assumption of geostrophy and q conservation (the red line). (middle) Time-mean, along-ridge current. Note that the jets have maxima at $x = \pm 200$ km, coinciding with the edge of the initial ridge. These jets are in a near geostrophic balance. (lower) Initial and final q (green and blue lines). Note that q of the numerical solution is almost unchanged by the process of geostrophic adjustment, as should have been the case. Also shown is the Sverdrup potential vorticity, $q = f/(H + \eta)$ (red line), which omits the relative vorticity. This is an acceptable approximation to the q of the steady, basin-scale circulation. However, it fails here, because the relative vorticity of the along-ridge jets makes a very significant contribution to q .

Notice that the length scale for the adjusted ridge is $R_d = C/f$, which has a clear physical interpretation in this problem. Recall from Section 5.3 that $1/f$ is the time it takes for rotation to turn a parcel (started from rest) by one radian with respect to the applied force. R_d is thus the distance that a gravity wave will propagate in the time $1/f$, and hence R_d is proportional to the distance that the ridge will spread outward (as a gravity wave) before being arrested by the Coriolis force. The experiment of Section 7.1 in which $f = 0$ can now be seen as the limit $R_d/L \rightarrow \infty$ in which rotational effects would be expected to be negligible — literally zero in that case — compared to spreading by gravity wave processes.

Continuing on we, can construct the complete profile $v(x)$, of the q -conserving, linear, geostrophic solution and find that it matches very well with the numerical solution (Fig. 27, upper, red curve and blue curve). The part of the adjusted ridge that slumps during the geostrophic adjustment process has a half-width (e-folding) R_d ; the full width of the edge adjusted ridge is then about 3 or 4 times R_d . This analysis provides a definite meaning to the phrase 'large scale' as applied to a mass anomaly or eddy of radius L : the appropriate standard against which to compare (or measure) a horizontal length is once again found to be the radius of deformation, $R_d = C/f$. Thus an eddy having a radius of $L = 50$ km

would be large scale and would survive geostrophic adjustment if found in a polar ocean where $R_d \approx 10$ km, but the same eddy would be decidedly small scale if found in the tropics, where R_d may be several hundred km.⁵⁰

The geostrophic currents, or 'jets' since they have a well-defined maximum, have a relative vorticity (Fig. 27, middle) that we can readily understand from the change in thickness and q conservation. For example, over the right-most segment, $x > L$, the layer thickness $H + \eta$ increased, and hence the shear of the geostrophic current in that region must have been $\partial v / \partial x \geq 0$, or cyclonic. By similar reasoning one can understand the sign of the relative vorticity over both jets.⁵¹ If a calculation of the final, geostrophically balanced state had been our only goal, then the best route would surely be the analytic solution built upon q conservation and geostrophy. On the other hand, if we had needed to know the inertio-gravity waves that accompany geostrophic adjustment, then we would have to solve the momentum and continuity equations that contain q -conservation plus the gravity wave dynamics.

Over longer times, say 50 days, this (numerical) ridge would slowly dissipate on account of either linear drag (if that has been included in the numerical model equations) or just by numerical viscosity, a numerical error that is endemic to most finite differencing and integration schemes. Dissipation aside, it is fair to say that nothing especially interesting happened in the f -plane problem after the geostrophic adjustment had been completed.

Summary: The f -plane shallow water model supports gravity waves as in the previous case, and two new modes of motion dependent upon f ; free inertial oscillations and steady geostrophic motion. The intrinsic horizontal length scale is the radius of deformation, $R_d = C/f$. If an anomaly of layer thickness is wide compared with R_d , say $L > 6R_d$, then it will survive geostrophic adjustment. A narrow ridge, say $L < 2R_d$ will be largely dispersed by gravity waves before coming into geostrophic balance. These results were found in numerical solutions of the momentum and continuity equations, but are most readily understood as a consequence of potential vorticity conservation.

7.3 Case 3, $\mathbf{f} = \mathbf{f}_o + \beta\mathbf{y}$, a β -plane,

The mesoscale eddies of Fig. 3 and the gyres of Fig. 2 have north-south horizontal scales of several hundred and several thousand kilometers respectively. The Coriolis parameter f varies a little or a lot

⁵⁰Using the Matlab script `geoadj_1d.m` to construct new solutions, verify that the width of the geostrophic current along the flank of the adjusted ridge is proportional to R_d . Show that variations of g' and of H are (almost) irrelevant except as they enter R_d . What happens when the thickness anomaly is made very large, say $\eta_o = 200$ m? The solution shown here was made with a very small value of the linear damping coefficient. What happens to the wave response and to the geostrophic response when damping is made significant? Connect the results you obtain here with the notion of an Ekman number developed in Section 5.

⁵¹Can you go a step further and reconstruct the velocity scale, $C\eta_o/H$, used to nondimensionalize the currents? How would you test this scaling law? For example, for a given g' , how does the magnitude of the along-ridge geostrophic current vary with latitude? How and why does the current magnitude vary with H ?

over these north-south scales, and it isn't clear that the f -plane model of Section 7.2 is entirely appropriate for these phenomena. To learn some of the consequences of the north-south variation of f we will carry out an adjustment experiment styled loosely on the oceanic mesoscale eddies of Fig. 3. The initial thickness anomaly will be made circular, with radius $L = 200$ km but otherwise the stratification and central latitude are as before. The spatial domain is two-dimensional and extends for several thousand kilometers around the eddy center. The important new feature of this experiment is that the north-south variation of the Coriolis parameter will be acknowledged. From Section 4.2 you may recall that $f = 2\Omega \sin(\phi)$ is the projection of Earth's rotation vector onto the local vertical unit vector. This form $f(\phi)$ could be used in the numerical model, but for a number of purposes it is helpful to utilize a linear approximation found by expanding f in a Taylor series about a central latitude, ϕ_0 (this repeats Eqn. 57):

$$f(y) = f(\phi_0) + \beta y + HOT, \quad (95)$$

where $y = R_e(\phi - \phi_0)$ is the north-south (Cartesian) coordinate, and R_e is Earth's nominal radius, approx. 6370 km. The coefficient of the linear term is beta,

$$\beta = \frac{df}{dy} = \frac{2\Omega}{R_e} \cos(\phi_0) \quad (96)$$

When the higher order terms (HOT) are ignored, the resulting linear model $f(y)$ is often called a beta-plane. The leading factor, $2\Omega/R_e = 2.29 \times 10^{-11} \text{ m}^{-1} \text{ s}^{-1}$, looks to be a very small number, but β will be multiplied by a north-south distance y of megameters. Notice that β is positive in both hemispheres, has a maximum along the equator and zeroes at the poles.

7.3.1 Beta-plane phenomena

When the eddy was released into the β -plane environment, the initial response included gravity wave propagation away from the center (Fig. 28), more or less as expected from the previous one-dimensional case with rotation, Section 7.2. There are several differences in detail compared to the one-dimensional case: 1) the outward traveling waves had a decreasing amplitude with distance on account of geometric spreading $\propto 1/r$, and 2) the region inside the expanding wave front continued to oscillate, though with decreasing amplitude in time. In these respects, this two-dimensional adjustment process looks much more like the wave response to a rock thrown into a pond than did the previous one-dimensional cases.

The first few days of the gravity wave response looked fairly symmetric azimuthally (isotropic), but after about five days there developed a noticeable north-south asymmetry, Fig. 29. The inertio-gravity waves that propagated poleward (northward in this case) were propagating toward higher f . Within a few thousand kilometers these waves reached a latitude at which their intrinsic frequency approached f . Recall from the previous section that free inertio-gravity waves can not exist at a latitude where $\nu < f$; this is true approximately also on a beta-plane. The poleward-travelling waves were reflected equatorward, and after about ten days, the poleward (northern) side of the eddy was nearly free

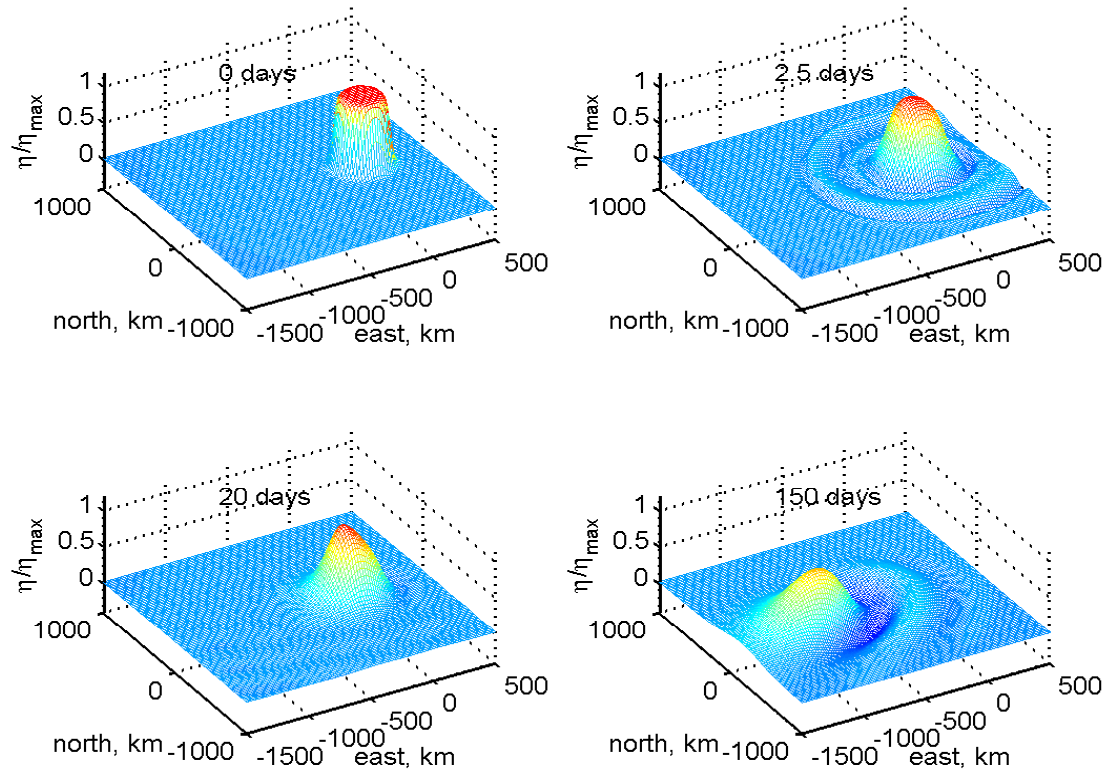


Figure 28: An experiment in geostrophic adjustment on a beta-plane solved by the numerical model `geoadj_2d.f` (Section 9). The anomaly of the layer thickness, η , is shown at four times: (upper left) the initial state of rest at $t = 0$; (upper right) at $t = 2.5$ days after the eddy was released, and while inertio-gravity waves were prominent; (lower left) at $t = 20$ days; and (lower right) at $t = 150$ days, by which time the beta-induced westward translation of the eddy peak was pronounced. This experiment is shown as an animation in the cover graphic.

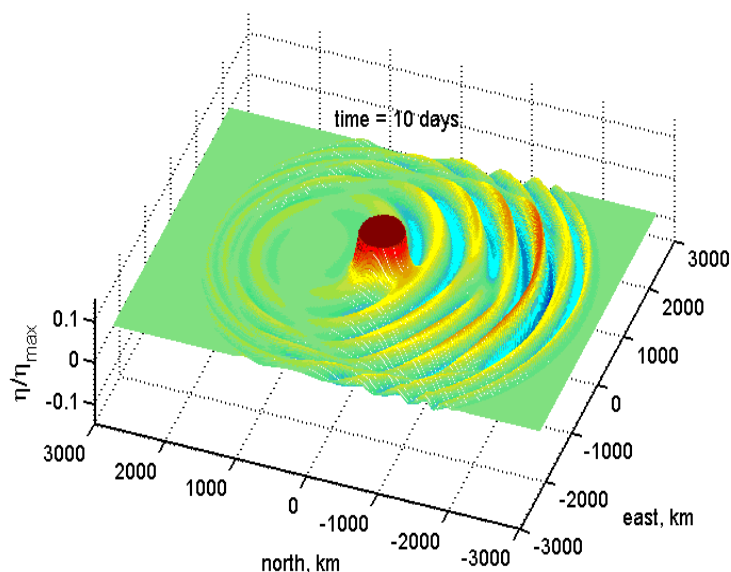


Figure 29: A snapshot at $t = 10$ days from the beta-plane adjustment experiment. Compared with Fig. 28, this figure shows a larger area, and the vertical scale is severely truncated to emphasize the comparatively small amplitude inertio-gravity waves. Notice that the wave amplitude was much reduced on the northern (poleward; toward the left in this figure) side of the eddy. This north-south asymmetry was due to a beta-induced reflection of poleward-travelling inertio-gravity waves. An animation of this case is available in the supplementary material (Section 9).

of inertio-gravity waves while the equatorward side was still fairly energetic. This beta-induced reflection of inertio-gravity waves is inherently interesting and is an important process of the ocean's internal wave sea state. However, our emphasis from here on will be mainly the low frequency phenomenon and we won't discuss this any further.

The inertio-gravity waves had largely diminished after several weeks, and the high pressure anomaly associated with the elevated layer thickness was nearly balanced by the Coriolis force acting on the anticyclonic currents that encircled the eddy (Fig. 30). In other words, the eddy had settled into a near geostrophic balance.⁵² Aside from the details of the wave radiation, the geostrophic adjustment process *per se* was about as we would have expected from our experience with the previous one-dimensional case (Section 7.2).

Over a longer period there emerged a wholly new process that followed from the seemingly small change in the representation of the Coriolis parameter — the nearly geostrophically balanced eddy moved steadily westward at a rate of about 5 kilometers per day. This slow, steady propagation persisted until the eddy reached the western boundary of the computational domain.⁵³ An apparently

⁵²Some near-inertial oscillations persisted for a week or more, as we noted above. Can you explain why that might be expected from the dispersion relation, Fig. (24)? If inertial motions persist, then in what sense can we claim that the eddy is in geostrophic balance?

⁵³The subsequent evolution of the eddy depended entirely upon the boundary condition imposed on the western edge of the domain. The radiation boundary condition used here, $\partial(\cdot)/\partial t = -C\partial(\cdot)/\partial x$ with $C = \sqrt{g'H}$, Eqn. (79), is effective at minimizing the undesirable reflection of gravity waves. However, this comparatively large gravity wave C acts to push the eddy through the boundary more rapidly than it would otherwise go. An adaptive C might be preferable.

similar westward propagation of mid-ocean eddies is a striking feature of the sea surface height field of all of the major ocean basins, e.g., the North Atlantic in Fig. 2. Along with westward propagation, there was also a significant change in the eddy amplitude and shape. The eddy amplitude slowly diminished, and a trough (low pressure ridge) formed to the southeast of the eddy center, almost in the initial location of the eddy. Our goals for the remainder of this section are to develop an understanding of the westward propagation of the eddy peak and of the apparent smearing of the eddy over time.

7.3.2 Rossby waves; low frequency waves on a beta plane

The (mainly) westward propagation of this eddy is reminiscent of the gravity wave propagation seen in Section 7.1. However, the eddy propagation was, by comparison, very slow, only a few percent of C . At a fixed point the time rate of change (and thus the frequency) was correspondingly much less than f . Is there a useful wave description of this phenomenon? The corresponding wave motion is not contained within the f -plane model, since no free motion exists in the frequency band $0 \leq \omega \leq f$ (Fig. 24) and too, the eddy remained in place in the f -plane experiment. An understanding of this low frequency motion will evidently require that we take explicit account of the variation of f with latitude. The straightforward and appealing technique of looking for plane wave solutions directly in the governing equations (Section 7.2) does not go through when $f = f(y)$ since all of the coefficients in Eqs. (85) are then not constant.

How to proceed? Two clues: 1) The velocity and pressure fields associated with the propagating eddy were very nearly geostrophic (Fig. 30); it is hard to see any discrepancy between the velocity direction and the local pressure isolines, though we know that geostrophy can not hold exactly. 2) The low frequency and nearly geostrophic motion of the eddy may be contained within the q -conservation relation, Eqn. (82), which we have seen gives a complete account of the spatially-varying geostrophic fields. These two taken together imply that we might take geostrophy as the basic state, $u = -(g'/f)\partial\eta/\partial y = 0$ and $v = (g'/f)\partial\eta/\partial x = 0$, and substitute into the linear q conservation law to arrive at a governing equation for the slowly evolving, nearly geostrophic η and \mathbf{V} .⁵⁴

The shallow water q -conservation equation expanded is just

$$\frac{Dq}{Dt} = \frac{1}{H + \eta} \left(\frac{D\xi}{Dt} + \frac{Df}{Dt} \right) - \frac{f + \xi}{(H + \eta)^2} \frac{D\eta}{Dt} = 0.$$

To put this into a form that might permit plane wave solutions we will use that $Df/Dt = \beta v$ (since $\partial f/\partial t = 0$), and linearize; $H + \eta \approx H$ wherever it appears in denominators, the material derivative is

⁵⁴A more formal and so more reliable approach to the same result is a perturbation method known as successive approximations, i.e., that we use the geostrophic basic state to estimate the small departures from geostrophy. This method is the starting point for much of the theory that has been developed to describe the slowly evolving, nearly geostrophic (often called quasi-geostrophic) phenomenon of the atmosphere and ocean (see Cushman-Roisin (1994)⁸ for a particularly clear exposition of this technique).

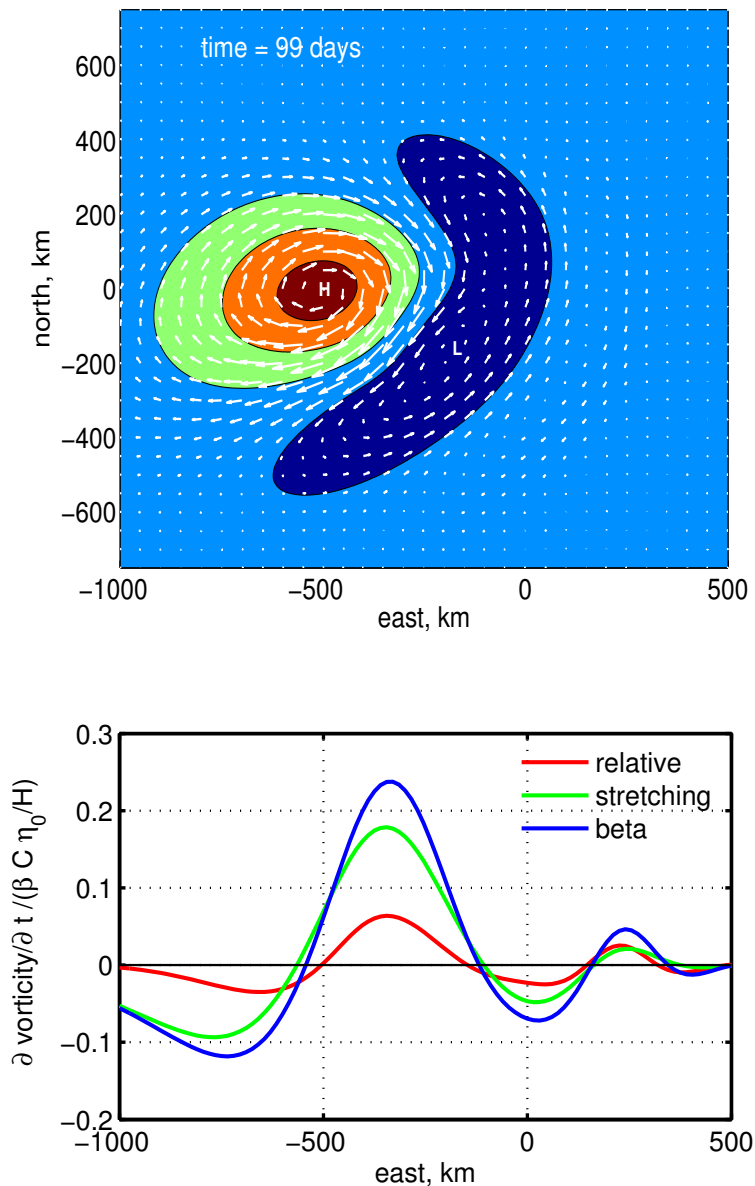


Figure 30: (upper panel) The horizontal currents and thickness anomaly η (color contours, proportional to pressure) associated with the two-dimensional geostrophic adjustment problem of Fig. (28). This is a snapshot at $t = 99$ days; click on this figure to start an animation. The currents were very nearly parallel to the lines of constant η suggesting a nearly geostrophic balance and yet were clearly time-dependent. Notice that the current swirling anti-cyclonically around the high pressure eddy peak varied with y , being larger to the south, i.e., toward the equator. This gives rise to the β -induced divergence mechanism that is characteristic of long, divergent Rossby waves discussed in Section 7.3.2. (lower panel) Terms of the linear potential vorticity balance Eqn. (97) evaluated at $t = 99$ days on the fields above along the line $y = 0$. The beta term (blue line) was very closely balanced by the sum of the time rate of change of relative vorticity (red line) and the stretching (green line), confirming that the potential vorticity balance was nearly linear in this small amplitude experiment. Near the eddy peak, the stretching term was about three times the magnitude of the relative vorticity term. Over the eastern-most portion, $x \geq 100$ km, the relative vorticity and stretching terms were about equal.

reduced to the partial time derivative, and finally note that $\xi \ll f$, as we can verify for the mesoscale eddies of Fig. 3. To this stage the linearized q -conservation equation reduces to

$$\frac{\partial \xi}{\partial t} - \frac{f}{H} \frac{\partial \eta}{\partial t} = -\beta v \quad (97)$$

relative + stretching = beta,

where it is understood that f and β are evaluated at the central latitude of interest. Next we substitute the geostrophic relation for the north-south velocity, $v = (g'/f)\partial\eta/\partial x$, and for the vorticity, $\xi = (g'/f)\nabla^2\eta$, and after a little further rearrangement come to a linear, third order governing equation for η ,

$$\left(1 - \frac{g'H}{f^2}\nabla^2\right)\frac{\partial\eta}{\partial t} = -\frac{\beta g'H}{f^2}\frac{\partial\eta}{\partial x}. \quad (98)$$

Notice that the time derivative of η is proportional to the first derivative of η in one direction, east-west, which is thus a special direction on a β -plane. If $\partial\eta/\partial x = 0$, which means that the north-south (meridional) geostrophic $v = 0$, then one possibility is that $\partial\eta/\partial t = 0$ and the η field could be steady. The mechanism that causes time-dependence in this system is evidently the north-south movement of fluid through a varying planetary vorticity, βv (Fig. 21, right). In this respect, north-south also looks like a special direction, and indeed it is. What we can conclude is that the β -plane shallow water system is anisotropic (not isotropic) though in different ways for different variables.

Substitution of a presumed plane wave solution $\eta(x, t) = \eta_0 \exp(i(k_x x + k_y y - \omega t))$ into Eqn. (98) yields a dispersion relation for waves on a beta-plane, sometimes called planetary waves, but more often termed Rossby waves, Fig. (31),

$$\frac{\omega}{f} = -\frac{\beta R_d}{f} \left(\frac{R_d k_x}{1 + R_d^2(k_x^2 + k_y^2)} \right), \quad (99)$$

which is very different from the dispersion relation of inertio-gravity waves (Eqn. 24). In the first place, these are very low frequency waves; the factor in parentheses is $O(1)$ for the scales of interest here in which K is $O(R_d)$, and the frequency is determined largely by the leading factor, $\beta R_d/f \approx R_d/R_e \approx 0.03$, where $R_d = 60$ km, appropriate to the subtropical (baroclinic) ocean. Secondly, this dispersion relationship is anisotropic; for a given wavelength, the frequency is a maximum when the wave vector is directed east or west ($k_y = 0, K = k_x$) and the frequency is zero if the wave vector is directed due north or due south. Zero frequency implies steady and exactly geostrophic motion, and hence any purely zonal (east-west) motion satisfies Eqn. (99) regardless of k_y . The north-south component of phase velocity can have either sign, while the east-west component is always negative, i.e., always westward (Fig. 32). This crucial distinction between north-south and east-west can be attributed to Earth's rotation vector (Fig. 4), which defines a specific direction for everything that is significantly effected by Earth's rotation, and to the thin-fluid form of the Coriolis force. A more general version of this dispersion relation includes also the variation of bottom depth

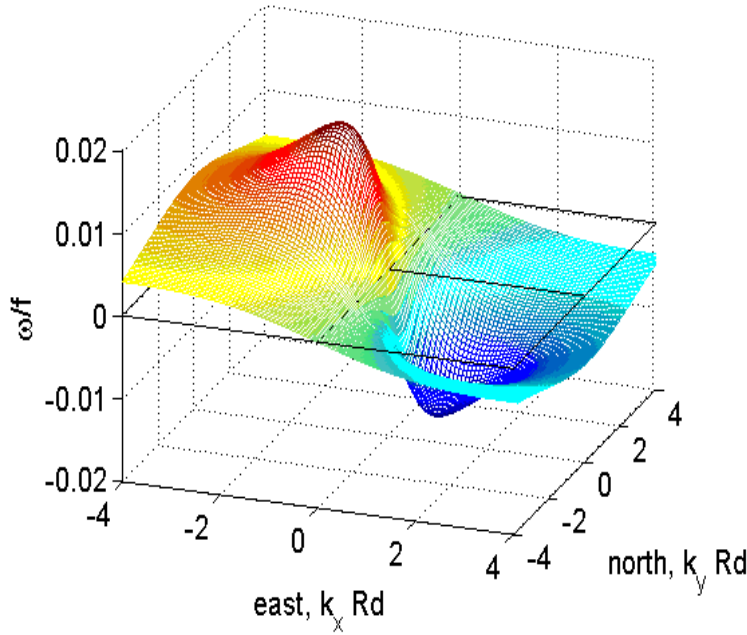


Figure 31: The dispersion relation for planetary Rossby waves, Eqn. (99). The R_d was 60 km, appropriate to a baroclinic ocean. The surface is symmetric north-south, and anti-symmetric east-west.

(noted briefly in Section 7.3.3). In that case, Rossby waves propagate in the direction that has higher background $q = f/H$ to the right of the wave vector.

The dispersion relation for planetary Rossby waves Eqn. (31) is symmetric north-south, and since we are concerned with east-west propagation it is helpful to simplify to the case of an east-west wave vector, i.e., $(K, 0) = (k_x, 0)$, Fig. (32),

$$\frac{\omega}{f} = -\frac{\beta R_d}{f} \left(\frac{R_d K}{1 + R_d^2 K^2} \right). \quad (100)$$

This dispersion relation has two distinct limits: long waves, $K R_d \ll 1$, and short waves, $K R_d \gg 1$.⁵⁵ This implies that there are two distinct mechanisms for Rossby waves that we will discuss further in Section 7.3.3. For now we note the consequences for wave dispersion. Long Rossby waves have a zonal phase velocity $C_p = -\beta R_d^2$ that is westward, and independent of K . Hence, long Rossby waves are nondispersive and their zonal group velocity, $C_g = C_p = -\beta R_d^2$, is also westward (and the same as the phase velocity). This is a candidate mechanism for the westward translation seen in the oceanic eddy field (Fig. 3). Short Rossby waves have a zonal phase speed $C_p = -\beta K^{-2}$. Thus short Rossby waves are highly dispersive and will not maintain an initial wave form.⁵⁶ The zonal group velocity of short Rossby waves is $C_g = -C_p = \beta K^{-2}$ and opposite the phase velocity.

⁵⁵This is now the third time that the radius of deformation has arisen as the appropriate length scale against which to compare (or measure) horizontal scales, in this case the wavelength of Rossby waves. Are we being overly enthusiastic about

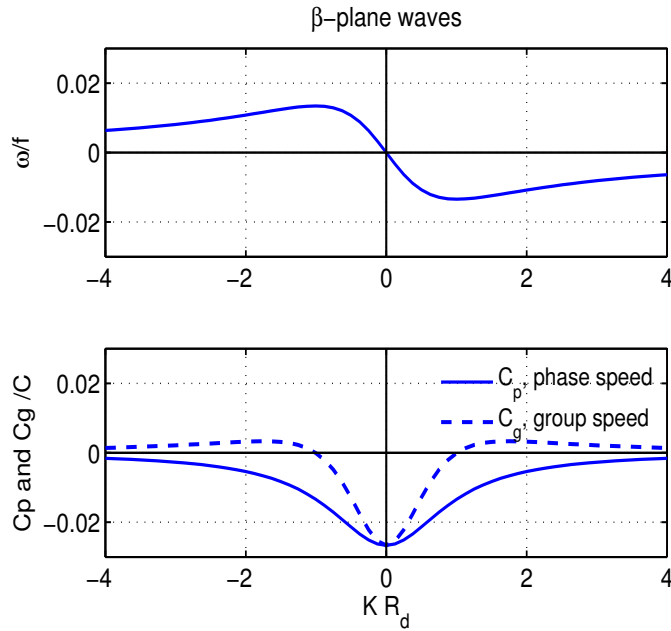


Figure 32: (upper panel) The dispersion relation for baroclinic, oceanic Rossby waves. This is a slice through the previous figure along $k_y = 0$ and $K = k_x$. Notice that the frequency of these waves is a very small fraction of f . The phase speed (lower panel, solid line) is always negative, meaning that phase propagates westward only. The group speed is also westward for long waves, $KR_d \leq 1$ but is eastward and small for medium to short waves, $KR_d \geq 1$.

The westward translation of the eddy seen in the solution is consistent with the westward group (and phase) speed of long Rossby waves, and so a wave description appears hopeful, at least. To make a quantitative estimate of phase or group speed from Eqn. (100) requires that we characterize our discrete (and two-dimensional) eddy by a wavelength, i.e., we will have to do a rough Fourier transform. As a first guess, we might try to estimate a dominant wavelength, the peak in the spectrum, while keeping in mind that other wavelengths will also be present. This eddy has a diameter of 400 km, and since it has one sign over that distance, a plausible equivalent wavelength would be twice that or 800 km. Given the baroclinic $R_d = 60$ km, then $KR_d \approx 2\pi 60 \text{ km}/800 \text{ km} \approx 0.4$. Hence, the dominant horizontal scale of this eddy appears to be consistent with a fairly long wave, although not $KR_d \ll 1$. From Fig. (32) the group speed at this KR_d is $C_g \approx 0.01C \approx 3 \text{ km day}^{-1}$, which is somewhat less but comparable to the westward translation of the eddy peak seen in the numerical solution (Fig. 28).

So far so good, but recall the trough that developed to the east of the eddy center; something more than an elementary (single) plane wave description will be required to explain this feature of the solution. One bleak possibility is numerical error. We have been careful to emphasize that all numerical

R_d , or is it just that there is nothing else suitable? What about the layer thickness, H ? Surely it too is an intrinsic length scale.

⁵⁶Rossby waves exhibit normal dispersion in that longer waves have greater phase speed. It can happen that shorter waves have a greater phase speed, a property dubbed anomalous dispersion. An example of anomalous dispersion that you can readily investigate is that of capillary waves (<http://www.terrapub.co.jp/journals/JO/pdf/5404/54040343.pdf>) generated by the movement of a small object across the surface of still water. If the object moves more slowly than the slowest gravity/capillary wave, about 0.2 m s^{-1} , there are no waves. But when the speed of the moving object exceeds this minimum wave speed, a wave pattern will suddenly appear around and in front of the object. Short capillary waves lead the pack. Anomalous and normal dispersion may be investigated also via numerical experiments that solve an initial value problem, `ftransform.m` (Section 9).

solutions are less than perfect, and the question is whether the errors swamp the physical, intended behavior or vice versa. A second possibility is wave dispersion. The Rossby waves that (we can imagine) make up this particular eddy are not expected to have a common phase speed since the estimated dominant scale does not satisfy $K R_d \ll 1$, and hence Rossby wave propagation would not be expected to preserve the initial shape of this eddy (compare with the gravity wave pulses of Section 7.1). To decide this question we will have to look within the solution for evidence of dynamically consistent behavior that goes beyond just the sign and approximate magnitude of westward propagation.

7.3.3 Modes of potential vorticity conservation

We identified two limits of the Rossby wave dispersion relationship: short waves, $K R_d \gg 1$, and long waves, $K R_d \ll 1$. These limits correspond to modes (two-term balances³⁵) of the q -conservation equation (82) and by examining the mechanisms and phase relationships that go along with each mode we can understand how westward propagation (and anisotropy generally) arises on a β -plane. The restoring force provided by the β -effect is slightly subtle compared to, say, the elastic restoring force that acts upon a plucked string. Westward propagation arises when there is a specific phase relationship between η and $\partial\eta/\partial t$, that the former lags the latter by $\pi/2$, or between north-south displacement, y , and the north-south velocity, v . However, wave propagation is not guaranteed by q -conservation alone, as the first q -conservation mode described below illustrates.

Stretching and relative vorticity. Consider that the balance of q -conservation is between the stretching term and the relative vorticity term (the case sketched in Fig. 21, left) so that the change in relative vorticity occurs in phase with the stretching. If stretching stops, so does the rate of change of relative vorticity; there is no inertia or overshoot, and so there is no restoring force that might lead to wave propagation. This first mode of q -conservation is (or can be) local in time and space and does not lead to wave propagation.

When the β term is a part of the q balance there will be westward propagation. To follow along with this discussion it will be very helpful for you to make sketches of $\eta(x)$, $v(x)$, *etc.* as you fill in the very brief calculations outlined here.

Beta and stretching. A very important mode of q -conservation is a balance between stretching and planetary vorticity, i.e., $f/(H + \eta) = \text{const}$. To see how this may support a wave, presume a sinusoidal thickness anomaly, $\eta(x, y, t) = \eta_0 \cos(Kx - \omega t)$, that is in geostrophic balance with a north-south (meridional) current, $v(x, y, t) = (g'/f(y))\partial\eta/\partial x$, where $f(y)$ is given by a beta-plane approximation. Whether there is an ω that is consistent with westward propagation is to be determined. The key point is that this meridional geostrophic current will vary with y simply because f varies with y , *viz.*, $\partial v/\partial y = (-g'\beta/f^2)(\partial\eta/\partial x)$, evident in Fig. (30). The meridional geostrophic current will thus be convergent, $\partial v/\partial y < 0$, and water will pile up where $\partial\eta/\partial x > 0$. A convergent flow will cause a positive rate of change of the layer thickness, $\partial\eta/\partial t \approx -H\partial v/\partial y$ from the continuity equation (78)

and hence $\partial\eta/\partial t = (g'H\beta/f^2)(\partial\eta/\partial x)$. The maximum positive rate of change of layer thickness will thus correspond to the maximum positive $\partial\eta/\partial x$, which is just the phase relationship that is required to produce a westward propagation of the η phase lines. The dispersion relation for this mode is readily calculated to be $\omega = -\beta R_d^2 K$, the small $K R_d$ limit (i.e., the long Rossby wave limit) of Eqn. (99). Because the mechanism of long Rossby waves is the beta-induced divergence of the north-south geostrophic current, long Rossby waves are sometimes called divergent Rossby waves. This beta-effect plus forcing by wind stress curl are important mechanisms for the westward intensification of the wind-driven ocean gyres (Fig. 2).

Beta and relative vorticity. Now suppose that the geostrophic current is nondivergent so that column thickness $H + \eta$ is effectively constant and the q -balance is $\xi + f = \text{const.}$, i.e., the absolute vorticity is conserved (Fig. 21, right). It is easiest to see the resulting phase relationships if we use the north-south velocity v and the y -displacement as the dependent variables. In terms of these variables, the conservation of absolute vorticity reads $\partial v/\partial x + \beta y + f_0 = \text{constant}$, and with no loss of generality we can take the $\text{constant} = f_0$. Thus a northward displacement, $y > 0$, induces negative relative vorticity, $\partial v/\partial x < 0$. The implied phase relation between v and y is consistent with a westward propagating wave (you will have to make the appropriate sketches to see this). The dispersion relation associated with this mode is $\omega = -\beta K^{-1}$, the short Rossby wave limit. Because the stretching term (divergence) is not involved in the q balance of this mode, short Rossby waves are sometimes referred to as non-divergent Rossby waves.

Beta, relative and stretching vorticity. For Rossby waves having a wavelength that yields $K R_d \approx 1$, all three terms are important in the q -balance. The lower panel of Fig. (30) shows these terms evaluated for the somewhat smeared out eddy at $t = 99$ days. The ratio of relative vorticity to stretching vorticity is $(K R_d)^2$, i.e., there is more contribution from relative vorticity for shorter wavelengths. Said a little differently, if the wavelength is sufficiently long, e.g., as it is for the ocean gyres (Fig. 2), there will be very little contribution by the relative vorticity term.⁵⁷

⁵⁷An elementary Rossby wave description appears to give a semi-quantitative account of the eddy translation found in this single numerical experiment, and appears to be at least roughly consistent with the oceanic mesoscale eddy observations of Fig. 3 as well. To gain some confidence in this tentative result, we would surely need to verify that the parameter dependence of the eddy translation speed is in common between the wave theory and the numerical solutions. For example, does the eddy translation speed vary with latitude and g' as predicted by Eqn. (99)? Much better that you design and run the experiments that you deem relevant, but a few cases with varying latitude are made available as animations listed in Section 9. An elementary wave description certainly does not account for the apparent dispersion of the eddy with time (the appearance of a low pressure trough in our geostrophic adjustment experiment, Fig. 28). How could we test the conjecture that the relevant mechanism is wave dispersion vs. some gross numerical error? For example, how does the initial horizontal scale of the eddy effect its translation speed and the apparent dispersion? More generally, does the vorticity balance in our numerical experiment follow the expected tendency toward greater relative vorticity contribution at larger $K R_d$? (a start on this is Fig. 30, lower).

7.3.4 Some of the varieties of Rossby waves

Topographic: Topographic Rossby waves are an important phenomenon of many coastal oceans and other regions having a sloping sea floor. The simplest form of these waves occurs when the fluid is homogeneous (not density stratified) and the flow is uniform with depth as in the shallow water model. The relevant, background potential vorticity is then $f/h(y)$, with $h(y) = H + b(y)$ the water column thickness (Fig. 20), here allowed to vary in y only. A fluid column that moves across bottom contours will then necessarily be stretched (or squashed), inducing relative vorticity exactly as does flow across lines of constant f . The ratio of planetary to topographic vorticity change over a typical continental shelf is

$$\frac{\text{planetary}}{\text{topographic}} = \frac{\frac{1}{f} \frac{\partial f}{\partial y}}{\frac{1}{h} \frac{\partial h}{\partial y}} = \frac{h}{\alpha R_e} \text{ is } O(10^{-1}),$$

given a bottom slope $\alpha = 10^{-3}$ and nominal depth $H = 200$ m. The magnitude of the topographic term can easily exceed the planetary β term since the bottom depth typically varies on much shorter spatial scales than does f (radius of Earth, R_e). Topographic effects would prevail over much of the deep, open ocean as well, except that stratification partially shields the upper water column from a direct bottom slope effect (something outside the domain of a single layer model).

Assuming that topographic variation dominates the gradient of the background $q = f/H$, and that the fluid is homogeneous, then the frequency of the resulting topographic Rossby waves is given by

$$\frac{\omega}{f} = \frac{\alpha g}{fC} \left(\frac{R_d K}{1 + R_d^2 K^2} \right),$$

where $R_d = C/f$ is the barotropic radius of deformation, with $C = \sqrt{gH}$ computed from a nominal H and the full gravity. For a nominal shelf water depth $H = 200$ m, $C \approx 45$ m s⁻¹ and $R_d \approx 900$ km (mid latitudes). Topographic Rossby waves require a non-zero planetary vorticity, f , but not the gradient of f . These waves have considerably higher frequencies than do planetary Rossby waves, with 5 - 20 day periods being common. They have correspondingly greater phase and group speeds as well. Just as planetary Rossby waves propagate phase westward - with higher background potential vorticity to the right of the wave vector - so too these topographic Rossby waves propagate phase with shallower water and thus larger f/H on their right.⁵⁸

Equatorial: At the subtropical site chosen here, the initial geostrophic adjustment was completed in about four or five days, and the subsequent westward propagation of the nearly balanced eddy became evident only after several weeks (though westward propagation started as soon as there was an appreciable north-south current). There is evidently a significant gap in time scales between two very different kinds of dynamics that are represented in this experiment: fast time scale inertio-gravity waves

⁵⁸An excellent description of (baroclinic) topographic Rossby waves observed under the Gulf Stream is available at <http://www.po.gso.uri.edu/dynamics/wbc/TRW.html> An analysis of a short-lived topographic Rossby wave is in the companion essay, 'Lagrangian and Eulerian Representations of Fluid Flow', <http://ocw.mit.edu/ans7870/resources/price/index.htm>

and geostrophic adjustment, and much slower Rossby wave, quasi-geostrophic dynamics that lead to westward propagation. If one's interest was mainly one or the other of these regimes, then it would make sense to treat these processes with a model designed to handle specific requirements efficiently. Here we have not done that, in part because we wanted to see that these two regimes emerge naturally from an initial value problem. And too, there is a very interesting and important case, central latitude = 0, that blurs the otherwise sharp distinction between gravity waves and Rossby waves. Here we go, back to the equator, again. On this trip we are ready to acknowledge that f varies toward both poles, i.e., we can envision an equatorial beta plane. f is very small (but of course non-zero just off the equator) and β is as large as it gets. The result is that the frequency difference between gravity and Rossby waves is much less than is found at subtropical and higher latitudes. Some equatorial waves appear to be a blend of gravity and Rossby waves (see the animation of the equatorial case in Section 9).

Westerlies: Rossby waves and the associated dynamics are a very significant phenomenon in the atmosphere. Indeed, the pioneering study of this phenomenon was carried out by Carl G. Rossby and colleagues in the late 1930s⁸ with the aim of understanding the zonal motion of the often prominent, wave-like undulations of the westerly winds (Fig. 1). These waves on the westerlies may have a planetary wavenumber (waves per circumference of the Earth) of anywhere from 3 to 15. The longest such waves (Fig. 1 is an example) often appear to be nearly stationary, despite that the westerly winds in which they are embedded have a spatially averaged speed, \bar{U} of $O(30 \text{ m s}^{-1})$ toward the east. The longest waves have a westward propagation speed that is just sufficient to stem this eastward advection and may appear to be nearly stationary with respect to the Earth. Quasi-stationary waves of this sort are very common in fluid flows around fixed obstacles: 'rapids' on the surface of a river and ripples on the flow of water from a faucet are familiar examples. On the other hand, the shortest waves on the westerlies, which may dominate the instantaneous pattern of the westerlies at other times (the web site noted in footnote 3 shows instances of this) clearly translate from west to east. In some cases short waves move eastward at a speed that is not much less than \bar{U} . Short westerly waves (which still have wavelengths of several thousand kilometers) thus appear to be more or less passively advected by the westerly wind. Rossby proposed that westerly waves may propagate zonally within a zonal mean flow \bar{U} as

$$C_w = \bar{U} - \beta K^{-2}, \quad (101)$$

which is the short (non-divergent) limit of the Rossby wave dispersion relation Eqn. (99). This relation, and the analysis that led to it, proved to have great merit, both as a fundamental explanation of the observations and as a practical guide for weather forecasting.⁵⁹

Summary: When the northward increase of f is included in the shallow water model there arises a

⁵⁹Rossby's highly readable papers are available at <http://www.aos.princeton.edu/WWWPUBLIC/gkv/history/general.html> An analysis of westerly waves is available from <http://journals.ametsoc.org/toc/atsc/1/3> A comprehensive, modern resource for oceanic Rossby wave observations and theory is <http://www.noc.soton.ac.uk/JRD/SAT/Rossby/index.html> The wide variety of mainly atmospheric phenomenon is reviewed by <http://carlsbad.princeton.edu/~dynamics/wiki/images/e/e9/Rhines.pdf> (you may have to type this address into your web browser).

low frequency wave motion, often called a Rossby wave. These are a very useful idealization of some of the most important low frequency phenomenon observed in the atmosphere and the ocean. Rossby waves are markedly anisotropic, in that they propagate phase westward only. Long (divergent) Rossby waves are nondispersive, while short (non-divergent) Rossby waves are highly dispersive.

8 Summary of the essay.

This essay has come two parts. In Part I, Sections 2 - 5, we used a very simple, single parcel model to examine the kinematics of a steadily rotating reference frame. The Coriolis force accounts for rotationally-induced accelerations, and is one of the most significant forces that shape the pattern and evolution of winds and currents. In Part II, Sections 6 and 7, we utilized a single layer fluid model, often called the shallow water model, to solve several problems in geostrophic adjustment. In the context of a fluid model, Earth's rotation is very important in the conservation of potential vorticity, the fluid equivalent of angular momentum conservation. To summarize further we will return to the questions raised in Section 1.2.

Q1) The origin of the term $2\boldsymbol{\Omega} \times \mathbf{V}'$: The Coriolis and centrifugal forces arise from the rotational acceleration of a reference frame rather than from an interaction between physical objects. Since there is no physical origin for these forces, neither should we expect a physical explanation of their origin. The sole, reliable explanation of the Coriolis force is the transformation law for acceleration (Section 2.5). Whether we should call the Coriolis term a force (as we have done) or an acceleration is less clear. The latter is sensible insofar as the Coriolis term arises from the transformation of acceleration, and too because it is independent of the mass of the parcel. However, when we use a rotating reference frame we seek to analyze (and necessarily observe) the acceleration seen in the rotating frame, $d^2\mathbf{X}'/dt^2$, and not the rotated acceleration, $(d^2\mathbf{X}/dt^2)'$, of which the Coriolis term is a part (Section 2.5). To understand the contribution of the Coriolis term to the acceleration that we observe, it is then natural to regard the Coriolis term as the *Coriolis force*.

The choice of reference frames is binary, as is the existence or not of the Coriolis and centrifugal forces; either it's inertial, in which case there is no Coriolis or centrifugal force, or it's rotating, and there definitely is (notwithstanding that they may be negligible in a given circumstance). If we choose to (or must) use a rotating frame, then the centrifugal and Coriolis forces are exact consequences of transforming the equation of motion (Section 2.4). There is nothing *ad hoc* or discretionary about their appearance in the rotating frame equation of motion, and there is no good in calling or thinking of the Coriolis force as a 'pseudo force', or a 'fictitious correction force' or any usage that might seem to question whether the Coriolis force is a full-fledged member of the equation of motion.

Q2) Global conservation and the absence of the centrifugal force: Because the centrifugal and Coriolis are not central forces between physical objects, they contribute peculiar and unphysical

behavior to the rotating frame dynamics. Recall the elementary trajectory of Section 3.4; when observed from a rotating frame the parcel veered to the right as expected from the deflecting Coriolis force. However, there was no object in the environment that revealed a corresponding reaction force. Similarly, the parcel speed and kinetic energy increased with time due to work by the centrifugal force, and yet there was no source for the energy. The rotating frame equation of motion thus does not support global conservation of momentum and neither does it preserve invariance to Galilean transformation. At first these would appear to be dire failings, but in practice they are not an issue, so long as we recognize and expect them. The overriding point is that the analysis and interpretation of geophysical flow phenomena is far simpler when viewed from an Earth-attached, rotating reference frame. In the special case of a reference frame attached to a rotating planet, the centrifugal term is cancelled by a small deformation of the planet. Because the atmosphere and the oceans are thin, when viewed in the large, and stably stratified, the horizontal component of winds and currents is generally much larger than the vertical component. In place of the full three-dimensional Coriolis force, we usually need consider only the horizontal component of the Coriolis force acting upon the horizontal wind or currents, $\mathbf{f} \times \mathbf{V}$, where f is the Coriolis parameter times the vertical unit vector.

Q3) New modes of motion: In the very simple, single parcel model (Section 5) we found that there were two modes of motion that depended directly upon the Coriolis force. The rotational modes include a free oscillation, usually called an inertial oscillation, in which an otherwise unforced current rotates at the inertial frequency, f . Inertial oscillations are often a prominent feature of the upper ocean current following the passage of a moving storm. A crucial, qualitative effect of rotation is that it makes possible a non-trivial, steady motion that is in balance between an external force (wind stress or buoyancy force) and the Coriolis force. The characteristic of this steady mode is that the velocity is normal to the applied force. We have to be cautious not to over-interpret the single parcel model, but a correct inference from this result is that rotation (and the Coriolis force) is indeed the basis for the nearly steady winds and currents that make up majority of atmospheric and oceanic circulation outside of equatorial regions.

Q4) Establishment of geostrophy: In Sections 6 and 7 we considered a much more realistic model of a geophysical flow, a single layer model, often termed a shallow water model. This model allows for gravity wave motions that, in the absence of rotation, have a phase and group speed $C (= \sqrt{g'H})$, where H is layer thickness). Absent rotation, these gravity waves will rapidly disperse any anomaly in the layer height (Section 7.1). With rotation present (Section 7.2), and provided that friction is not large ($E = r/f \ll 1$, where r is the linear friction parameter and E is the Ekman number) a thickness anomaly will evolve toward a state of geostrophic balance. The currents that accompany the geostrophic adjustment process may be characterized as gravity waves, inertial oscillations and geostrophic currents. One mode or the other may dominate depending upon the time and place, but in general all occur at once.

Perhaps the most important result of the f -plane experiments (Section 7.2) was that the fraction of a ridge of width λ that survived to reach a steady geostrophic balance was found to depend upon $K R_d$,

where $K = 2\pi/\lambda$ and $R_d = C/f$ is the radius of deformation. Most of a wide ridge, $K R_d \ll 1$, will survive in the geostrophic state. On the other hand, a narrow ridge, $K R_d \gg 1$ will be dispersed by gravity waves. These important results are best understood as a consequence of potential vorticity conservation which links changes in layer thickness with changes in f and changes in relative vorticity.

Q5) Departures from geostrophy: The end state of a geostrophic adjustment process may be an almost exact geostrophic balance (assuming small E). An exact geostrophic balance would be exactly steady. It is clear that the atmosphere and the ocean evolve continually, though generally fairly slowly compared to f , so that geostrophic balance must be an approximation of the momentum balance of real winds and currents. From this perspective, it can be fruitful to take (near) geostrophy for granted, and then focus attention on the the small departures from geostrophic balance that are most clearly revealed in the balance of potential vorticity. Earth's rotation enters as the planetary vorticity, f . The variation of f with latitude, often called the beta-effect, gives rise to a westward propagation tendency for all large scale, nearly geostrophically balanced eddies, waves or gyres.

9 Supplementary material.

The most up-to-date version of this essay plus the Matlab and Fortran source codes noted in the text may be downloaded from the author's public access web site:

<http://www.whoi.edu/science/PO/people/jprice/education/aCt.update.zip>

9.1 Matlab and Fortran source code

All of the following are public domain for all educational purposes.

coriolis.m solves for the motion of a parcel as seen from an inertial and a rotating reference frame. Used to make Fig. 29. It is much easier to see the results in the onscreen plotting vs. the hardcopy figure.

partslope.m solves for the motion of a single dense parcel on a slope and subject to buoyancy, bottom drag and Coriolis forces. Used to make the figures of Section 5, and configured to carry out additional experiments.

twowaves.m shows the result of superposing two sine waves whose dispersion relation may be specified arbitrarily.

ftransform.m solves an initial value problem in one-dimension and without rotation. Shows the wave forms that result from dispersion that is normal, anomalous or none.

geoadj_1d.m is a one-dimensional, shallow water model used for the geostrophic adjustment experiments of Sections 7.1 and 7.2. The latitude, layer depth, friction parameter, etc. may be easily

varied from experiment to experiment.

geoadj_2d.for is a two-dimensional shallow water model used to do the beta-plane geostrophic adjustment experiments of Section 7.3. Written in a very simple Fortran. Solutions like those shown in Section 7.3 can be generated on a reasonably capable PC in a few minutes. Model parameters including latitude, the kind of f model, eddy amplitude, etc. are entered from the keyboard. Output is saved to disk. This model was written for educational rather than research purposes, and the numerical methods are simple rather than optimal. As would be true for any numerical model, the results should be approached with considerable caution.

geoadj_2d_plot.m is a Matlab script used to plot the data generated by **geoadj_2d.for**.

9.2 Additional animations

Some additional animations are available as follows:

igwaves_beta.mpg; an animation of the beta-plane geostrophic adjustment case shown here in Fig. 29.

ga2d_eta_lat0.mpg; animation of layer thickness anomaly, η , for an equatorial beta-plane geostrophic adjustment experiment. Unlike the other adjustment experiments listed below, this case employed no normal flow boundary conditions on walls set at $x = \pm 3000$ km. The northern boundaries were specified by radiation boundary conditions.

ga2d_eta_latxx.mpg; animations of thickness anomaly, η , for latitude $xx = 10, 20, 40,$ and 60°N .

ga2d_u_latxx.mpg; the currents that go with the η animations above.

MIT OpenCourseWare
<http://ocw.mit.edu>

Resource: Online Publication.Fluid Dynamics
James Price

The following may not correspond to a particular course on MIT OpenCourseWare, but has been provided by the author as an individual learning resource.

For information about citing these materials or our Terms of Use, visit: <http://ocw.mit.edu/terms>.